10.14751/SZIE.2013.026

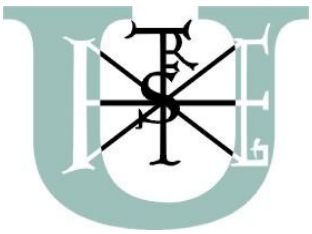

SZENT ISTVÁN UNIVERSITY

Energetic modelling of photovoltaic modules in grid-connected systems

PhD Dissertation

by

Dani Rusirawan

Gödöllő, Hungary
2012

10.14751/SZIE.2013.026

Doctoral school denomination: Mechanical Engineering PhD School

Science: Energetics of Agricultural and Environmental Engineering

Leader: Prof. Dr. István Farkas
Dr. of Technical Sciences
Faculty of Mechanical Engineering
Szent István University, Gödöllő, Hungary

Supervisor: Prof. Dr. István Farkas
Dr. of Technical Sciences
Institute for Environmental Engineering Systems
Faculty of Mechanical Engineering
Szent István University, Gödöllő, Hungary

...……...……....…….. ……

Affirmation of the Doctoral School Leader Affirmation of supervisor

10.14751/SZIE.2013.026

CONTENTS

10.14751/SZIE.2013.026

NOMENCLATURE AND ABBREVIATIONS

A	Area (m^2)
AM	Air mass ratio
$En_{ph}(\lambda)$	Energy of a photon (J)
E	Electrical energy (J) or (kWh)
E_{arr}	Solar irradiation on the plane array position (kWh/m^2)
E_G	The band gap energy of semiconductor used in the cell (eV)
E_{hor}	Global solar irradiation (kWh/m^2)
Ex	The exergy in general (J)
$Ex\_loss\ or$ Ex_{loss}	The major loss exergy (exergy destroy) as a consequence of the irreversibilities of the process (W/m^2)
$\dot{E}n_{chemical}$	Available of photonic energy or Chemical potential (W)
$\dot{E}x^{Q}$	The exergy transfer associated with $\dot{Q}$ (W)
$\dot{E}x^{W}$	The exergy transfer associated with $\dot{W}$ (W)
en	Specific energy (J/kg)
ex	Specific exergy (J/kg)
FF	Fill Factor
G	Solar irradiance (W/m^2)
h_{ca}	Convection and radiation heat transfer coeff. ($W/m^2.K$)
I	Currrent produced by solar cell (A)
I_l	Light-generated current/photocurrent (A)
I_o	The dark saturation current (A)
I_r	System exergy consumption (W)
K	Boltzmann's constant (1.381×10^{-23} J/K)
L_C	Capture losses (kWh/kWp)
L_s	System losses (kWh/kWp)
$\dot{m}$	Mass flow rate (kg/s)
N	Ideality factor (1-2)
$N_p\ or\ N_s$	Number of modules in parallel and series
N_{ph}	Numbers of photon falling per second per unit area on the Earth ($1/m^2.s$)
$NOCT$	Nominal Operating Cell Temperature (^oC) or (K)
P	Electric power (Watt)
PR	Performance Ratio (-)
Q	Electron charge (1.602×10^{-19} C)
$\dot{Q}$	Heat transfer across system boundary (W)
q_s	Heat transfer from the sun (W/m^2)
q_r	Reflected solar radiation (W/m^2)
q_c	Useful heat absorbed by solar cell (W/m^2)
q_k	Convection heat to environment (W/m^2)
q_o	Radiation heat to environment (W/m^2)

R	Resistance (Ω)
S_{gen}	Entropy generated by system (W/K)
T	Temperature (^{o}C) or (K)
V	Output/applied voltage (V)
v	Wind velocity (m/s)
$\dot{W}$	Work transfer across system boundary (W)
Y	The yield of energy (kWh/kWp)

Subscripts:

a	Ambient
Arr or *A*	Array
c	Solar cell/module
ch	Chemical
dest	Destructive
en	Energy
ex	Exergy
f	Final
hor	Horizontal
in	Input
k	Kinetic
mp	Maximum point
mpp	Maximum power point
max	Maximum (theoretical) value
oc	Open circuit
out	Output
p	Potential
pc	Power conversion
ph	Physics
pv	Photovoltaic
Ref or *r*	Reference
s	Series
s	Sun
sc	Short circuit
sh	Shunt

Greek symbols:

β	PV plane tilt angle (^{o})
δ	Solar declination (^{o})
ϕ	Latitude angle (^{o})
γ	PV plane azimuth angle (^{o})
η	Efficiency (%)
λ	Wavelength of spectrum the light (nm)
μ_i	The cell's short-circuit current temperature coefficient (A/K)

μ_t	Temperature coefficient of the PV cell ($^oC^{-1}$)
θ	Angle between direct beam and normal of collector (^{o})
θ_z	Zenith angle (^{o})

ABBREVIATIONS

a-Si	Amorphous silicon
pc-Si	Polycrystalline silicon (or multicrystalline silicon)
I-V-P	Current-Voltage-Power
PV	Photovoltaic
STC	Standard Test Conditions
SZIU	Szent István University

10.14751/SZIE.2013.026

1. INTRODUCTION AND OBJECTIVES

In this chapter, the importance of the research topic is presented along with the objectives of this research.

1.1. Introduction

Developing a clean and renewable energy has become one of the most important tasks in field of modern science and engineering. Solar energy can be recognized as one of the most promising renewable energy sources. Photovoltaic (PV) systems, presently is accepted as the most important way to convert solar energy into electricity, due to pollution free and abundantly available anywhere in the world. It is well known that most of the radiation (solar energy) absorbed by a PV system is not converted into electricity (electrical energy) but contributes also to increase the temperature of the module (thermal energy), thus reducing the electrical efficiency. In thermodynamic point of view, PV system performance can be evaluated in terms both energy and exergy, and in applications level, PV module is basic building block to construct PV systems.

Testing (conducted to an experimental data) and modelling efforts are typically to quantify and then to replicate the measured phenomenon of interest. Testing and modelling of PV system performance in the outdoor environment is very complicated and influenced by a variety of interactive factors related to the environment and solar cell physics. In order to effectively design, implement, and monitor the performance of photovoltaic systems, a performance model must be able to separate and quantify the influence of all significant factors. In view of this, it is now becoming essential to look for various aspects in order to increase the PV energy conversion into electricity on its application in the field.

1.2. Objectives

In this research, comprehensive evaluation of two PV modules technologies will be performed based on points of view energetic and exergetic. As a subject, polycrystalline silicon, pc-Si (included wafer based crystalline silicon technology) and amorphous silicon, a-Si (included thin-film technology), as components of grid-connected PV array system at Szent István University (SZIU), are used under Gödöllő climatic conditions. It is well known that energy analysis is more suitable for energy balance when we design a system, while exergy analysis is more appropriate when we evaluate the performance of a system qualitatively.

The objectives of this research can be described as follow:

1. Evaluation of an existing grid-connected PV array system in view of macro PV model, based on theoretical and experimental.

2. Evaluation of surface orientation (tilt and azimuth angles) effect on the yield energy in grid-connected PV array system.
3. Elaborates the mathematical model of PV cell/module, and its correlation in the PV panel/array, in view of energetic.
4. Evaluation of *I-V-P* (current-voltage-power) characteristic of the PV modules and its correlation in the PV panel/array, using a relevant software packages, such as: NSol, RetSCreen, Homer, etc.
5. Elaborates the thermodynamic performances of PV modules in view of energetic and exergetic.
6. Evaluation of PV modules performances in view energetic and exergetic based on theoretical (mathematical model) using PV*SOL and experimental.
7. Comparing an exergetic performances based on ”thermodynamic approach for solar energy ” and ”photonic energy (chemical potential) from the sun” models.
8. Study of spectral irradiations effects on energetic and exergetic PV performance.

2. LITERATURE REVIEW

Solar energy can be recognized as one of the most promising renewable energy sources. Along with other forms of renewable energy sources, i.e. biomass energy, geothermal energy, wind energy, fuel cell, ocean energy, it has a great potential for a wide variety of applications because of its abundance and accessibility. Direct conversion of solar energy (the energy contained in photons of light) into electricity (an electrical voltage and current) usually refers to a photovoltaic (PV) system (solar cell/module/panel/array).

PV system use semiconductor materials to convert sunlight into electricity. The technology for doing so is very closely related to the solid-state technologies used to make transistors, diodes, and all of the other semiconductor devices that we use so many of these days (Masters, 2004).

PV systems produce DC electricity when sunlight shines on PV solar cell, without any emissions. The DC power is converted to AC power with an inverter and can be used to power local loads or fed back to the utility. Principally, there are two methods to convert solar radiation into electric energy i.e. by photovoltaic (PV) and by concentrated solar thermal (CST). In the PV method, a certain semi conductor materials absorbed a light and directly converted into electricity (photo-effect). Meanwhile, in CST method, a direct light is focused into one point in order to heat a liquid, and the heat is subsequently used to drive a generator like in a conventional power station (such as turbine power plant).

PV systems, presently is accepted as the most important way to convert solar energy into electricity. According to predictions by many energy experts, photovoltaic electricity will necessarily play a significant role in any sustainable energy future. The future competitiveness of PV depends on many factors, such as technological advances, production volume of PV components, ecological tax on traditional energies, and also on the most judicious use of this new energy technology (especially in advance material aspects). The latter point in particular relates to the performance of PV system generators under site-specific climatic conditions. The question is: What energy output of different generators can be expected under actual operating conditions at climatologically different sites? To answer this question, the physical behavior of solar cells and photovoltaic modules under varying solar illumination and changing climatic conditions needs to be known. Usually these data are not provided by the manufacturers and suppliers of PV products. Moreover, the data provided at Standard Test Conditions (STC) most often are taken under test conditions which never occur in practice (Durisch et al., 2000).

2.1. State of the art of photovoltaic technologies

In case of technology, until this time, the PV technologies can be classified into three generation as can be seen in Table 2.1.

Table 2.1. PV modules technologies based on history

History of photovoltaic technology	1st generation	Wafer based crystalline silicon technology
	2nd generation	Thin film technology
	3rd generation	Nanostructure technology: Concentrating photovoltaic (CPV), Dye sensitized solar cell/DSSC (organic photovoltaic (OPV)

The output power of PV systems can be affected by many factors, such as environment (irradiance and temperature) and material (semiconductor material). In view of material, PV system (or the most commercial of PV) mainly can be categorized into silicon and compounds, as shown in Table 2.2.

The PV module cost depends on the total manufacturing cost of the module per square area and the conversion efficiencies. Fig. 2.1. gives an estimate of achievable cost with crystalline silicon (c-Si) technology and comparison with projected achievable costs with other technologies. It is generally agreed that c-Si wafer technology would not be able to meet the low cost targets, whereas thin-film technologies have the potential to provide a viable alternative in the near future (Razykov et al., 2011).

Table 2.2. Commercial PV categories based on technology and material

	Technology	Material	Sub-material
PV	Wafer based crystalline silicon	Silicon	1. Mono/single crystalline silicon, sc-Si
			2. Poly/multi – crystalline silicon, mc-Si
			3. Heterojunction with intrinsic thin layer, HIT
	Thin film	Silicon	1. Amorphous silicon, a-Si
			2. Microcrystalline silicon, μc-Si
			3. Multi Junction (Tandem), example: a-Si/a-Si and micromorph silicon (a-Si/μc-Si)
		Compound	1. Copper - Indium - (Gallium) - Selenide, CI(G)S
			2. Cadmium telluride, CdTe

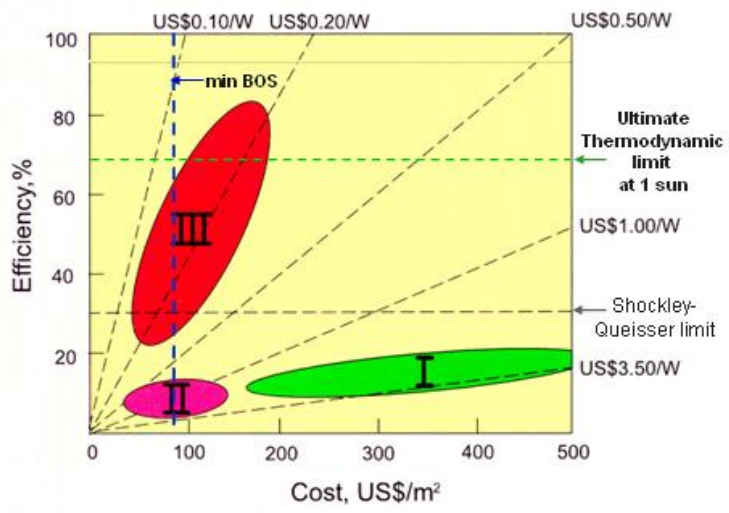

Fig. 2.1. Cost – efficieny of PV for all technologies (Walukiewicz, 2012)

The thermodynamic efficiency for an ideal single-homojunction cell is ~31% (see Fig. 2.1). The 31% detailed balance limit for a single junction solar cell (proposed by Shockley and Queisser) is based upon the reduction of the ultimate efficiency limit of 44% due to entropic losses (Abrams et al., 2012). In view of solid state subject, the efficiency of a single-junction device is limited by transmission losses of photons with energies below the bandgap and thermal relaxation of carriers created by photons with energies above the bandgap. The illustration of losses in commercial c-Si is shown in Fig. 2.2.

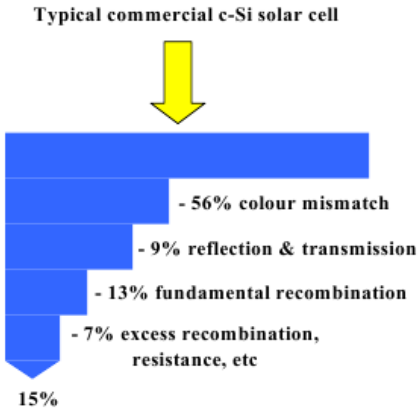

Fig. 2.2. Losses in PV cell for c-Si (Zeman, 2012)

In other form, state of the art of a PV material in view of "cell cost vs cell efficiency" can be illustrated such as in Fig. 2.3. This matrix shows that the most efficient, but also most costly remains the multi-junction material. It is clear that the material aspect is the most important to be developed in order to get the best efficiencies Note that this picture only shows the relationship between photovoltaic efficiency and cost of photovoltaic material rather than cost of the total system**.** Low efficiency may impact on costs for mounting, wiring and land

ownership, as more area needs to be covered for the same rated power. Hence, costs could go up further even when module costs per kWh are the same (www.greenrhinoenergy.com/solar/technologies/pv_modules.php, 2012).

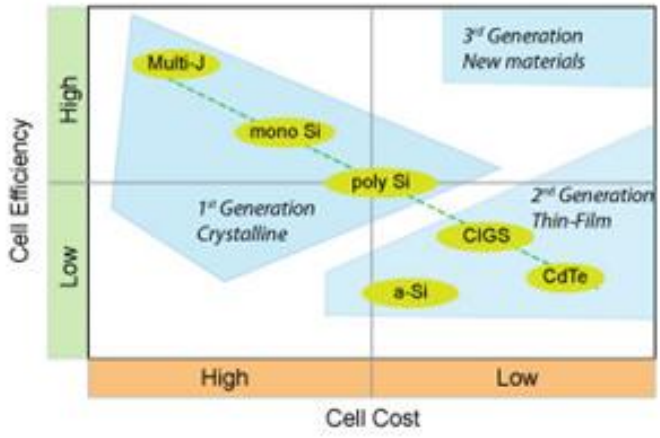

Fig. 2.3. PV cell power conversion efficiency vs. PV cell cost

As a comparison, the world evolution of PV cell efficiencies (in Laboratory scale) is shown in Fig. 2.4 (www.nrel.gov/ncpv/images/efficiency_chart.jpg, 2012). Improving PV cell efficiencies while holding down the cost per cell is one of the most important tasks of the PV industry.

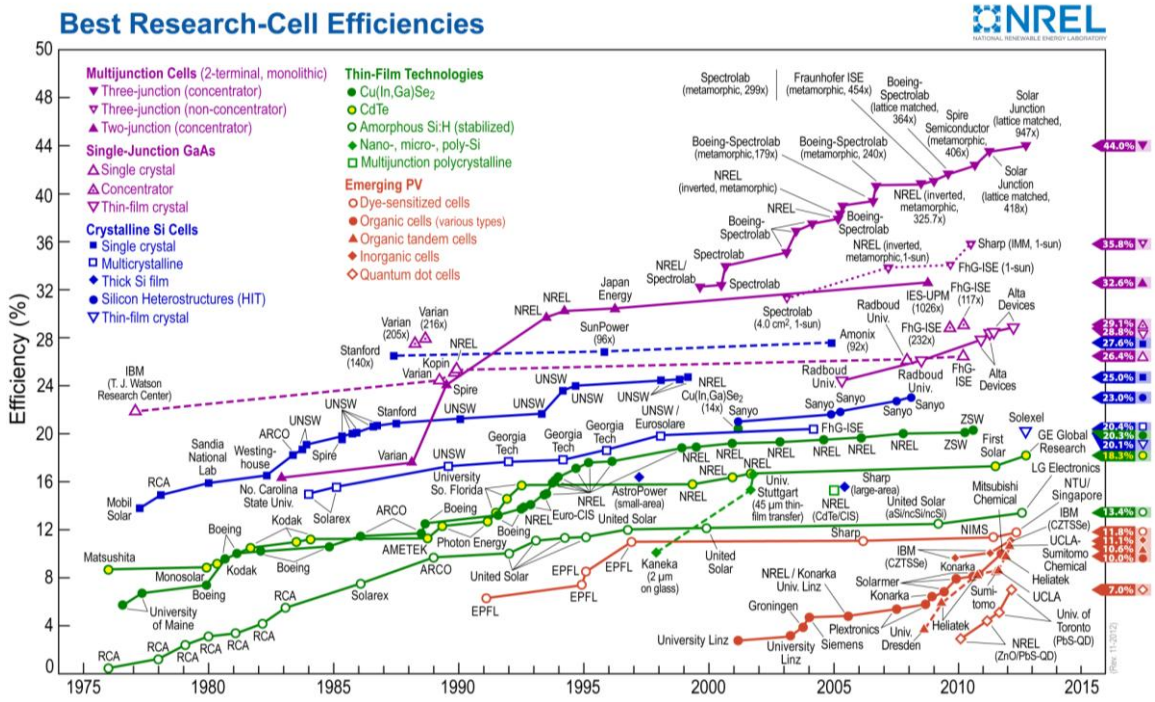

Fig. 2.4. PV cell efficiency versus cost for all technologies

Several methods have been offered to increase the power conversion efficiency of PV cells, including tandem cells, impurity-band and intermediate-band devices, hot-electron extraction, and carrier multiplication (Razykov et al., 2011).

2.2. Configuration of photovoltaic system

There are two main of PV system configurations i.e. stand-alone and grid-connected, as can be seen in Fig. 2.5 (Pearsall and Hill, 2001). As its name implies, the stand-alone PV system operates independently of any other power supply and it usually supplies electricity to a dedicated load or loads. It may include a storage facility (e.g. battery bank) to allow electricity to be provided during the night or at times of poor sunlight levels. Stand-alone systems are also often referred to as autonomous systems since their operation is independent of other power sources. Otherwise, the grid PV system operates in parallel with the conventional electricity distribution system. It can be used to feed electricity into the grid distribution system or to power loads which can also be fed from the grid.

It is also possible to add one or more alternative power supplies (e.g. diesel generator, wind turbine) to the system to meet some of the load requirements. These systems are then known as hybrid system (see Fig. 2.6).

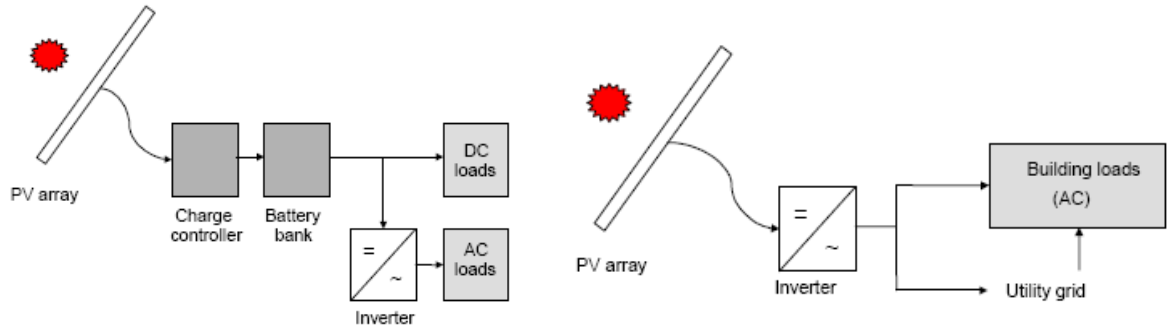

a) Stand-alone b) Grid-connected

Fig. 2.5. Two type of PV system configuration

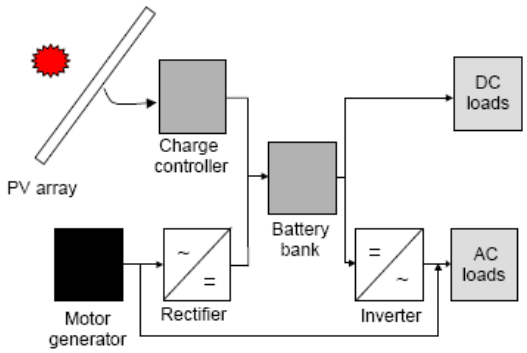

Fig. 2.6. Schematic diagram of ”hybrid system” incorporating a PV array system and generator system

Hybrid systems can be used in both stand-alone and grid-connected applications but are more common in the former because, provided the power supplies have

been chosen to be complementary, they allow reduction of the storage requirement without increased loss of load probability.

Principally, a PV array frames can be fixed (non tracking), adjustable or tracking. Adjustable frames allow the tilt angle to be varied manually throughout the year to maximize output year round. Tracking array frames follow the sun as its path across the sky varies throughout the day and year. They are controlled either by an electric motor. Trackers are more expensive than fixed array frames but by following the sun they provide more power throughout the day.

In order to capture as much solar energy as possible, the PV cell must be oriented towards the sun. If the photovoltaic cells have a fixed position, their orientation with respect to the south (for northern hemisphere location), and tilt angle with respect to the horizontal plane, should be optimized.

2.2.1. Grid-connected photovoltaic system

PV can be used in grid-connected mode in two ways: as arrays installed at the end use site, such as on rooftops, or as utility-scale generating stations.

A grid-connected PV system consist mainly of a PV array and an inverter. In order to evaluate the energetic performance such a system, the energy yield and losses at the different conversion steps are normalized to the power values under STC. Yield and losses can be allocated to the different components of a grid-connected PV system as shown in Fig. 2. 7 (Woyte, 2003).

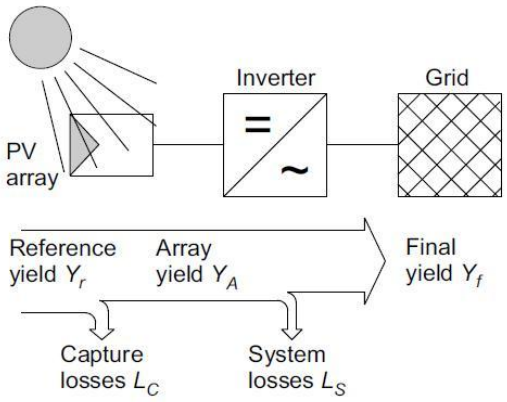

Fig. 2. 7. Energy flow in grid-connected PV system

The reference yield (Y_r) is defined as solar irradiation on the tilted plane normalized to the solar irradiance under STC, hence,

$$Y_r = \frac{G_\beta}{G_{STC}}. \tag{1}$$

It is expressed in hours or ”kWh/kWp”.

Array yield (Y_A) and final yield (Y_f) are calculated by normalizing the energy before, respectively after passing the inverter, to the rated power of the PV array under STC. In practice, these values are mostly given in ”kWh/kWp”. Accordingly, the capture losses and system losses are calculated as

$$L_C = Y_r - Y_A, \tag{2}$$

$$L_S = Y_A - Y_f . \tag{3}$$

For a grid-connected PV systems, the system losses are mainly inverter losses.

In order to assess and compare the performance of PV systems over several years and for different sites, independently of variations of the solar resource, array yield and final yield are normalized to the reference yield. The performance ration is defined as

$$PR = \frac{Y_f}{Y_r} . \tag{4}$$

It can be interpreted as the ratio between the actual system yield and the yield of an ideal system, always operating with the conversion efficiency of the PV array under STC.

2.2.2. Inverter

Two main types of inverters can be used to achieve AC power at the voltage used in the main grid. These are (Wenham, et al., 2007):

1. line-commutated-where the grid signal is used to synchronise the inverter with the grid,
2. self-commutated-where the inverter’s intrinsic electronics lock the inverter signal with that of the grid.

For DC-AC conversion usually self-commutated inverters with pulse-width modulation (PMW) are applied. Some inverters for the application in microgrid are further equipped with a control algorithm, permitting the formation of a stable grid by multiple distributed geneeration units.

The inverter in Fig. 2.8 is based on a PMW-controlled full bridge. The PV array is directly connected to the DC bus of the inverter. The transformer mainly serves as galvanic separation while, in addition, transforming the inverter output voltage to grid voltage.

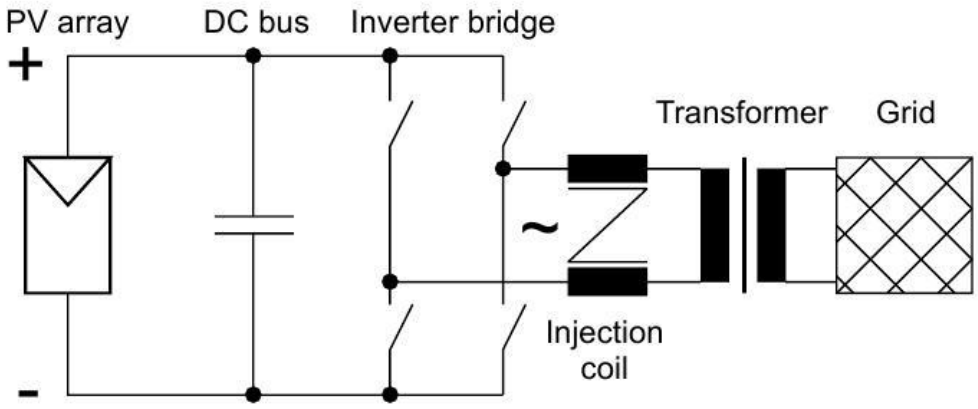

Fig. 2.8. Basic scheme of a PWM inverter with low-frequency transformer for PV grid connection

2.3. Surface orientation

Solar radiation incident on a solar PV collector is composed of three components, i.e. the direct beam, diffusion and reflection from the ground, which has different dependence on the slope of collector, the sum of these three components is called global radiation. Installing a collector properly can enhance its application benefit because the amount of radiation flux incident upon the collector is mainly affected by the surface orientation i.e. azimuth and tilt angles that it is installed. In the northern hemisphere, the best azimuth is due south (facing equator), but the tilt angle varies with factors such as the geographic latitude, climate condition, utilization period of time, etc (Chang, 2008).

Generally, the amount of solar radiation that will be intercepted by a surface on the earth, influenced by several factors as follow:

- day of the year (due to tilt of earth),
- geographic location (latitude and longitude),
- time of day (where the sun is in the sky),
- surface orientation,
- local atmospheric conditions (cloud/fog cover, ambient temperature, wind).

The surface orientation a module with respect to direction of the sun, consisted of two parameters, i.e. tilt and surface azimuth angles, as presented in Fig. 2.9. Tilt angle is the angle between the plane of the module and horizontal. Meanwhile, azimuth angle is between plane of module and due South (due North).

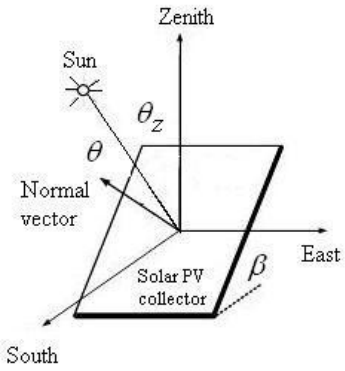

a) Tilt angle (β)

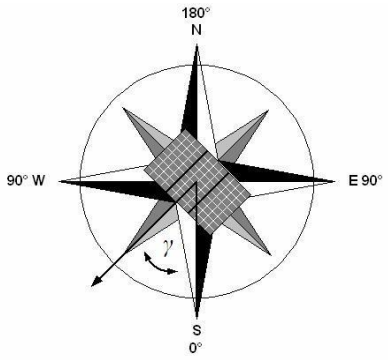

b) Surface azimuth angle (γ)

Fig. 2.9. Definition of surface orientation

As shown in Fig. 2.9.a), the global radiation incident on a south-facing solar PV collector tilted at an angle β to the horizontal surface. Where, θ is the instantaneous angle between direct beam and the normal of collector, θ_z is zenith angle.

Principally, the optimum tilt angle depends on several parameters:

- the type of application, i.e. stand-alone or grid-connected,
- maximization of the PV energy for the whole year or a certain period of time,
- actual climatic condition of the site, regarding snow fall, dust storm or polluted air.

In order to get the optimum surface orientation, several literatures (for example Hussein et al., 2004) reported that for the Northern hemisphere, the optimum orientation is south facing and the optimum tilt angle depends only on the latitude (ϕ). Definite value is rarely given by researcher for optimum tilt angle. Lunde and Garge suggested $\beta_{opt} = \phi \pm 15^0$, Duffie and Beckman suggested $\beta_{opt} = (\phi \pm 15^0)$, Heywood suggested $\beta_{opt} = \phi \pm 15^0$ and Lewis suggested $\beta_{opt} = \phi \pm 8^0$ as mentioned in the following papers: Kacira (2004), Christensen and Barker (2001) and Azmi and Malik (2001). Plus and minus sign are used in winter and summer respectively.

It is generally accepted that for low latitudes, the maximum annual output is obtained when the array tilt angle is roughly equal to the latitude angle and the array faces due south (in the northern hemisphere) or due north (for the southern hemisphere). For higher latitudes, such as those in northern Europe, the maximum output is usually obtained for tilt angles of approximately the latitude angle minus 10-15 degrees (Pearsall and Hill, 2001).

Generally, in the central European region (included Hungary), the optimal tilt angle which maximized yearly output energy is between 30° and 45°. It is usually close to the latitude angle (Marcel et al., 2007).

2.4. General photovoltaic models

Solar cell is basically a p-n junction fabricated in a thin wafer or layer of semiconductor. The electromagnetic radiation of solar energy can be directly converted to electricity through a photovoltaic effect. Being exposed to the sunlight, photons with energy greater than band-gap energy (E_G) of the semi conductor are absorbed and create some electron-hole pairs proportional to the incident irradiation. Under the influence of the internal electric fields of the p-n junction, these carriers are swept apart and create a photocurrent which is directly proportional to solar irradiance. A PV system naturally exhibits non-linear *I-V* and *P-V* characteristics which vary with the radiant intensity and cell temperature (Tsai et al., 2008).

2.4.1. PV and connecting cells and modules

Solar cells are rarely used individually. Rather cells with similar characteristics are connected to form modules which, in turn, are the basic building blocks of PV arrays. Since the maximum voltage from a single silicon cell is only about 600 mV, cells are connected in series in order to obtain the desired voltage. Usually about 36 series cells are used for a nominal 12 V charging system.

Under peak sunlight (G = 1000 W/m^2), the maximum current delivered by a cell is approximately 30 mA/cm^2. Therefore, cells are paralleled to obtain the desired current. Fig. 2.10 illustrates the terminology used to describe a typical connection of PV installation (from smallest to biggest) and the standard terminology used to describe such connections (King et al., 2004 and Wenham, 2007).

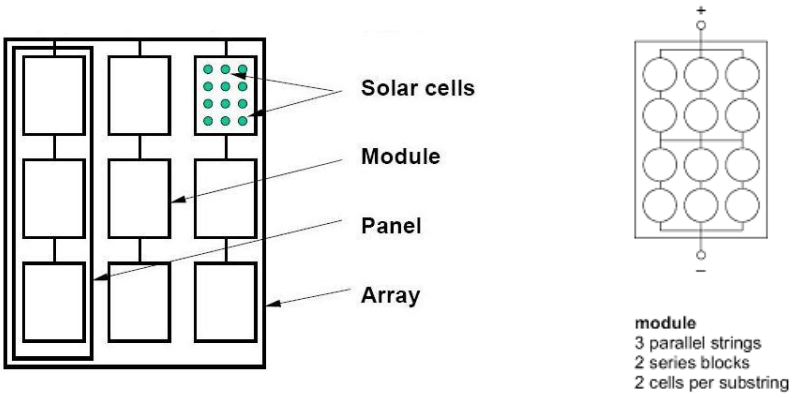

(a) (b)

Fig. 2.10. (a) Identification of solar photovoltaic system components and (b) terminology used in module circuit design

2.4.2. Solar cell model

The basic component of PV system is the PV cell (solar cell). A simplified equivalent circuit model is used since it is quite simple to implement and is

compatible with the electrical behaviour of the actual cell. The equivalent electric circuit diagram of PV cell is shown in Fig. 2.11, which consists of a photocurrent source, a diode, a parallel resistor (R_{sh}) expressing a leakage current and a series resistor (R_s) describing internal resistance to the current flow (Wenham, 2007).

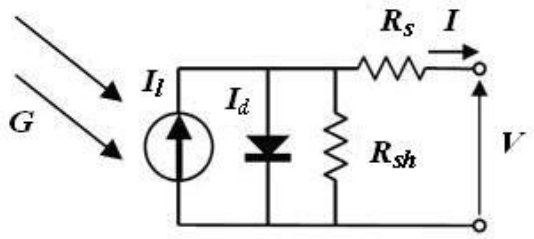

Fig. 2.11. General model of PV cell in a single diode model (five model parameter)

The PV cell's electric characteristic under solar irradiance (G) is given in terms of PV cell output current (I) and PV cell voltage (V).

Refers to Fig. 2.11., based on the First Law of Kirchoff, the basic equations which describing *I-V-P* characteristics of the PV cell model, can be elaborated through the following set equations:

$$I = I_l - I_d - I_{sh}, \tag{5}$$

$$I_d = I_o\left[exp\left(\frac{V_d}{\frac{nkT_c}{q}}\right)-1\right] = I_o\left[exp\left(\frac{V_d}{V_t}\right)-1\right], \tag{6}$$

$$I_o = I_{o,ref}\left(\frac{T_c}{T_{c,ref}}\right)^3 exp\left[\frac{qE_G}{nk}\left(\frac{1}{T_{c,ref}}-\frac{1}{T_c}\right)\right], \tag{7}$$

$$V_t = \frac{nkT_c}{q}, \tag{8}$$

$$V_{sh} = V_d, \tag{9}$$

$$V_d = V + IR_s, \tag{10}$$

$$I_{sh} = \frac{V_{sh}}{R_{sh}} = \frac{V_d}{R_{sh}}, \tag{11}$$

$$I_{sh} = \frac{V + IR_s}{R_{sh}}, \tag{12}$$

$$I = I_l - I_o \left[exp\left(\frac{V + IR_s}{\frac{nkT_c}{q}} \right) - 1 \right] - \frac{V + IR_s}{R_{sh}}, \tag{13}$$

where I is the current produced by the solar cell (A), I_l is a light-generated current or photocurrent (A), I_o is the dark saturation current (the diode leakage current density in the absence of light) (A), V is the output voltage/applied voltage (V), q is an electron charge (=1.602 x 10^{-19} C), k is the Boltzmann's constant (= 1.381 x 10^{-23} J/K), T_c is the cell working temperature (K), n is an ideality factor (a number between 1 and 2 that typically increases as the current decreases), R_{sh} is shunt resistance of the cell (Ω) and R_s is a series resistance of the cell (Ω), $I_{o,ref}$ is the cell's short circuit current at temperature and solar radiation reference, E_G is the band gap energy of the semiconductor used in the cell (eV).

The single exponential, expressed by equation (13) is derived from the physics of the p-n junction, and is generally accepted to reflect the behaviour of the PV cell. For an ideal condition of solar cell, there is no series loss and no leakage to ground. In this case, R_s = 0 (very small) and R_{sh} = ∞ (very large), and with considering this assumption, the equation (13) can be rewritten as:

$$I = I_l - I_o \left[exp \frac{V}{\left(\frac{nkT_c}{q} \right)} - 1 \right]. \tag{14}$$

Equations (13), (14) can be used in computer simulation to obtain the output characteristics of PV cell, as shown in Fig. 2.12.

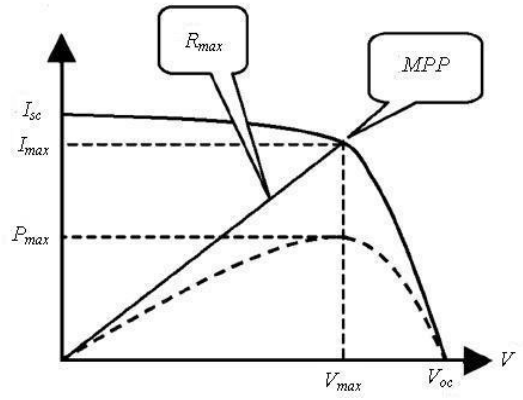

Fig. 2.12. *I-V-P* characteristics

This curve clearly shows that the output characteristics of a PV cell are non-linear and are crucially influenced by solar radiation G, operating cell temperature T_c and load condition R. Each curve has a maximum power point (*MPP*), at which the solar array operates most efficiently (Air Jiang et al., 2005).

The PV system characteristic present three important points: the short circuit current I_{sc}, the open circuit voltage V_{oc} and the optimum power P_{max} delivered by PV system to an optimum load R_{op} (or R_{max}) when the PV system operate at their MPP. Short circuit current (I_{sc}) is the maximum current, at $V = 0$. In the ideal condition, if $V = 0$, $I_{sc} = I_l$. Open circuit voltage (V_{oc}) is the maximum voltage, at $I = 0$. The power curves on Fig. 2.12 shows that the optimum power point corresponds to a load connected to the PV system that varies with the ambient conditions of irradiation and temperature. In practice this variable optimal load will be achieved through the use of a variable duty cycle of the control part of MPPT converter, which controls directly the operating voltage which corresponds to this optimal load.

The complete behavior of a single diode model PV cells is described by five model parameters (I_l, n, I_o, R_s, R_{sh}) which are representative of a physical PV cell/module. These five parameters of PV cell/module are in fact related to two environmental parameters i.e. solar insolation (irradiation) and temperature.

The photocurrent mainly depends on solar insolation and the cell's working temperature, which is described as (Tsai et al., 2008):

$$I_l = \frac{G}{G_{Ref}}\left[I_{l,ref} + \mu_i\left(T_c - T_{c,ref}\right)\right], \tag{15}$$

$$I_{l,ref} = I_{sc,ref}, \tag{16}$$

$$\mu_i = \frac{I_{sc} - I_{sc,ref}}{T_c - T_{c,ref}}, \tag{17}$$

where $I_{l,ref}$ is the cell's short-circuit current at a 25°C and 1000 W/m^2, μ_i is the cell's short-circuit current temperature coefficient (A/K), $T_{c,ref}$ is the cell's reference temperature (K), G is the solar irradiance (kW/m^2) and G_{ref} is the solar radiation under standard condition (kW/m^2).

There are a lot of correlations which can be used to predict the cell/module temperature, T_c. Based on Nominal Operating Cell Temperature (*NOCT*), T_c can be estimated as:

$$T_c = T_a + \frac{G}{G_{ref}}\left(NOCT - T_{a,ref}\right), \tag{18}$$

The temperature of the individual cells (actually, that of their p-n junctions) within a PV module, i.e. T_c, is the proper temperature to use in order to predict the electrical performance of the module. However, it may be higher by a few degrees from the back surfaces (back-side) temperature, T_b, and this difference depends mainly on the materials of the module substrate and on the intensity of the solar radiation flux. The relation between the two temperatures can be expressed by the simple linear expression (Skoplaki et al., 2008):

$$T_c = T_b + \frac{G_T}{G_{ref}} \Delta T_{G_{ref}} , \tag{19}$$

In which G_T is irradiance on module's tilted plane, G_{ref} is a reference solar radiation flux incident on the module (1000 W/m^2), and ΔT_{Gref} is the temperature difference between the PV cells and the module back side at this reference solar radiation flux.

Refers to equation (13) and Fig. 2.11, if we take account of R_s and consider R_{sh} is very large (∞), equation (13) can be written as:

$$I = I_l - I_o \left[exp\left(\frac{V + IR_s}{\frac{nkT_c}{q}} \right) - 1 \right]. \tag{20}$$

At $V = 0$, $I = I_l = I_{sc}$, and with definition above equation can be elaborated as follow:

$$\frac{I - I_{sc}}{I_o} = -\left[exp\left(\frac{V + IR_s}{\left(\frac{nkT_c}{q} \right)} \right) - 1 \right], \tag{21}$$

$$\frac{I_{sc} - I}{I_o} = \left[exp\left(\frac{V + IR_s}{\left(\frac{nkT_c}{q} \right)} \right) - 1 \right], \tag{22}$$

$$exp\left(\frac{V+IR_S}{\left(\frac{nkT_c}{q}\right)}\right)=\frac{I_{sc}-I}{I_o}+1, \tag{23}$$

$$\frac{V+IR_S}{\left(\frac{nkT_c}{q}\right)}=ln\left[\frac{I_{sc}-I+I_o}{I_o}\right], \tag{24}$$

$$V=-IR_S+\frac{nkT_c}{q}ln\left[\frac{I_{sc}-I-I_o}{I_o}\right]. \tag{25}$$

The production of electrical energy, E [kWh], is given by the integral:

$$E=\int_{\Delta t}Pdt=\int_{\Delta t}(IV)dt. \tag{26}$$

2.4.3. Model of PV module/panel/array

PV cells are grouped together in order to form PV modules/panel/array, which are combined in series and parallel to provide the desired output power. When the number of the cells in series is N_s and the number of cells in parallel is N_p, the relationship between the output current and voltage is given by:

$$I_{l,tot}=N_pI_l, \tag{27}$$

$$I_{o,tot}=N_pI_o, \tag{28}$$

$$n_{tot}=N_sn, \tag{29}$$

$$R_{s,tot}=\frac{N_s}{N_p}R_s, \tag{30}$$

$$I=N_pI_l-N_pI_o\left[exp\left(\frac{\left(V+I\frac{N_s}{N_p}R_s\right)}{N_s\left(\frac{nkT_c}{q}\right)}\right)-1\right]-\frac{V+I\frac{N_s}{N_p}R_s}{R_{sh}}, \tag{31}$$

$$I = N_p I_l - N_p I_o \left[exp\left(\frac{\left(\frac{V}{N_s} + \frac{IR_s}{N_p} \right)}{\left(\frac{nkT_c}{q} \right)} \right) - 1 \right] - \frac{\frac{N_p}{N_s} V + IR_s}{R_{sh}}. \quad (32)$$

For ideal condition, R_s is very small (R_s = 0) and R_{sh} is very large (R_{sh} = ∞), therefore:

$$I = N_p I_l - N_p I_o \left[exp\left(\frac{\left(\frac{V}{N_s} \right)}{\left(\frac{nkT_c}{q} \right)} \right) - 1 \right]. \quad (33)$$

Generally, the evaluation of PV module characteristics, such as in Fig. 2.12 can be summarized in Fig. 2.13 (Markvart, 1996).

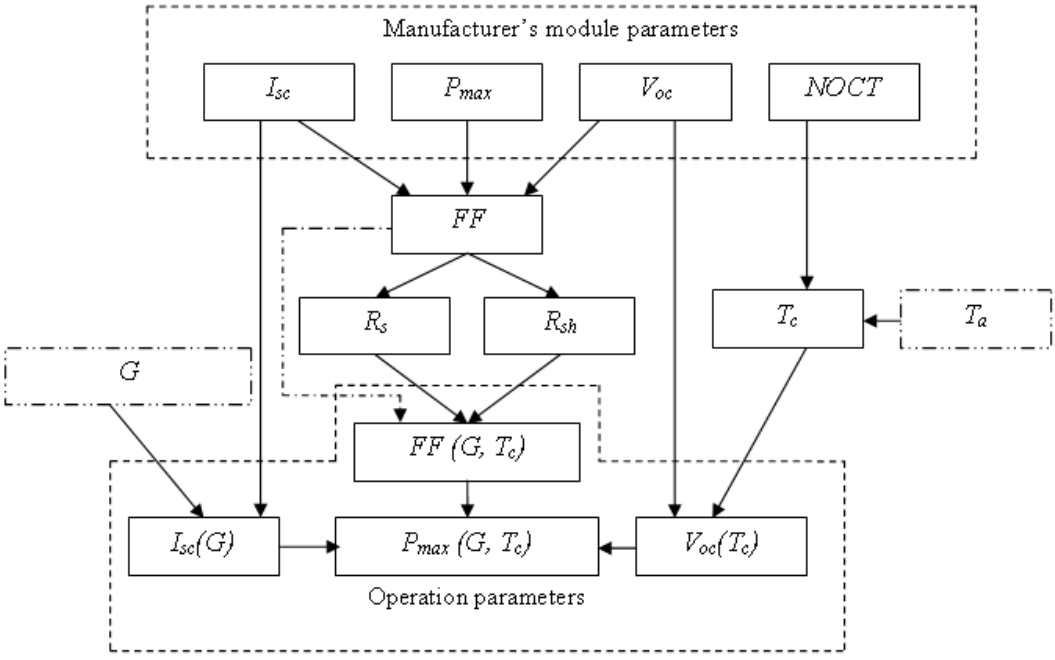

Fig. 2.13. Bridge parameters for evaluating of the PV module performances

It can be seen that there is an inter correlation of Manufacturer's module parameters and the real operation parameters, which influenced by ambient temperature (T_a) and irradiation (G) or respect to changes of environmental parameters.

Based on Fig. 2.13., it clears that a short circuit current (I_{sc}) is influenced greatly

by solar irradiance (G); an open circuit voltage (V_{oc}) is influenced greatly by the cell temperature (T_c); meanwhile the fill factor (FF) and max. power (P_{max}) are influenced by both of solar irradiation (G) and the cell temperature (T_c). It can be drawn also that climatic conditions (solar irradiance, G and ambient temperature, T_a) great affected on the whole operation parameters (mostly electrical) of PV module, which directly affected on PV module performance.

2.5. Thermodynamics of photovoltaic

Most of thermodynamic systems (included PV) possess energy, entropy, and exergy, and thus appear at the intersection of these three fields, such as shown in Fig. 2.14 (Dincer et al., 2001). The forms of energy can be expressed as enthalpy (h), internal energy (u), chemical energy (en_{ch}), work (w), heat (q), electricity (e), etc.

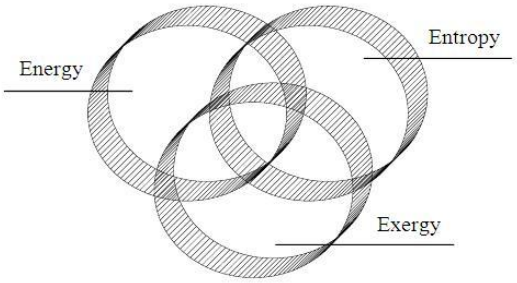

Fig. 2.14. Interactions between the domains of energy, entropy and exergy

The thermodynamic efficiency of PV system is a wide interest because the relevance of this parameter for energy conversion (efficiencies).

Energy analysis (energetic) is based on the First Law of Thermodynamics meanwhile exergy analysis (exergetic) is based on both the First and the Second Laws of Thermodynamics.

The energy balance is basic method to estimate of energy conversion processes. Exergy is defined as the maximum amount of work which can be produced by a system or a flow of matter or energy as it comes to equilibrium with a reference environment. In principle, four different types of exergy, ex, can be identified and are denoted, respectively, as kinetic (ex_k), potential (ex_p), physical (ex_{ph}) and chemical exergy (ex_{ch}). With this identification, the specific exergy (J/kg) of a flow of matter can be expressed as:

$$ex = ex_k + ex_p + ex_{ph} + ex_{ch} \,. \tag{34}$$

Kinetic and potential exergy have the same meaning as the corresponding energy terms, and generally these two term can be neglected for purposes of process analysis. For the exergy analysis, the characteristics of reference environment must be specified and commonly is done by specifying the

temperature, pressure and chemical composition of the reference environment. The exergy of a system is zero when it is in equilibrium with the reference environment. A different point of view between energy and exergy is shown in Fig. 2.15.

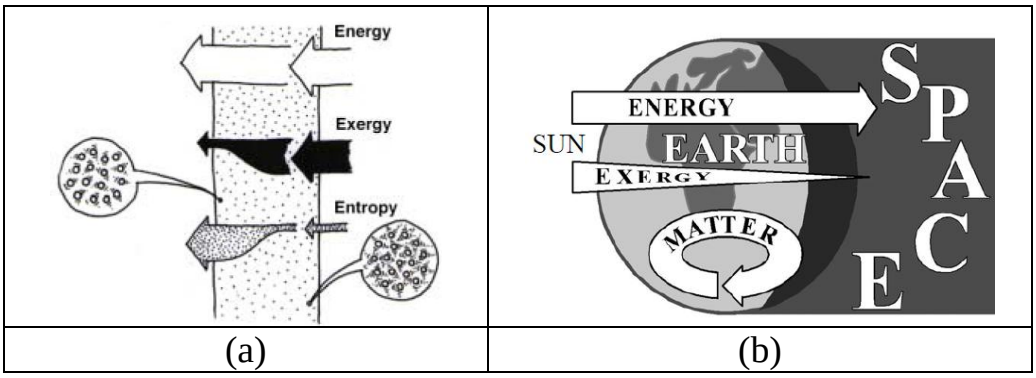

(a) (b)

Fig. 2.15. Energy, exergy, and entropy flow in and flow out a system (Shukuya, et al., 2002) and illustration energy and exergy from the sun (Wall, 2007)

Refers to Fig. 2.15 (a), the amounts of energy flowing in and out are the same under thermally steady-state condition according to the first law of thermodynamics (energy conservation); on the other hand, the amount of entropy flowing out is larger than flowing in according to the second law of thermodynamics (production of entropy). The amount of exergy flowing out is smaller than flowing in, since exergy is consumed within the system to produce entropy, due to irreversibility. Exergy deals with the quantity and quality of energy, while energy deals with the quantity only. Difference between analysis of energy and exergy can be seen in Table 2.3.

Table 2.3. Difference point of view analysis of energy and exergy

Energy analysis	Exergy analysis
1. Dependent on the parameters of matter or energy flow only, and independent of the environment parameters.	2. Dependent both on the parameters of matter or energy flow and on the environment parameters.
3. Guided by the First Law of Thermodynamic for all processes.	4. Guided by the First and Second Law of Thermodynamics for all irreversible processes.
5. Measure of quantity.	6. Measure both of quantity and quality.

For a steady state flow system, energy and exergy balances through a system can be expressed as (Sahin et al., 2007):

$$\sum_{in} en_{in}\dot{m}_{in} - \sum_{out} en_{out}\dot{m}_{out} + \sum \dot{Q} - \dot{W} = 0, \tag{35}$$

$$\sum_{in} ex_{in}\dot{m}_{in} - \sum_{out} ex_{out}\dot{m}_{out} + \sum \dot{E}x^{Q} - \dot{E}x^{W} - I_r = 0, \tag{36}$$

where $\dot{m}_{in}$ and $\dot{m}_{out}$ are mass flow rate input and output across system boundary (kg/m); ex_{in} and ex_{out} are specific exergy input and output, respectively (J/kg); $\dot{Q}$ is the heat transfer across system boundary (W); $\dot{E}x^{Q}$ is the exergy transfer associated with $\dot{Q}$ (W); $\dot{W}$ is the work (including shaft work, electricity, etc.) transferred out of the system (W); $\dot{E}x^{W}$ is the exergy transfer associated with $\dot{W}$ (W); and I_r is the system exergy consumption due to irreversibility during a process (W), and given by:

$$I_r = T_a S_{gen}, \tag{37}$$

where T_a is the ambient temperature (K) and S_{gen} is entropy generated by system (W/K).

The solar energy absorbed by the PV modules is converted to electric energy and also thermal energy. The thermal energy is dissipated to the ambient as a heat loss; by convection, conduction, and radiation. The rate of the heat transfer process depends on the design of the PV system. To achieve the efficiency of a PV cell/module/panel/array, its operating temperature (T_c) must be determined, and homogeneous assumption on the whole plate can be applied for simplicity.

The principle of a solar cell based on thermal energy point of view can be considered for an ideal simple situation in which the sun irradiates the flat surface of the solar cell on earth. The energy streams exchanged by the solar cell are schematically shown in Fig. 2.16.

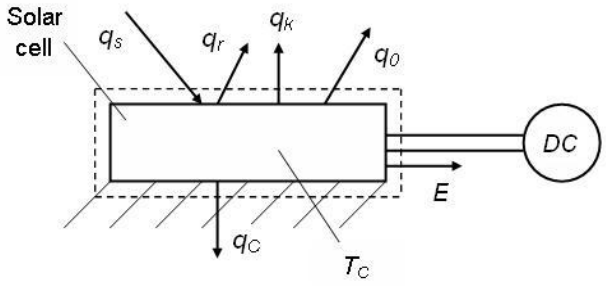

Fig. 2.16. Model description of solar cell in view of thermal energy

The representative temperature of the solar cell is T_c. Generally, the heat transferred (q_s) from the sun's surface at temperature T_s to the outer surface of the solar cell on the earth is distributed to the generated electrical energy (E), the

reflected solar radiation (q_r), the useful heat absorbed by the solar cell (q_c), and to the convection and radiation heat, q_k and q_o, respectively, both transferred to the environment (Petela, 2010).

The energy balance equation for the considered system can be written as follows:

$$q_s = q_r + q_k + q_o + q_c + E\,. \tag{38}$$

In case of energy, entropy and exergy transfer in a situation where the temperature of a reservoir, T_1, is reduced to T_2 across an interface (e.g. a wall), and where the external surrounding have a temperature T_0 is shown in Fig. 2.17. In compliance with the 1st Law of Thermodynamics, the transferred heat remains constant in quantity. The reduction in temperature across the boundary is however accompanied by an entropy generation, and the exergy content of the energy is reduced.

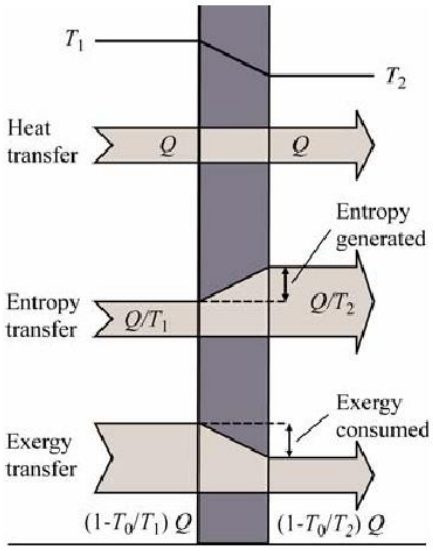

Fig. 2.17. Exergy is consumed (and entropy generated) when heat is transferred from a higher to lower temperature reservoir (Sandness, 2003)

The quantity of exergy can be used to assess and improve the efficiencies energy system, and can help better understand the losses in energy systems by providing more useful and meaningful information than energy provides (Rosen et al., 2009).

2.6. Energetic and exergetic analysis

2.6.1. Energy analysis of PV modules

For each point on the *I-V* curve such as in Fig. 2.12, the product of the current and voltage represents the power output for that operating condition, and

mathematically can be expressed as:

$$P = IV\,. \tag{39}$$

A solar cell can also be characterised by its maximum power point (*mpp*), when the product *V I,* reached the maximum value. The maximum power output of a cell is graphically given by the largest rectangle that can be fitted under the *I-V* curve.

$$P_{max} = P_{mpp} = V_{mp}\, I_{mp}\,. \tag{40}$$

FF is the ratio of the maximum power that can be delivered to the load and the product of I_{sc} (Short circuit current - the maximum current at zero voltage); and V_{oc} (Open circuit voltage - the maximum voltage, at zero current). Definition of I_{sc} and V_{oc} can be seen in Fig. 2.18:

$$FF = \frac{P_{max}}{V_{oc}\, I_{sc}} = \frac{V_{mp}\, I_{mp}}{V_{oc}\, I_{sc}}\,. \tag{41}$$

The fill factor is a measure of the real *I-V* characteristics (measure of cell quality). Its value is higher than 0.7 for good cells. *FF* diminishes as the cell temperature is increased. The production of electrical energy, *E* [kWh], is given by the integral, as described in equation (26).

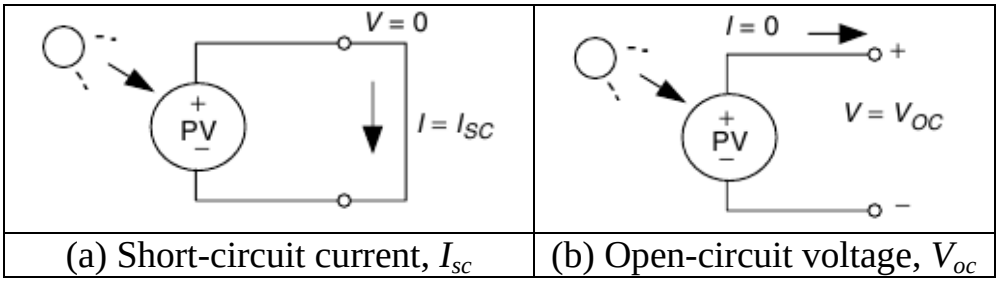

(a) Short-circuit current, I_{sc} (b) Open-circuit voltage, V_{oc}

Fig. 2. 18. Two important parameters in PV are the short-circuit current, I_{sc} and the open-circuit voltage, V_{oc} (Masters, 2004).

2.6.2. Exergy analysis of PV modules

Exergy is inversely related to entropy generation. Any given amount of energy consists of two parts; exergy, which represents the useful work potential, and the remaining fraction which under no circumstance can be converted to work, the anergy. Generally, it can be written as follow:

$$\text{Energy} = \text{Exergy} + \text{Anergy}. \tag{42}$$

Exergy analysis of PV model based on terminology fluxes energy and entropy, can be seen in Fig. 2.19. All in and outgoing fluxes in the thermodynamic balance equations for energy and entropy must be known. Radiation energy flux densities are denoted e (W.m^{-2}) , and entropy flux densities s (W/m^2.K). The arrows indicating the energy fluxes show the respective content of available energy (Labuhn et al., 2001).

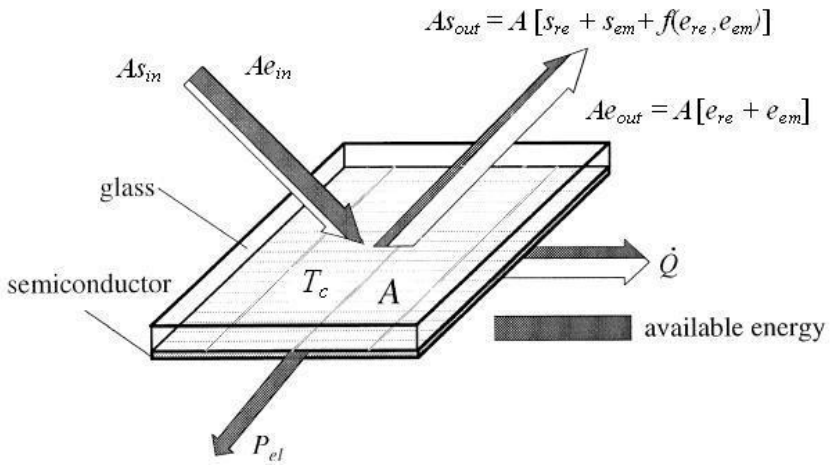

Fig. 2.19. Energy fluxes Model of solar cell I-V-P characteristics.

Based on Fig. 2.19, the electric power P_{el} (W) is calculated from the energy balance equation:

$$0 = A(e_{in} - e_{out}) - \dot{Q} - P_{el}\,, \tag{43}$$

and the entropy balance equation:

$$0 = A(s_{in} - s_{out}) - \frac{\dot{Q}}{T} + A\dot{s}_{ir}\,. \tag{44}$$

After elimination of the heat flux $\dot{Q}$, finally P_{el} can be determined as follow:

$$\frac{P_{el}}{A} = (e_{in} - e_{out}) + T(s_{out} - s_{in}) - T\dot{s}_{ir}\,. \tag{45}$$

The exergy consumption during a process is proportional to the entropy created due to irreversibilities associated with process. Exergy is a measure of the quality of energy which, in any real process, is not conserved but rather is in part destroyed or lost.

The illustration for concept of fluxes energy, such as reflection and emission can be seen in Fig. 2.20.

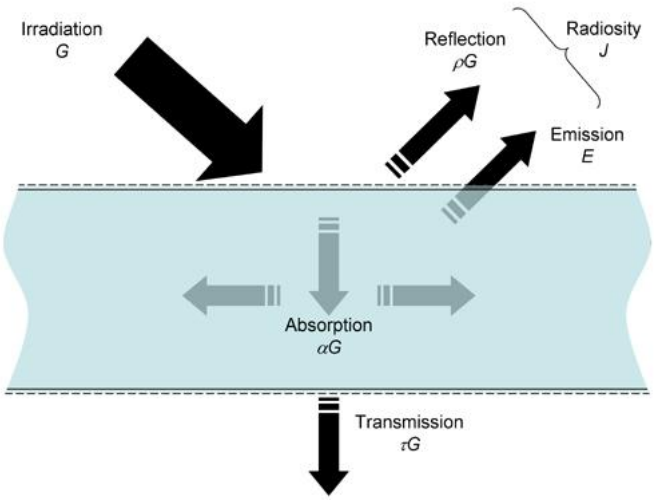

Fig. 2.20. Concepts of energy balance in semitransparent a medium.

The solar energy flux which reaches the terrestrial surface after passing through the atmosphere in the form of electromagnetic radiation is accompanied by an entropy flux. This entropy results, on the one hand, from the spatial divergence of the propagating electromagnetic wave and, on the other hand, from its wavelength dispersion. When incoming radiation energy is converted to electrical energy, as is the case in devices which employ the photovoltaic effect, the incoming entropy flux has to be conveyed to the environment, including the entropy produced within the device. This holds if a steady state condition is assumed. The energetic and exergetic energy conversion efficiencies depend decisively on the success of the entropy removal because an entropy flux always adheres to an energy flux which then is lost for the conversion output.

2.7. Feature of polycrystalline silicon and amorphous silicon

2.7.1. Performances of a-Si and pc-Si PV based on operational experienced

Based on information in section 2.1, it is obvious that presently two type of the PV module which frequently applied i.e. crystalline silicon and thin film. On the other hand, it is also clear that efficiency of thin film technology (2^{nd} generation) is lower than wafer based crystalline silicon (1^{st} generation). Nevertheles, one of main driving forces for thin film solar cell development was and still is the potential reduction of manufacturing cost, due to low material consumption in comparison to state of the art silicon wafer technology (Waldau, 2004).

An additional issue is the lower energy consumption for the production of thin film solar cells and consequently a shorter energy pay back time for these devices. However, one should bear in mind that the total energy payback time for a given module does not only depend on the solar cell used, but also on the module design, e.g. framed module, glass/glass, metal foil, EVA, etc.

In other side, Although the energy conversion efficiency of amorphous modules is lower than that of single-crystal units (an average of 6-7% compared to an average of 12-16%), as amorphous silicon thin film solar PV cells have more favorable temperature dependence compared to their mono-/polycrystalline counterparts, they work better in diffuse or low intensity light conditions and their yearly generated energy yield – under real life conditions – compared to their nominal power is higher as well (www.greensolar.hu/sites/default/files/EuropeanEnergyInnovation-GreenSolar .pdf, 2012).

A comparison about energy production between pc-Si and a-Si can be seen in the following Fig. 2.21.

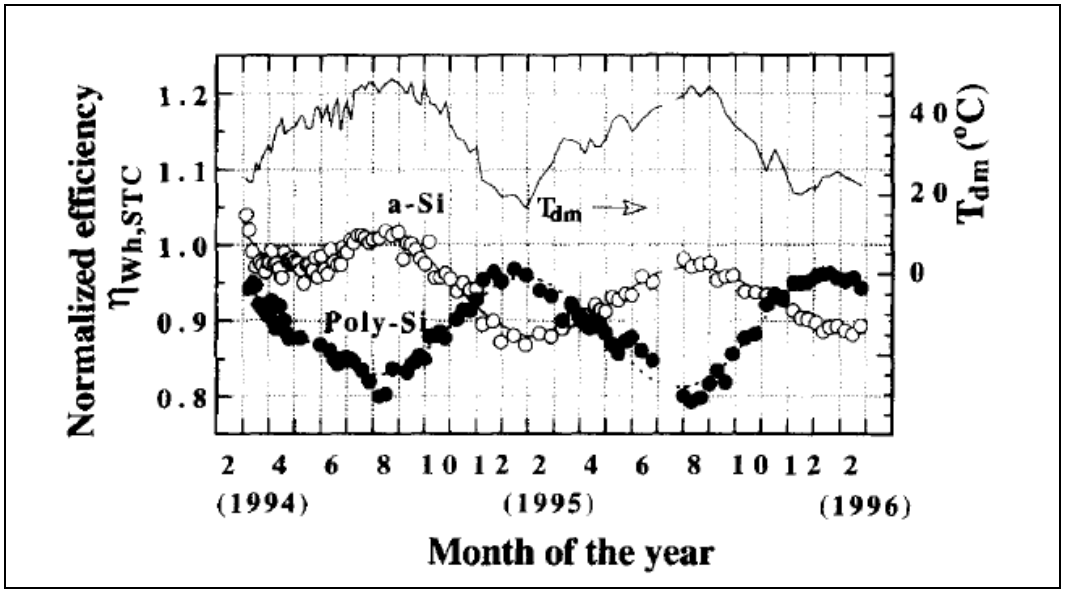

Fig. 2.21. The outdoor performance of pc-Si and a-Si in Japan weather's

Characteristis in Fig. 2.21 is resulted by Akhmad et al. In 1996 (published in 1997). They have performed experimental in order to compare the performance of two modules based on a-Si of p-i-n single junction and pc-Si during 2 years (March 1994 to February 1996), in Japan weather's. They showed the PV performance characteristics in form of normalized efficiency ($\eta_{wh,STC}$) versus time.

The PV module output parameters we have evaluated in our outdoor measurements are the normalized daily watt-hour efficiency ($\eta_{wh,STC}$) and normalized daily integrated output power ($P_{wh,\mathrm{STC}}$). Both performance parameters and other one parameter of daily average module temperature (T_{dm}) are defined as:

$$\eta_{wh,STC} = \frac{\eta_{wh}}{\eta_{STC}}, \tag{46}$$

$$\eta_{wh} = \frac{\sum_{i=1}^{N} P_{m,i} \Delta t}{\sum_{i=1}^{N} I_i \Delta t A} x100\%, \tag{47}$$

$$T_{dm} = \sum_{i=1}^{N} \frac{T_{bsm,i}}{N}. \tag{48}$$

They concluded that the annual average of η_{wh} of the a-Si module is about 95% and 92.5% of its efficiency at STC condition at the first and second year, respectively, while the values are nearly unchanged at about 89% for the poly-Si module. The manufacture specification of both PV module at STC condition can be seen in Table 2.4.

Table 2.4. Specification of a-Si and pc-Si modules at STC condition

Module	V_{oc} (V)	I_{sc} (A)	V_{mp} (V)	I_{mp} (A)	P_{mp} (W)	η (%)	A (m^2)
pc-Si	21.2	3.25	16.9	3.02	51	11.6	0.4383
a-Si	25.5	2.06	17.9	1.72	30.8	5.9	0.5224

Other case regarding to comparison about a-Si and pc-Si can be seen in Figs 2.22-23. These data is resulted from the installation test of PV field in Bulgaria (www.greensolar.hu/sites/default/files/EuropeanEnergyInnovation-GreenSolar .pdf, 2012). The monitored have been performed for 5 month. The modules were mounted under a fixed tilt angle optimal for annual average production. The total capacity was about 1.7 kWp for both types of modules connected to the same type of inverters under similar dc condition.

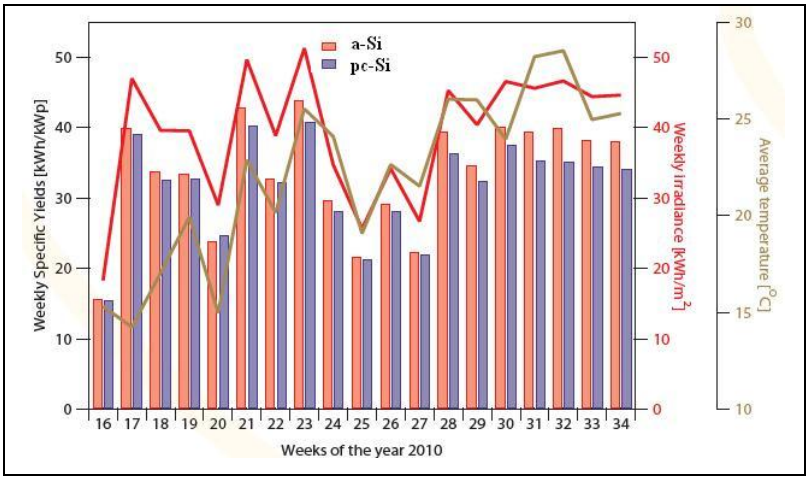

Fig. 2.22. Comparison of specific yield of a-Si and pc-Si PV modules

Based on Fig. 2.22, in average, specific yields energy of a-Si PV modules 6% higher than pc-Si PV modules.

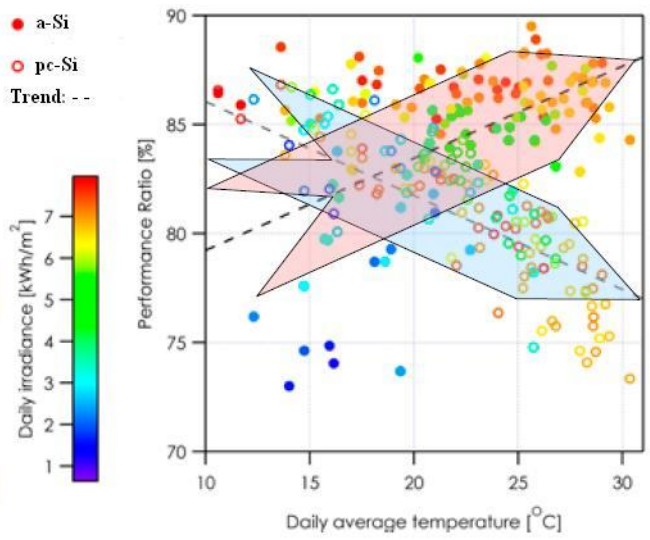

Fig. 2.23. Trend of performance ratio of a-Si and pc-Si PV modules

Based on Fig. 2.23, it is seen that a-Si PV modules may perform some 10-15% better under high irradiance (> 5 kWh/m2.day) and high average temperature (> 23^{o} C) conditions than the pc-Si PV modules.

2.7.2. General feature of crystalline silicon and thin film

The major types of PV materials are crystalline and thin films, which vary from each other in terms of light absorption efficiency, energy conversion efficiency, manufacturing technology and cost production.

Physically, difference of crystalline silicon and thin film, in view of matrial thickness can be seen in Fig. 2.24.

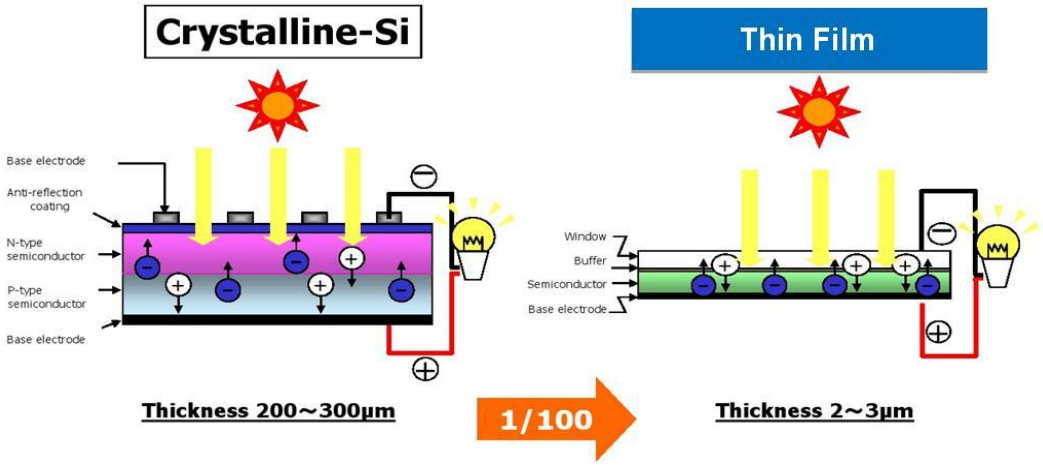

Fig.2.24. Different thickness of crystalline silicon and thin film PV modules

In atomic level, amorphous silicon (a-Si) differs from crystalline silicon in that the silicon atoms are not located at very precise distances from each other and the angles between the Si-Si bonds do not have a unique value.

The arrangement of silicon atoms in monocrystalline (mc-Si) cell is regular, and its transfer efficiency is comparatively high. The theoretical transfer efficiency of mc-Si cell is 15% to 18%, and 12-16% for mc-Si modules. Polycrystalline silicon (pc-Si) has advantage of low cost but disadvantage of less efficiency. The transfer efficiency of pc-Si module is about 10-14%. The arrangement of amorphous silicon (a-Si) is irregular, and the transfer efficiency of amorphous solar module is only 6-9% (Yu et al., 2008).

Based on Fig. 2.3 (see chapter 2), it's clear that improving of PV cell efficiencies, while holding down the cost per cell is one of the most important tasks of the PV industry today.

Practically, the current efficiencies of different commercial PV modules, is shown in Table 2.5 (International energy agencies, 2010).

Table 2.5. Current efficiencies of different PV technology commercial modules

Wafer based c-Si		Thin film		
sc-Si	pc-Si	a-Si; a-Si/μc-Si	CdTe	CIS/CIGS
14-20%	13-15%	6-9%	9-11%	10-12%

In Table 2.6. other general features of commercial wafer based crystalline silicon and thin film are presented (www.greenrhinoenergy.com).

Table 2.6. Current efficiencies of different PV technology commercial modules

No.	General features	Wafer based crystalline silicon	Thin film
1	Voltage rating (*Vmp*/ *Voc*)	80%-85%	72%-78%
2	*I-V* curve fill factor (*FF*)	73%-82%	60%-68%
3	Temperature coefficients	Higher	Lower
4	Radiation components: direct (beam) or diffuse	Direct light preferred, but diffuse light can be used as well.	Both direct and diffuse light
5	Module construction	With anodized aluminum and need to be mounted in a rigid frame	Frameless, sandwiched between glass; lower cost, lower weight

Higher of voltage rating is better for the PV module and the low temperature coefficients more suitable for the location with high ambient temperature.

2.8. Single and multi junctions of module structures

Both of PV module which used in this research is single junction type. As mentioned in section 2.1., one of method which can be used to increase the power conversion efficiency of PV system is tandem (multi-junction) solar cells.

Multi-junction solar cells or tandem cells are solar cells containing several p-n junctions. The different structures of the cells are intended to absorb different wavelengths of sunlight. By this way, as can be seen in Fig. 2.25, the entire light spectrum is used and the efficiency of the thin-film module will be increased.

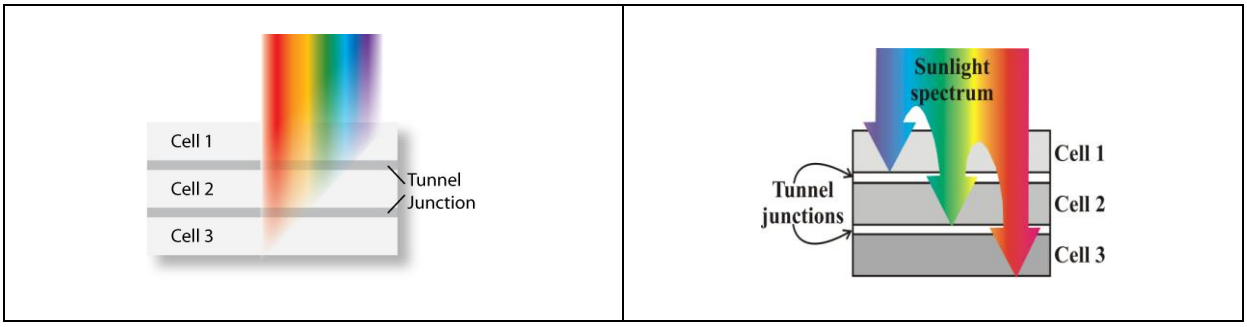

Fig. 2.25. Multi-junction concept (Walukiewicz, 2012)

In concept multi junction solar cell structure, the first cell convert the mainly shorter wavelength part (higher energy) of the spectrum of the incident light while the second cell and thee next cell converts the longer wavelength part (lower energy).

Absorption PV cell material in the range of spectrum solar radiation can be seen in Fig. 2.26 (Hahn-Meitner, 2012).

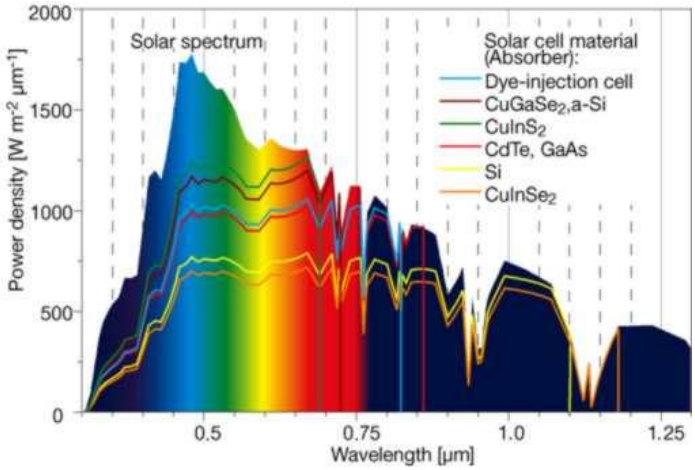

Fig. 2.26. Solar cell materials and solar radiation spectrum

Amorphous silicon has a higher bandgap (1.7 eV) than crystalline silicon (c-Si) (1.1 eV), which means it absorbs the visible part of the solar spectrum more strongly than the infrared portion of the spectrum.

As μc-Si has about the same bandgap as c-Si, the μc-Si and a-Si can advantageously be combined in thin layers, creating a layered cell called a tandem cell (multi-junction cell). The top cell in a-Si absorbs the visible light and leaves the infrared part of the spectrum for the bottom cell in μc-Si.

10.14751/SZIE.2013.026

3. MATERIAL AND METHODS

In this research, energy and exergy evaluation of two PV module technologies (from the first and second generation), as component of PV array system, will be performed, refers to installation of 10 kWp grid-connected PV array system at Szent István University, Gödöllő – Hungary.

The system description and the method of PV analysis in view of energy and exergy, as bases for evaluation, are presented in this chapter.

3.1. System description

The grid-connected PV array systems at Szent István University were installed on the flat roof of Dormitory building and are structured into 3 sub-systems. Sub-system 1 consists of 32 pieces of ASE-100 type modules (RWE Solar GmbH) from polycrystalline PV technology, and sub-system 2 and 3 consists of 77 pieces of DS-40 type of modules (Dunasolar Ltd.) from amorphous silicon PV technology, respectively. The total power of the system is 9.6 kWp with the total PV surface area 150 m^2. Every sub-system uses a separate inverter (Sun power SP3100-600 for sub-system 1 and SP2800-550 for others sub-system), that will convert the production of DC electrical energy to the 230 V AC, 50 Hz electrical grid (Farkas et al., 2008). The schematic installation of grid-connected PV array at Szent István University can be seen in Fig. 3.1., and the PV surface orientation can be seen in Fig. 3.2.

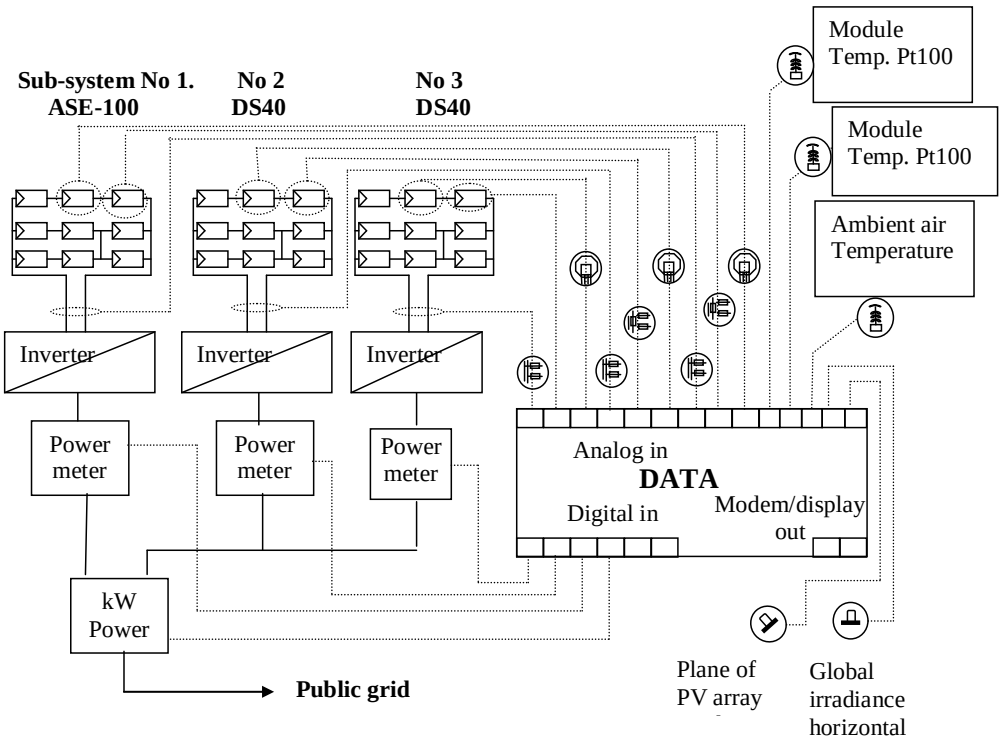

Fig. 3.1. The schematic diagrams of a 10 kWp grid-connected PV array at SZIU

The surface orientation for this system are 30° for tilt angle (β) and 5° to East (-5°) for azimuth angle (γ), for South facing.

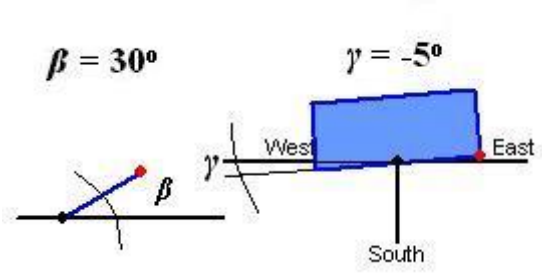

Fig. 3.2. Actual surface orientation of 10 kWp grid-connected PV array system at SZIU

A two different of PV module technology, as a components of grid-connected PV array system installed at SZIU, is shown in Fig. 3.3.

	
(a) ASE-100 Polycrystalline silicon (pc-Si)	(b) DS-40 Amorphous silicon (a-Si)

Fig. 3.3. Physical different of PV module technologies

The electrical parameters under Standard Test Conditions (STC), such as (short circuit current); (open circuit voltage); (current at maximum power point); (voltage at maximum power point) are provided by manufacturer sheets and shown in Table 3.1.

A PC based data logging systems is installed in order to get real measurement data. The following parameters are measured by the data logging system:

- irradiance (in the panel plane by a silicon reference sensor, and the global irradiation by a pyranometer),
- temperature (environmental/ambient and module temperatures for each type, measured by Pt100 sensors),
- PV array (DC) voltage, current and power,
- AC voltage, current and power supplied to the electrical grid.

The connection of the analog input channels with the description of the measured parameters is shown in Fig. 3.4.

Table 3.1. PV modules specifications in SZIU grid-connected PV array system

Module parameters	Sub-sys. 1 ASE-100	Sub-sys. 2 DS-40	Sub-sys. 3 DS-40
Electrical Module *			
Typical peak power (W)	105	40	40
Voltage at peak power (V)	35	44.8	44.8
Current at peak power (A)	3	0.8	0.8
Short circuit current (A)	3.3	1.15	1.15
Open circuit voltage (A)	42.6	62.2	62.2
Temperature coefficient of open circuit voltage (%/^{o}C)	-0.38	-0.2797	-0.2797
Temperature coefficient of short circuit current (%/^{o}C)	0.10	0.0897	0.0897
Approximate effect of temp. on power (%/^{o}C)	-0.47	-0.190	-0.190
Nominal operating cell temperature, NOCT (^{o}C)	45	50	50
Others			
Active surface area (m^{2})	0.83	0.79	0.79
Specific heat capacity (J/kg K)	920	920	920
Absorption coefficient (%)	70	70	70
Weight (kg)	8.5	13.5	13.5
Array			
No. of modules in series (per string)	16	7	7
No. of strings in parallel (per inverter)	2	11	11
Total module area (m^{2})	27	61	61

* Under Standard Test Conditions (G = 1000 W/m^{2}, AM = 1.5 and Tc = 25^{o}C).

As the data logger computer are relatively far from the measurement point (inverter room and sensor connection boxes), signal converters were installed to the system to serve as an amplifier. The signal converters (ISC – isolated signal converter) converts all different output signals of the sensors (e.g. different voltage levels) to 4-20 mA signal, what is sent to the AD converter unit of the data logger PC. The signal converter modules can be seen in Fig. 3.5 (Seres et al., 2007).

As an example the electrical connection plan of the irradiation measurement in the module plain can be seen in Fig. 3.6. Such connection plans are developed for every used sensor.

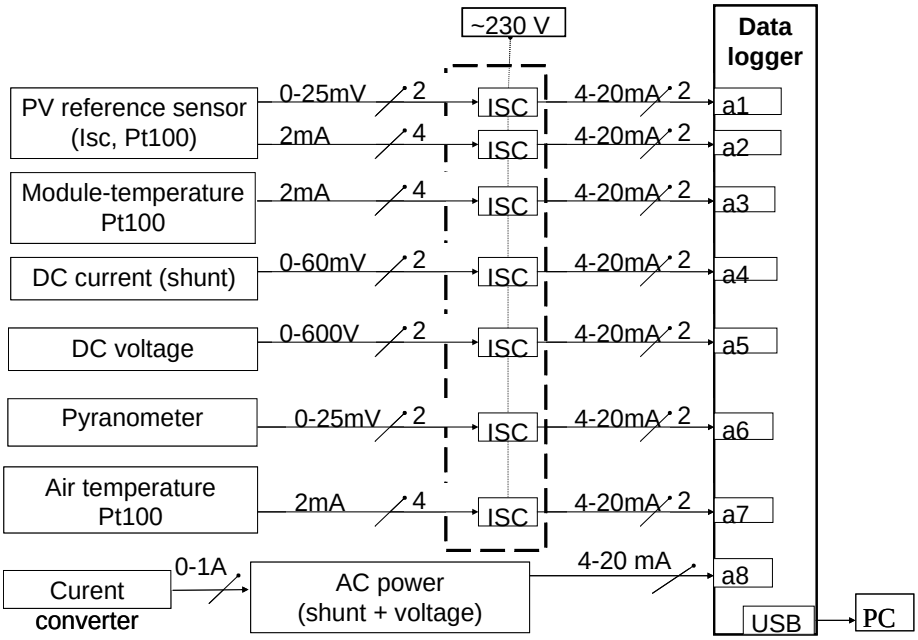

Fig. 3.4. The analog input quantities of the data logger system

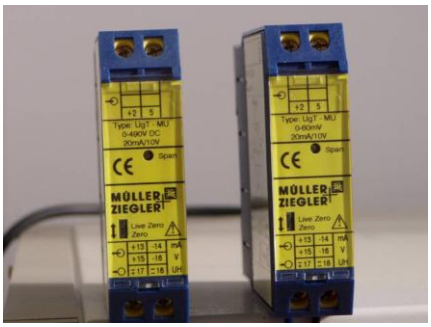

Fig. 3.5. Signal converter modules

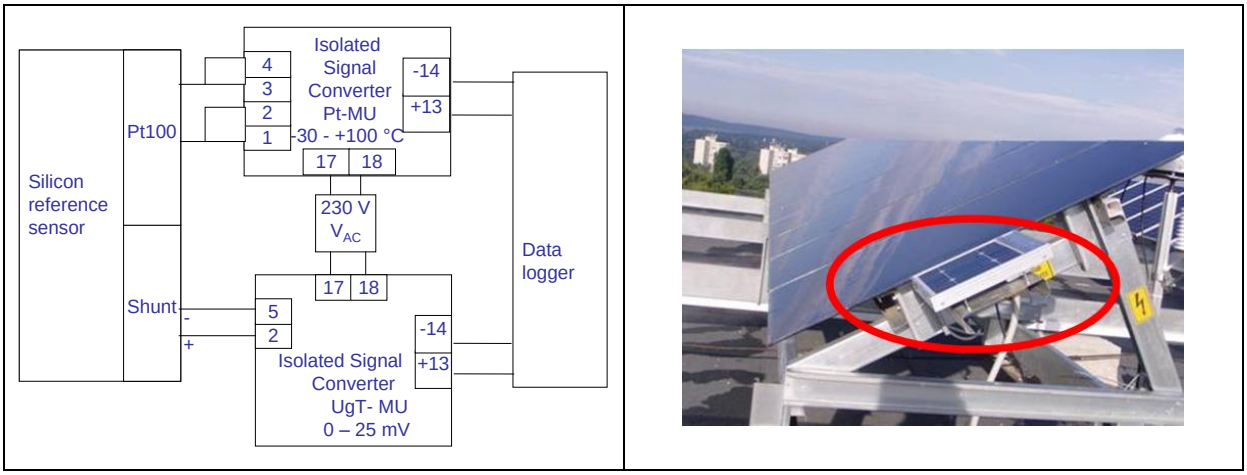

Fig. 3.6. The electrical connection and the realization of the irradiation measurement by a silicon reference sensor

The data logger runs every day from 4 am to 11 pm and measures continuously the mentioned variables. The measuring frequency is not fixed, it depends on the

measured signal, but it is below 1 second. Not all these data are recorded, the software calculates 10 minutes average values from the measured data and these averages are recorded to the hard drive of the PC. In Fig. 3.7, a screenshot of the data logger is presented during the energy collection.

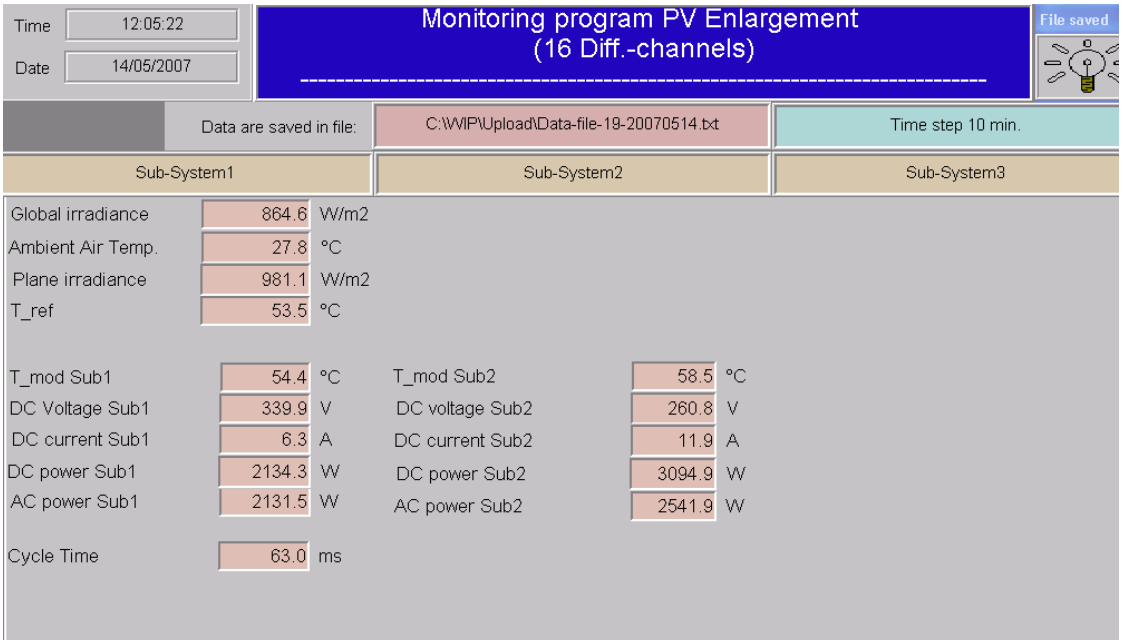

Fig. 3.7. Screenshot of the data logger PC during data acquisition process

Beside the installed own designed data logger, an authorized two way electrical meter was installed as a control unit for the energy data.

3.2. Evaluation of electric production of the PV array system in a macro views

In macro point of view, an electric production of PV power plant can be evaluated through the following mathematical model (Benard, 2006):

$$\dot{W}_{elec} = \eta_{pv} A_{pv} E_{arr}, \tag{49}$$

where:

η_{pv} : conversion efficiency of the photovoltaic cell,
A_{pv} : surface area of the PV collector (m^2),
E_{arr} : incident solar irradiation (insolation) ($kwh/m^2/day$).

The effeciency of the PV cell is given by:

$$\eta_{pv} = \eta_o \left[1 - \mu_t |T_o - T_c|\right], \tag{50}$$

$$T_c = T_{amb} + C_f \left(218 + 823\overline{K}_t\right)\frac{NOCT - 20}{800}\ , \tag{51}$$

where:

η_{pv}	:	conversion efficiency of the photovoltaic cell at the reference temperature,
T_o	:	reference temperature, 25°C,
μ_t	:	temperature coefficient of the PV cell ($^oC^{-1}$),
T_c	:	average PV cell temperature,
$\overline{K}_t$	:	monthly clearness index (comes from weather data),
$NOCT$	:	Nominal Operating Cell Temperature,
C_f	:	Tilt correction factor.

$$C_f = 1 - (1.17 \times 10^{-4})\,(\beta_M - \beta)^2, \tag{52}$$

where β_M is the optimum tilt angle and β is the actual tilt angle, both expressed in degrees.

$$\beta_M = Latitude - \delta, \tag{53}$$

where δ is solar declination, as can be seen in Fig. 3.8.

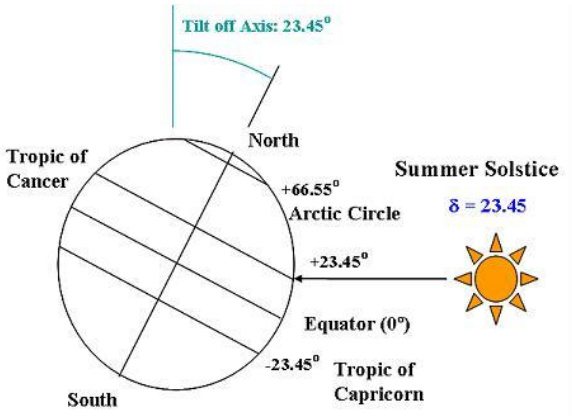

Declination (°)	Approximate dates
+23.45	June 22
+20	May 21, July 24
+15	May 1, Aug 12
+10	Apr 16, Aug 28
+5	Apr 3, Sept 10
0	Mar 21, Sept 23
−5	Mar 8, Oct 6
−10	Feb 23, Oct 20
−15	Feb 9, Nov 3
−20	Jan 21, Nov 22
−23.45	Dec 22

Fig. 3.8. Solar declination (www.geog.ucsb.edu/ideas/Insolation.html, 2012)

Solar Declination (δ) changes seasonally, and is calculated by the day of year using the following equation:

$$\delta = 23.45\frac{\pi}{180}\,sin\left(2\pi\left(\frac{284 + n}{365}\right)\right), \tag{54}$$

where *n* is the day number counted from January first throught the year (1-365).

The constants of η_o, *NOCT* and μ_t for the above equations are available in the Table 3.2 for several different types of PV cell technologies.

Table 3.2. PV Module characteristics for standard technologies

PV Module Type	η_o (%)	NOCT (^{o}C)	C_{OTPV} (%/^{o}C)
Mono-Si (mc-Si)	13.0	45	0.40
Poly-Si (pc-Si)	11.0	45	0.40
a-Si	5.0	50	0.11
CdTe	7.0	46	0.24
CIS	7.5	47	0.46

The production of electric energy of 10 kWp grid-connected PV array system as a function of tilt angle will be simulated using two commercial simulation software packages, i.e RETScreen V 3.2 and NSoL V4.4. Furthermore, prediction of the production energy of PV array using mathematical model approach as mentioned before will be performed.

The following data is required, as input parameters for simulation of PV array with software packages:

- location parameter (latitude, longitude)
- array parameter (tilt and azimuth angle)
- PV parameter (nominal power, number of module, V_{OC}, I_{SC}, etc.)
- inverter parameter (input/output voltage and nominal power, etc.)

The feature of data entry NSoL V4.4 sofware packages, as tools for evaluation and analysis can be seen in Figs 3.9-11.

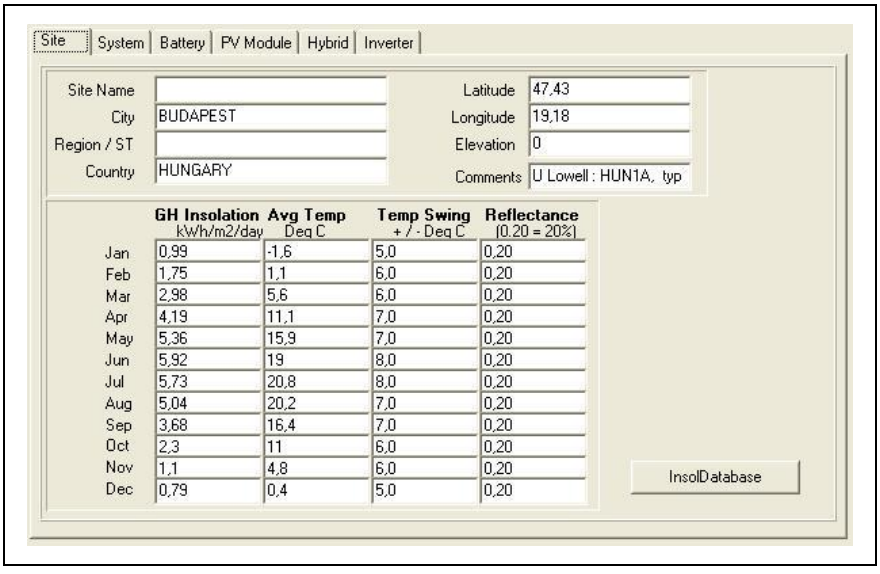

Fig.3.9. Input site location

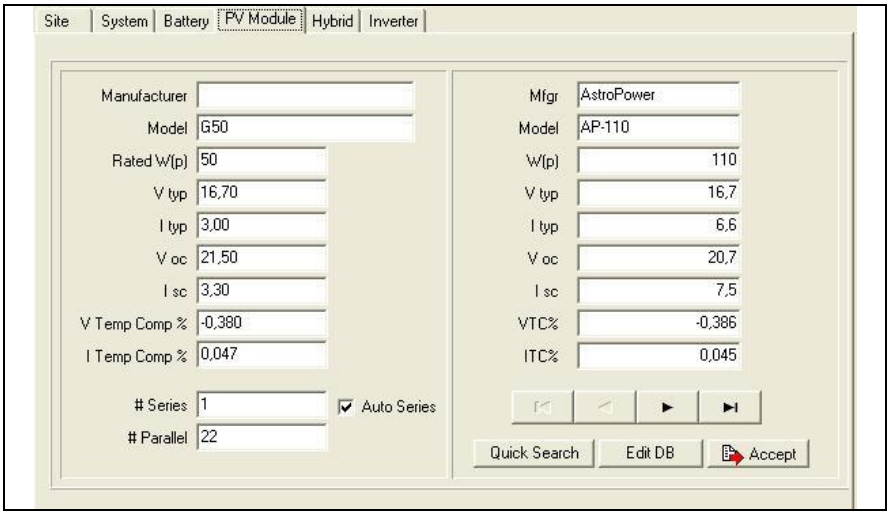

Fig.3.10. Input PV module

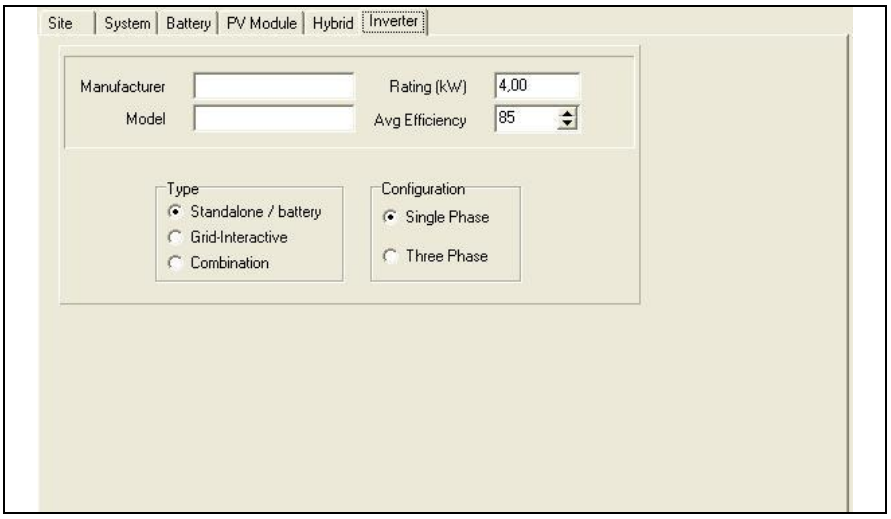

Fig.3.11. Input inverter

3.3. PV modules performances based on energy and exergy

The energy of a PV system depends on two major components namely electrical energy and thermal energy. While the electricity is generated by photovoltaic effect, the PV cells also get heated due to the thermal energy present in the solar radiation. The electricity generated by a photovoltaic system is also termed as the electrical exergy, as it is the available energy that can completely be utilized in useful purpose (Joshi et al., 2009).

The energy efficiency of a PV system can be defined as the ratio of the output energy of the system to the input energy received on the photovoltaic surface, and can be expressed as:

$$\eta_{en} = \frac{\dot{E}n_{out}}{\dot{E}n_{in}} = \frac{\dot{E}n_{electrical} + \dot{E}n_{thermal}}{\dot{E}n_{in}} = \frac{(V_{oc} I_{sc}) + \dot{Q}}{GA}. \quad (55)$$

Since the thermal energy available on the photovoltaic surface is not utilized for useful purpose, furthermore this energy called as heat loss to the ambient, and equation (55) can be rewritten as:

$$\eta_{en} = \frac{(V_{oc} I_{sc})}{GA}. \quad (56)$$

However, the above definition is restricted to theoretical cases only, and furthermore equation (56) is called as the maximum (theoretical) electrical efficiency (η_{max}). Other definition related to energy efficiency is efficiency of power conversion (η_{pc}) and in practice this efficiency is more applicable. The power conversion efficiency (η_{pc}) can be defined as:

$$\eta_{pc} = \frac{\dot{E}_{elec.}}{G A} = \frac{V_{mp} I_{mp}}{G A} = \frac{FF V_{oc} I_{sc}}{G A}, \quad (57)$$

$$\eta_{pc} = \frac{\dot{E}_{elec.}}{G A} = \frac{V I}{G A}. \quad (58)$$

This efficiency is also called electrical efficiency.

The exergy consumption during a process is proportional to the entropy created due to irreversibilities associated with process. Exergy is a measure of the quality of energy which, in any real process, is not conserved but rather is in part destroyed or lost.

The exergy efficiency of a system in general can be given as:

$$\eta_{ex} = \frac{\dot{E}x_{out}}{\dot{E}x_{in}} = \frac{\dot{E}x_{electrical} + \dot{E}x_{thermal} + \dot{E}x_{dest.}}{\dot{E}x_{solar}} = \frac{\dot{E}x_{electrical} + I_r}{\dot{E}x_{solar}}. \quad (59)$$

Exergy consumption (I_r) included both internal and external losses. Internal losses are electrical exergy destruction ($\dot{E}x_{dest,electrical}$) and external losses are heat losses ($\dot{E}x_{dest,thermal}$), which is numerically equal to $\dot{E}x_{thermal}$ for PV system (Joshi et al., 2009).

$$I_r = \sum Ex_{dest.} = \dot{E}x_{dest.thermal} + \dot{E}x_{dest.electrical}. \quad (60)$$

Referring to eq. (59), electrical exergy can be estimated as:

$$\dot{E}x_{electrical} = \dot{E}n_{electrical} - I_r = (V_{oc}\, I_{sc}) - \left((V_{oc}\, I_{sc}) - (V_{mp}\, I_{mp})\right),$$
$$\dot{E}x_{electrical} = V_{mp}\, I_{mp}, \tag{61}$$

while thermal exergy ($\dot{E}x_{thermal}$) can be calculated as:

$$\dot{E}x_{thermal} = \left(1 - \left(\frac{T_a}{T_c}\right)\right)\dot{Q}, \tag{62}$$

$$\dot{Q} = h_{ca}\, A(T_c - T_a), \tag{63}$$

$$h_{ca} = 5.7 + (3.8v), \tag{64}$$

$$T_c = T_a + \frac{G}{G_{ref}}(NOCT - T_{a,ref}), \tag{65}$$

where G_{ref} is solar irradiance reference, *NOCT* (Nominal operating cell temperature), A is PV surface area (m^2), h_{ca} is the convective (and radiative) heat transfer coefficient from photovoltaic cell to ambient (W/m^2K), v is wind velocity (m/s)and $\dot{Q}$ is heat transfer across the boundary.

By considering equations (59)–(65), a general formula for the exergy of a PV system can be defined as:

$$\dot{E}x_{out} = \dot{E}x_{pv} = V_{mp} I_{mp} - \left(1 - \frac{T_a}{T_c}\right)\left[(5.7 + (3.8v))A(T_c - T_a)\right]. \tag{66}$$

In a solar PV system, only electrical exergy is considered as the exergy of the system. A negative sign shows that the thermal part is a heat loss to the ambient and it is going to waste, any way.

To evaluate an exergy efficiency of PV system, the information about exergy of the total solar irradiation, is needed. The exergy of solar irradiance, $\dot{E}x_{solar}$ can be evaluated as (Santarelli et al., 2004 and Joshi et al., 2009):

$$\dot{E}x_{in} = \dot{E}x_{solar} = \left(1 - \frac{T_a}{T_s}\right) G\, A. \tag{67}$$

Other formula to evaluate the exergy of solar irradiance is given by Petela's formula (2003) as:

$$\dot{E}x_{solar} = G\,A\left(1-\frac{4}{3}\frac{T_a}{T_s}+\frac{1}{3}\left(\frac{T_a}{T_s}\right)^4\right), \tag{68}$$

where T_s is the Sun's temperature [K] (≈ 5777 K)

Referring to Eq (59) and Eqs (67-68), the exergy efficiency for the PV system can be given as:

$$\eta_{ex} = \frac{V_{mp}\,I_{mp} - \left(1-\left(\frac{T_a}{T_c}\right)\right)\left[\left(5.7+\left(3.8v\right)\right)A\left(T_c-T_a\right)\right]}{\left(1-\left(\frac{T_a}{T_s}\right)\right)G\,A}. \tag{69}$$

3.4. Theoretical exergetic assessment of PV performance

Exergetic performance of PV modules can be performed by (Joshi et al., 2009):

1. thermodynamic approach for solar energy,
2. photonic energy (chemical potential) from the sun" models.

Climates data for theoretical analysis is taken from PV*SOL 3.0 software packages, which acquires data from MeteoSyn, Meteonorm, PVGIS, NASA SSE, SWERA (Klise et al., 2009). The feature of PV*SOL 3.0 can be seen in Fig. 3.12.

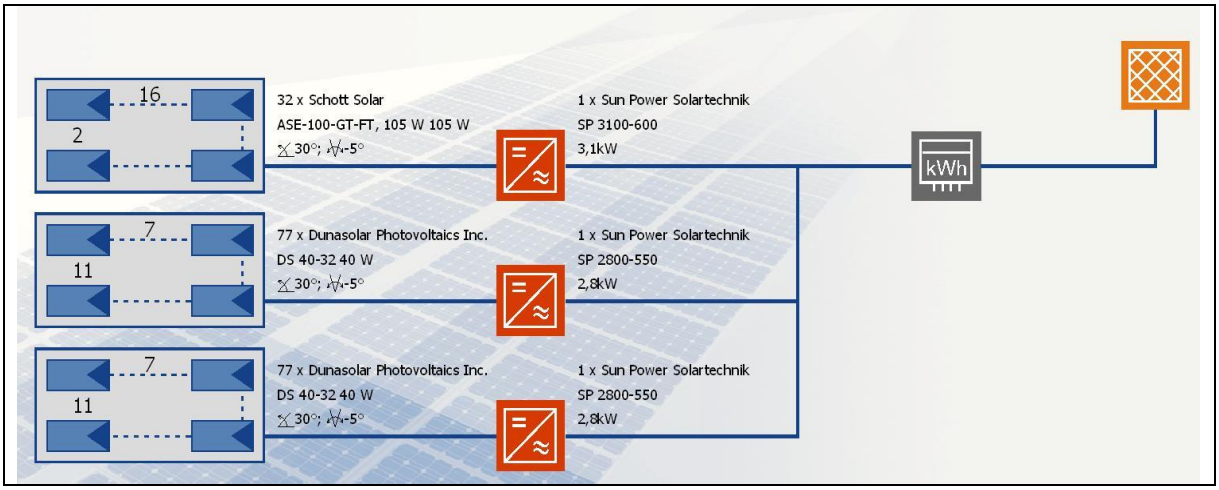

Fig. 3.12. Main feature of PV*SOL

3.4.1. Exergetic PV assessment by thermodynamic approach

Exergetic performance of photovoltaic by thermodynamic approach indirectly has introduced in section 3.3, meanwhile other method will be elaborated in

section 3.4.2. The set of equations as described in section 3.3, can be applied in order to evaluate the exergetic performances of PV modules based on thermodynamic approach for solar energy.

3.4.2. Exergetic PV assessment by photonic energy method

All matter regardless of its state or composition continuously emits electromagnetic (EM) radiation. The sun is the major source of the earth's energy. It emits a spectrum of energy that travels across space as electromagnetic radiation. Radiation can be viewed either as the transportation of tiny particles called photons or quanta; or as the propagation of EM waves. This so-called wave-particle duality, is very convenient in describing EM behavior (Clemente, 2005).

The EM spectrum, depicted in Fig. 3.13 can be thought as a map containing all types of EM radiation. The most energetic forms are located at the short wavelength end of the spectrum, left part of Fig. 3.13 (http://www.healthycanadians.gc.ca/environment-environnement/sun-soleil/radiation-rayonnement-eng.php), between 10^{-14} and 10^{-8} m. Gamma (γ) Rays and X-Rays are widely used in medicine, security and nondestructive testing. On the other hand, wavelengths ranging from 1 mm to several hundred meters, right part of Fig. 3.13, are transparent to the atmosphere, so they are mostly used for data transmission, *e.g.* radio, TV, mobile phones, etc. Many other kinds of waves used in numerous applications are enclosed between these two extremes.

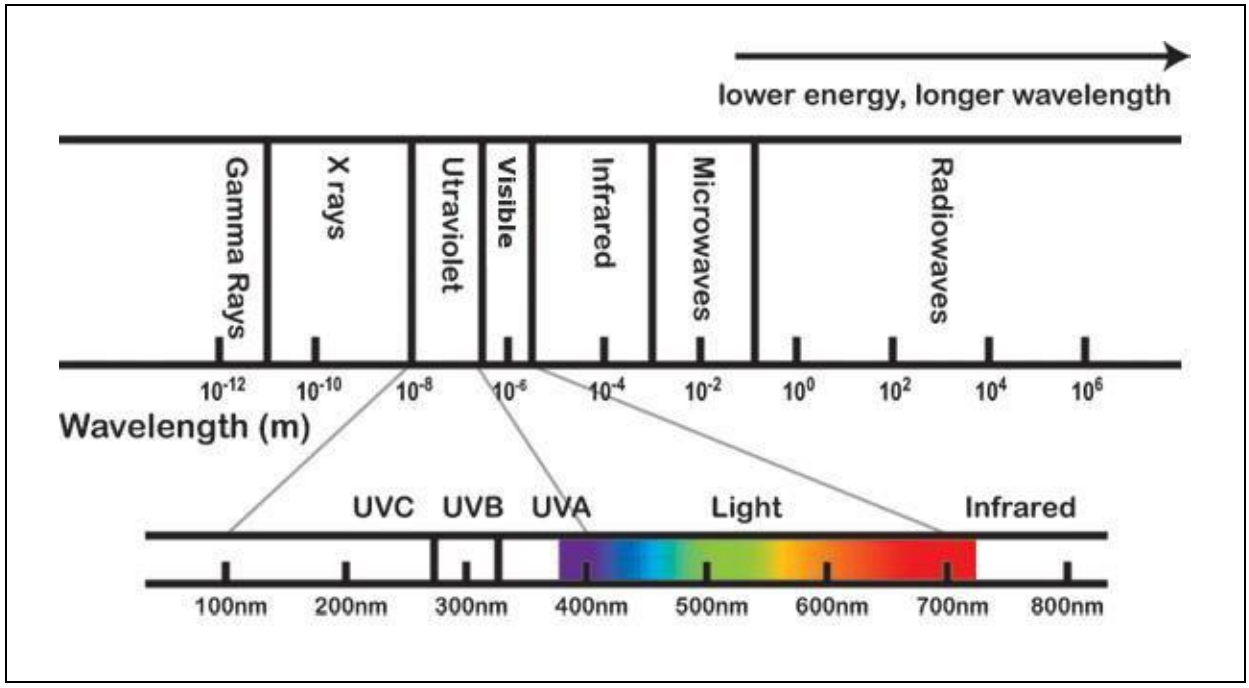

Fig. 3.13. Concepts of an electromagnetic radiation spectrum

The thermal radiation band is enclosed between 0.1 and 1000 μm of the spectrum, as shown in Fig. 3.13. The thermal spectrum can be divided into three spectral bands: the ultraviolet (UV) spectrum, the visible band and the infrared (IR). Moreover, it shows that the energy of the visible light region, in the range of wavelengths between 350 nm to 740 nm.

Solar cells respond differently to the different wavelengths of light. In summary, light that is too high or low in energy is not usable by a cell to produce electricity. Rather, it is transformed into heat.

In view of the visible light spectral band of the thermal radiation, the evaluation of the exergy of PV modules, namely based on photonic energy perspective, can be carried out.

Solar energy can be termed as photonic energy from the sun and this energy travels in the form of photons. The energy of a photon, En_{ph} (J), can be calculated as:

$$En_{ph}(\lambda) = \frac{hc}{\lambda}, \tag{70}$$

where h and c are physical constants; h is Planck's constant ($\approx 6.626 \times 10^{-34}$ J.s); c is speed of light in vacuum (2.998×10^{8} m/s); and λ is wavelength of spectrum the light (nm). For the clear sky day (with G = constant = 1367 W/m^2), the rate of photons falling on the PV surface, N_{ph} can be estimated as 4.4×10^{21}/s.m^2. In order to evaluation of photonic energy parameters, in given G, the sets equations as follow can be implemented:

$$N_{ph} = G\frac{4.4\times10^{21}}{1367}, \tag{71}$$

$$\dot{E}n_{ph}(\lambda) = En_{ph}(\lambda)N_{ph}\,A, \tag{72}$$

$$\dot{E}n_{chemical} = \dot{E}n_{ph}(\lambda)\left(1-\frac{T_C}{T_S}\right), \tag{73}$$

where N_{ph} is the numbers of photon falling per second per unit area on the Earth (1/m^2.s); $\dot{E}n_{ph}(\lambda)$ is the photonic energy falling on the PV system (W); $\dot{E}n_{chemical}$ is available photonic energy or Chemical potential (W) and T_s is the sun temperature (5777 K). In this method, $\dot{E}n_{chemical} = \dot{E}x_{in}$ and $\dot{E}x_{out}$ equal

with power generated by the PV modules, and can be calculated as the product of their output current (I) and the voltage across their terminals (V).

On the other hand, if available of photonic energy is known, the exergy of PV system can be determined also through the following correlation:

$$\dot{E}x_{chemical} = \eta_{pc}\, \dot{E}n_{chemical}\,. \tag{74}$$

3.5. Experimental exergetic assessment of PV performance

To simplify the process of exergy evaluation, a "Sankey diagram" as can be seen in Fig. 3.14 (Kabelac, 2008), can be implemented as guidance in order to understand the process and to get all the required parameters easily.

In exergy analysis, the characteristics of a reference environment need to be specified and in this study the outside temperature (T_o) or ambient temperature (T_a) is used as reference. In order to find exergy of solar radiation (radiation exergy), the data of the sun temperature, T_s is required, and as an approach T_s ~ 5777 K.

Based on Fig.3.14, efficiency energy (η_{en}) and efficiency exergy (η_{ex}) of the PV module can be expressed as follow:

$$\dot{E}n_{solar} = \frac{En_{in}}{\Delta t}\,, \tag{75}$$

$$\eta_{en} = \frac{\dot{E}n_{out}}{\dot{E}n_{in}} = \frac{P+\dot{Q}}{\dot{E}n_{in}} = \frac{(VI)+\dot{Q}}{GA}\,, \tag{76}$$

$$\dot{E}x_{solar} = \frac{Ex_{in}}{\Delta t}\,, \tag{77}$$

$$\eta_{ex} = \frac{Ex_{out}}{Ex_{in}} = \frac{\dot{E}x_{out}}{\dot{E}x_{in}} = \frac{P}{\dot{E}x_{solar}} = \frac{VI}{\dot{E}x_{solar}}\,. \tag{78}$$

It can be seen from Fig. 3.14 that not all incoming radiation energy can be said as useful radiation energy. Furthermore, not all useful radiation energy can be converted to useful energy, in this case electric energy.

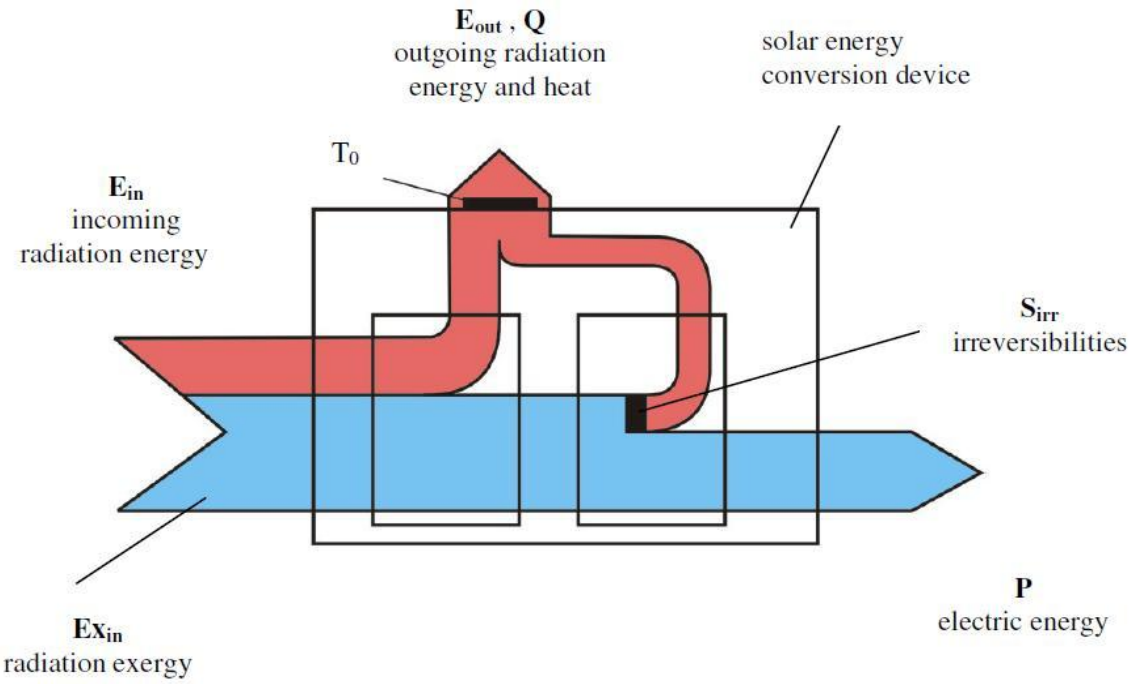

Fig. 3.14. Energy and exergy flow diagrams in solar energy conversion device

4. RESULTS

4.1. Climate data of the site

Generally, to evaluate the grid-connected PV array system characteristics, the main information as described in Fig. 4.1 are needed. However, if the evaluation focus only on the PV module performance, the information about inverter is not necessary.

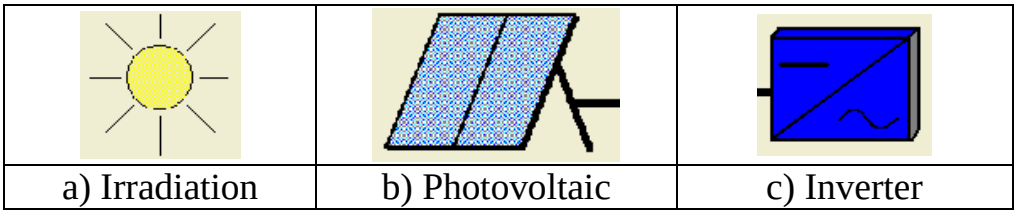

a) Irradiation | b) Photovoltaic | c) Inverter

Fig. 4.1. The main components of grid-connected PV system (NSoL)

For theoretical evaluation and analysis, secondary data of annual climates of Gödöllő, Hungary, which is located at 47.4° N lattitude and 19.3° E, were taken from PV*SOL 3.0 software packages, which acquires data from MeteoSyn, Meteonorm, PVGIS, NASA SSE, SWERA (Klise et al., 2009). Besides of that, other software packages such as NSoL 4.4.0 and online software such as Homer 2.68 Beta, Retscreen and PVGIS, also are used in this research.

The solar radiation (either in irradiation or irradiance) in yearly base, monthly base and daily base for Gödöllő, Hungary are presented in Figs 4.2-4.

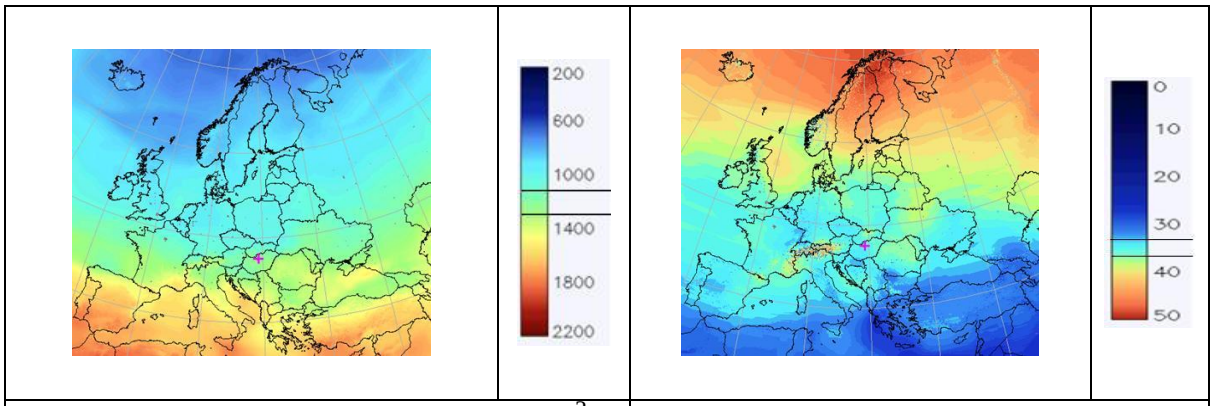

a) Yearly global irradiation (kWh/m^2) | b) Optimum tilt angle (degree)

Fig. 4.2. The global irradiation and and optimum tilt angle for Gödöllő, Hungary (http://re.jrc.ec.europa.eu/pvgis/)

Moreover, annual climate data in comprehensive, included solar irradiation (both in horizontal position, G_{hor}, and tilt array position, G_{arr}), ambient temperature (T_a), wind velocity (v) and solar irradiance (G), is presented in Table 4.1.

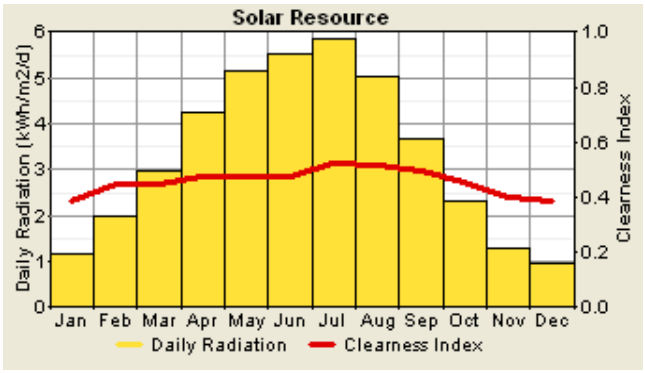

Gödöllő – Hungary
Lattitude: 47°26’ N (47,43° N)
Longitude: 19°21’ E
Average global solar irradiation: 3.4 kWh/m^2/day or 1.21 MWh/m^2/year

Fig. 4.3. The monthly radiation profile of Gödöllő, Hungary (Homer 2.68 Beta)

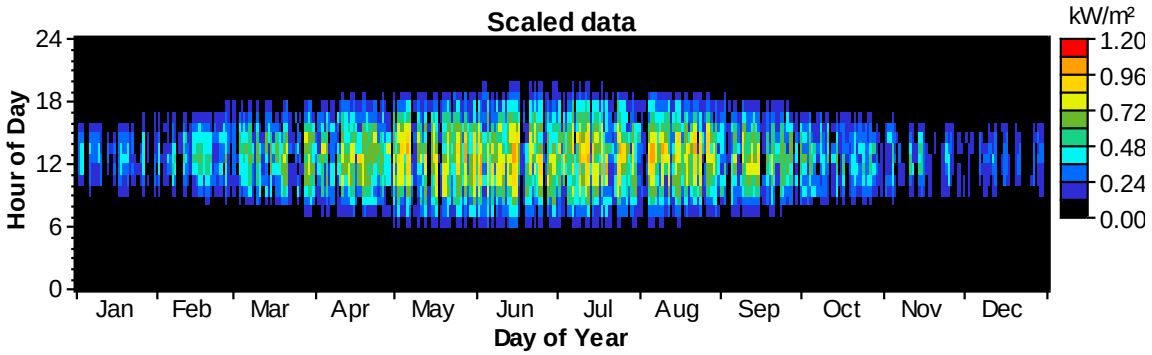

Fig. 4.4. The daily map irradiance characteristic of Gödöllő, Hungary (Homer 2.68 Beta)

Table 4.1. Annual climate data of Gödöllő, Hungary (PV*SOL 3.0)

Month	E_{hor}	E_{arr}	v	T_a	*Sun hours**	$G_{arr} = G$
	kWh/m^2	kWh/m^2	m/s	°C	h	W/m^2
January	29.79	44.57	2.65	-0.94	9	159.75
February	46.35	62.82	2.70	1.70	10	224.34
March	86.25	104.16	2.82	6.20	12	279.99
April	127.23	140.31	2.91	11.54	14	334.07
May	162.17	163.76	2.67	16.48	15	352.16
June	172.06	167.49	2.76	19.30	16	348.93
July	182.90	182.05	2.75	21.42	15	391.51
August	153.71	164.99	2.38	20.82	14	380.16
September	109.33	130.47	2.29	16.54	12	362.42
October	70.55	98.39	2.12	11.37	10	317.39
November	35.31	52.03	2.49	5.30	9	192.71
December	23.06	33.38	2.64	1.14	8	134.60
Annual	1,199.00	1,344.00	2.60	11.00		

*Based on average effective sun hours in Hungary

4.2. Energy production of 10 kWp grid-connected PV array system

The evaluation of energy production of 10 kWp grid-connected PV array system as a function of surface orientation (Fig. 4.5) have been simulated using two commercial simulation software packages, i.e RETScreen V 3.2 and NSoL V4.4. In addition, prediction of the performance of PV array using of general mathematical model approach has been performed.

In simulation process, the properties of both PV modules (polycrystalline silicon and amorphous silicon) are taken from Table 3.1 (PV modules specifications in SZIU grid-connected PV array system).

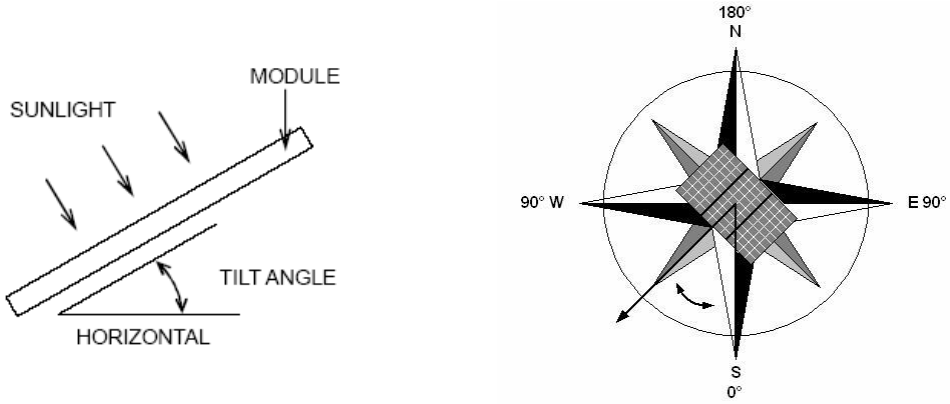

a) Tilt angle (β) b) Surface azimuth angle (γ)

Fig. 4.5. PV Surface orientation

In first of study, estimation of solar irradiation/insolation (in monthly base) as a function of PV surface orientation was carried out using NSol V4.4. In this study, seven position of tilt angle and five position of surface azimuth angle are selected as surface orientation. The five of surface azimuth angles (γ) as mentioned are: -90^o, -5^o, 0^o, $+5^o$, $+90^o$ (minus sign is respect to East, 0 is corresponds to surfaces facing directly towards the equator and positive sign is respect to West). For each surface azimuth angles, the following tilt angles (β) are considered: 0^o, 32^o, 39^o, 47^o, 55^o, 62^o, 90^o. These values are chosen based on Lunde-Garge and Lewis, in order to get optimum tilt angle (Lunde-Garge: $\beta_{opt} = \phi \pm 15^o$ and Lewis, $\beta_{opt} = \phi \pm 8^0$).

Based on simulations, characteristic information of the PV array system has been obtained. All information resulted from simulation and analysis, have been arranged and generally presented here in graphs and tables (see Figs 4.6-14).

Fig. 4.6 shows the monthly variation an average solar radiation/insolation, incident on the surfaces of PV modules mounted facing south (with azimuth angle 5^o to east) with different tilt angle. Fig 4.6 indicates that the tilt angle has very significant effect on the monthly average insolation during the summer season (June-August) while it has a lesser effect during the winter season (December-February). This is because the day length in the summer season is

longer than that in the winter season. In another form, Fig. 4.6 can be seen in Fig.4.7.

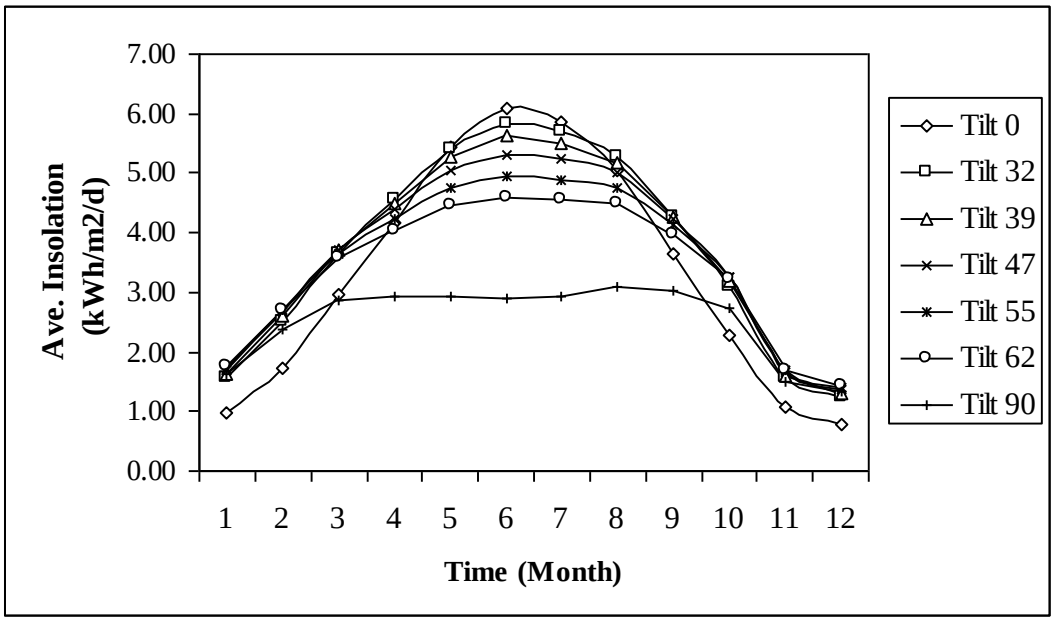

Fig. 4.6. Effect of tilt angle on monthly average incident insolation

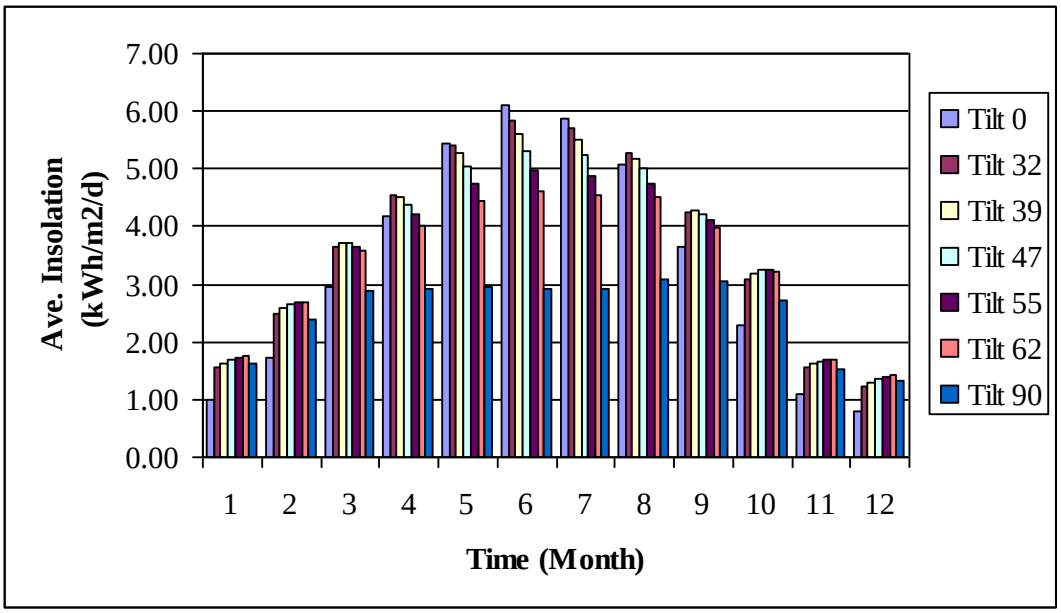

Fig. 4.7. Effect of tilt angle on monthly average incident insolation

In Table 4.2, average of insulation in different of surface orientation can be compared. Based on this Table, the best position of surface orientation for PV installation in Gödöllő, can be predicted.

Table 4.2 also informed that there is no significant effect on the average of insolation, in the small difference of azimuth angle (in this case 5, 0, -5). It is

mean that for an existing condition, a 10 kWp PV array system at SZIU has a proper installation (can be said also an equal facing to South/equator).

Table 4.2. The average of insolation (kWh/m^2/d) for several surface orientations

Tilt Angle (^{o})	Azimuth Angle (^{o})						
	90	45	5	0	-5	-45	-90
0	3.34	3.34	3.34	3.34	3.34	3.34	3.34
32	3.15	3.57	3.72	3.72	3.72	3.57	3.15
39	3.07	3.54	3.70	3.70	3.70	3.54	3.07
47	2.96	3.46	3.63	3.63	3.63	3.46	2.96
55	2.83	3.34	3.51	3.51	3.51	3.34	2.83
62	2.70	3.21	3.37	3.37	3.37	3.21	2.70
90	2.10	2.46	2.52	2.52	2.52	2.46	2.10

Fig. 4.8 shows the peak and the lowest period of daily average insolation at the predetermined tilt angle. Further calculation based on this characteristics, gives the Hungary yearly global irradiation 1.2 MWh/m^2 (in the range of GIS prediction values, as shown in Fig. 4.2).

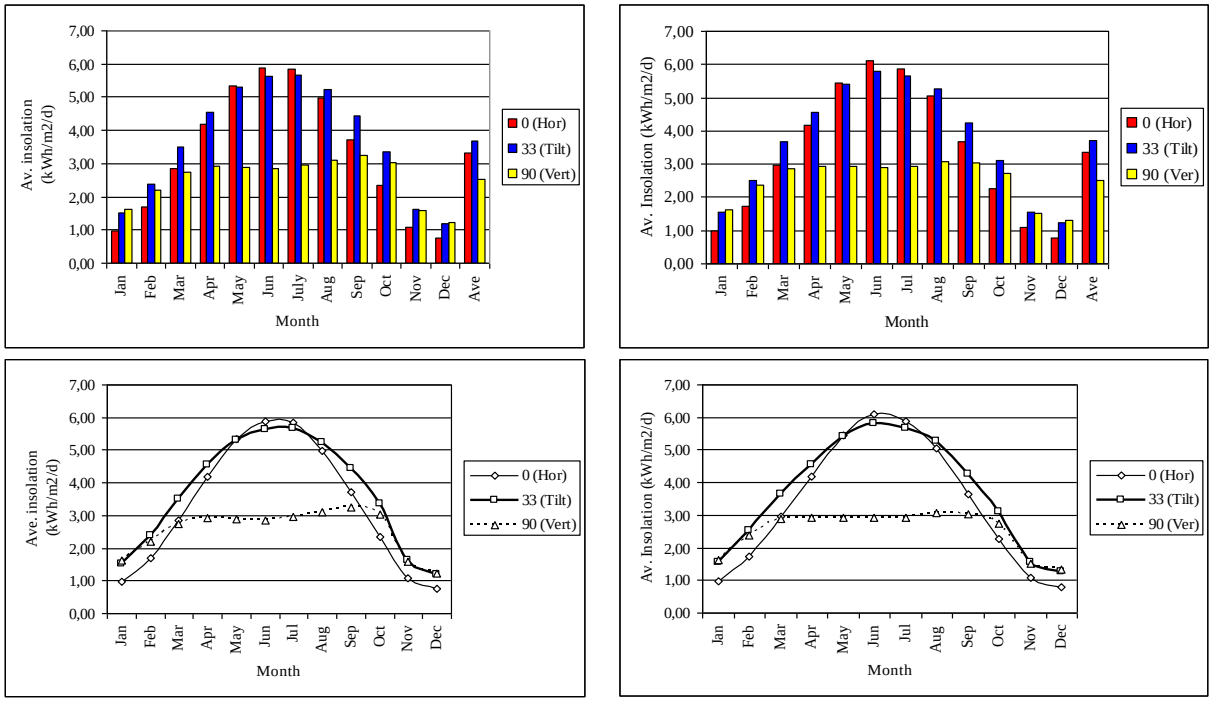

a) By RETScreen b) By NSoL

Fig. 4.8. Comparison daily average insolation for fixed azimuth at three different tilt angle

Refers to previous insolation characteristics, the annual output of grid-connected PV array at various tilt angle in the best azimuth angle can be estimated. In this

evaluation, the efficiencies data's of the PV module and inverter as basic for calculation are taken from the first operational data, as shown in Fig. 4.9 (performed in April 2007).

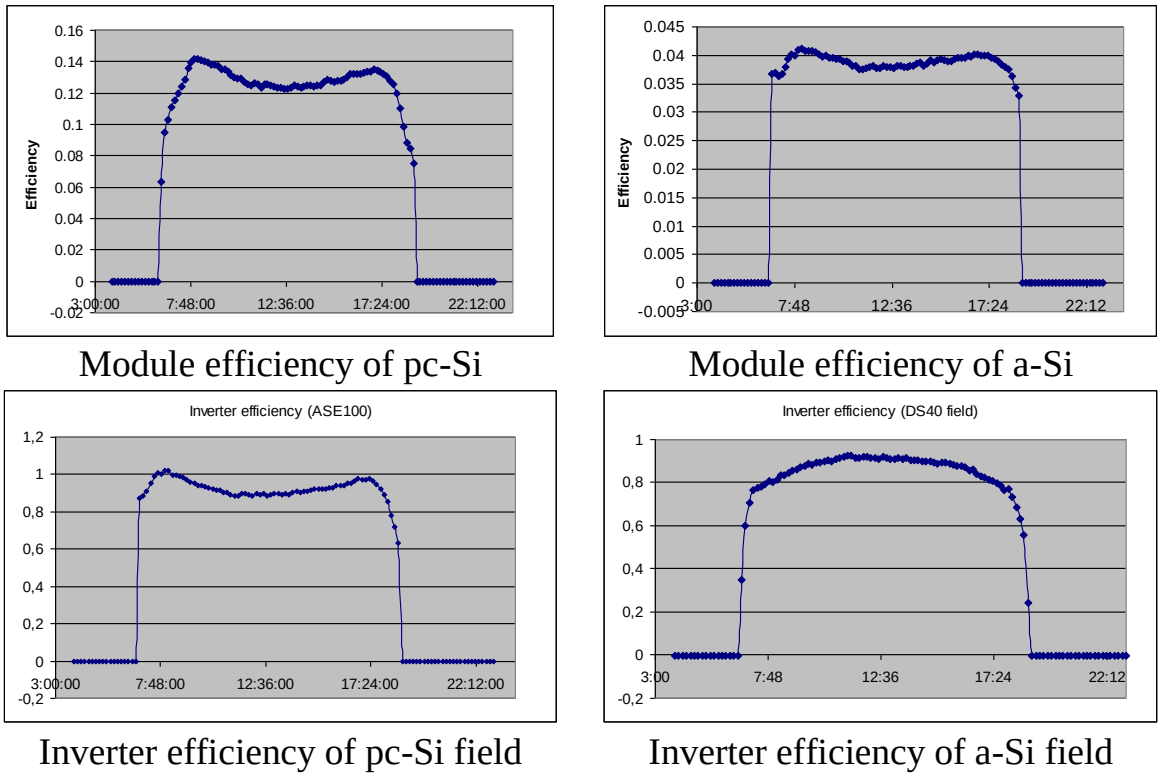

Module efficiency of pc-Si | Module efficiency of a-Si

Inverter efficiency of pc-Si field | Inverter efficiency of a-Si field

Fig. 4.9. Efficiencies of PV modules and inverter (from the measured data)

The average module efficiencies can be read from the curves as about 13% for the polycrystalline and 4% for the amorphous silicon modules. From the figures it also can be seen that the module efficiency is a little bit lower in the hottest hour (in the hottest condition). The highest module temperature was reached about 45ºC at noon (Seres et al., 2007). The phenomena expressed the temperature dependence of the PV efficiency.

The inverter efficiency was calculated from the measured DC and AC power values. Similarly to the PV array efficiency, only an overall rate was calculated. As the data logging is set to record 10 minute average values, this efficiency was also calculated in series for the same day as the module efficiencies (see in Fig. 4.9). Based on this curves, it can be seen that the average efficiency (even in the most important midday period) is above 90%.

Figs 4.10-12 show the influence of tilt angle on the annual output of PV array system at fixed azimuth angle, for existing condition (south facing), based on NSol and RETScreen.

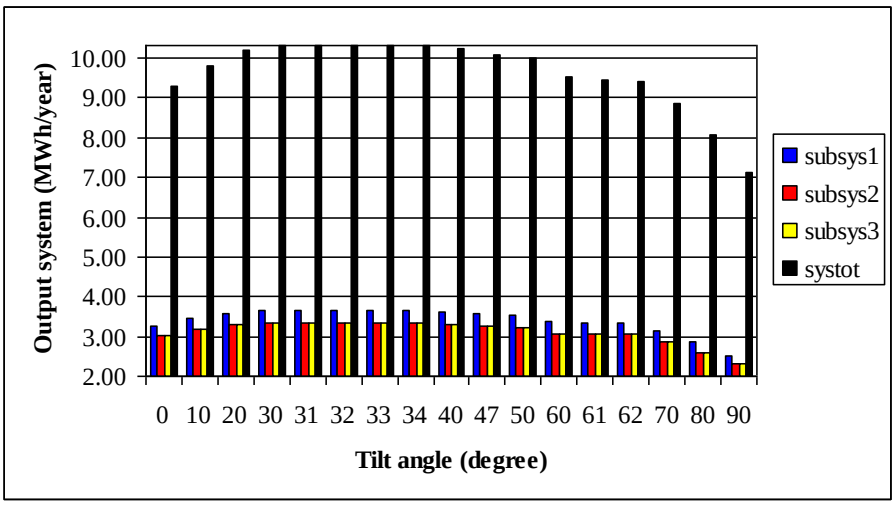

Fig. 4.10. Annual energy output PV array system at various tilt angle (NSol)

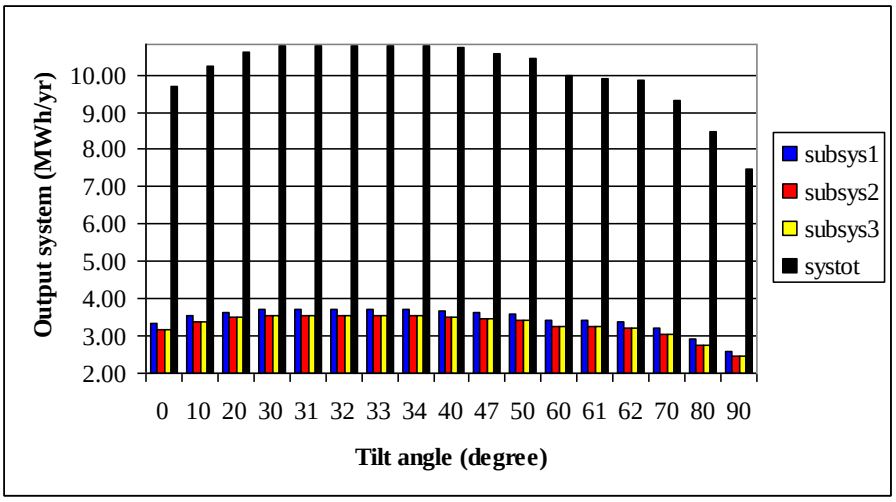

Fig. 4.11. Annual energy output of PV array system at various tilt angle (RETScreen)

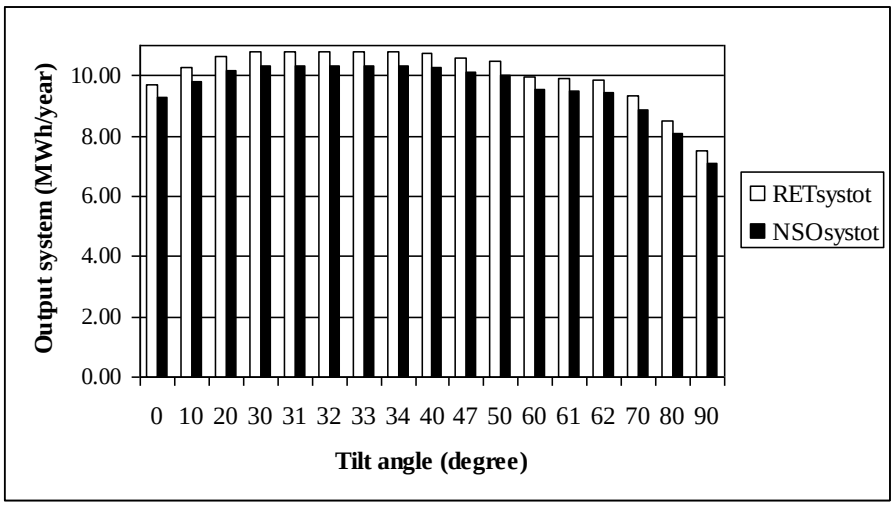

Fig. 4.12. Comparison of output system based on simulation

Comparison of the annual output of the PV array and output in different season, at different tilt angles can be seen in Table 4.3.

Table 4.3. Evaluation of energy output for each season

Tilt Angle	Energy Output (kWh)				
	Spring	Summer	Fall	Winter	Annual
0	2955	3761	1605	836	9157
32	3192	3798	2073	1262	10325
39	3159	3687	2108	893	9847
47	3083	3525	2123	1367	10098
55	2970	3318	2108	1397	9793
62	2838	3097	2070	1403	9408
90	2078	2056	1709	1274	7117

Based on Table 4.3 it can be seen that in the summer, a 10 kWp grid-connected PV array system with tilt angle 32^o would produce highest of energy. On the other hand, the PV array at tilt angle 62^o would produce the highest of energy in the winter. For the whole year, a PV array at tilt angle 32^o would produce highest energy. Referring to this evaluation, tilt angle 32^o can be recommended to be used.

Figs 4.13-14 show the comparison between modeling and measurement and Fig. 4.15 shows the influence of various tilt and azimuth angles on the output system.

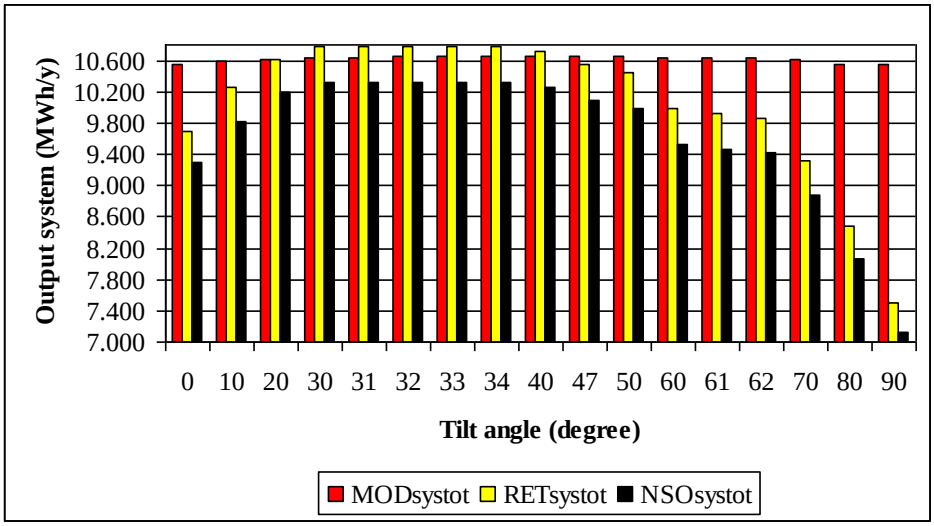

Fig. 4.13. Comparison of output system simulation and mathematical model

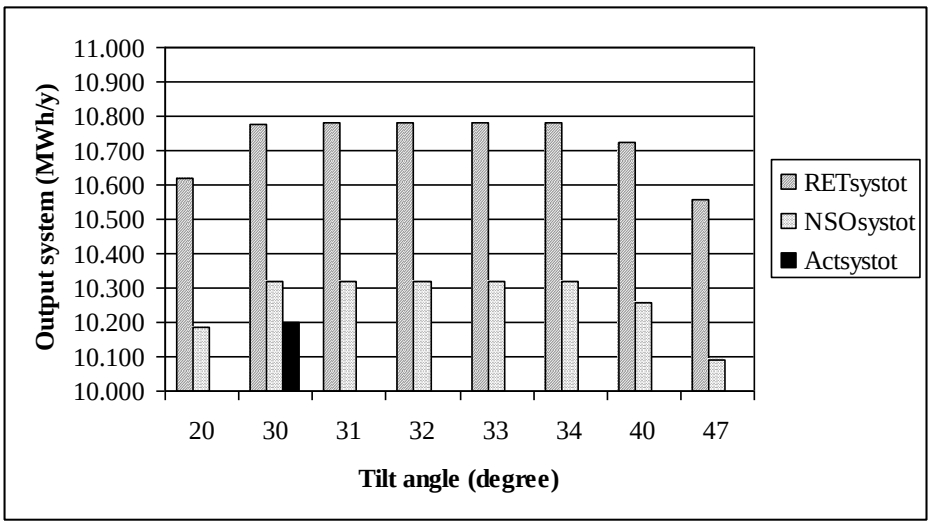

Fig. 4.14. Comparison of output system based on simulation and real data operation (surface azimuth -5^o)

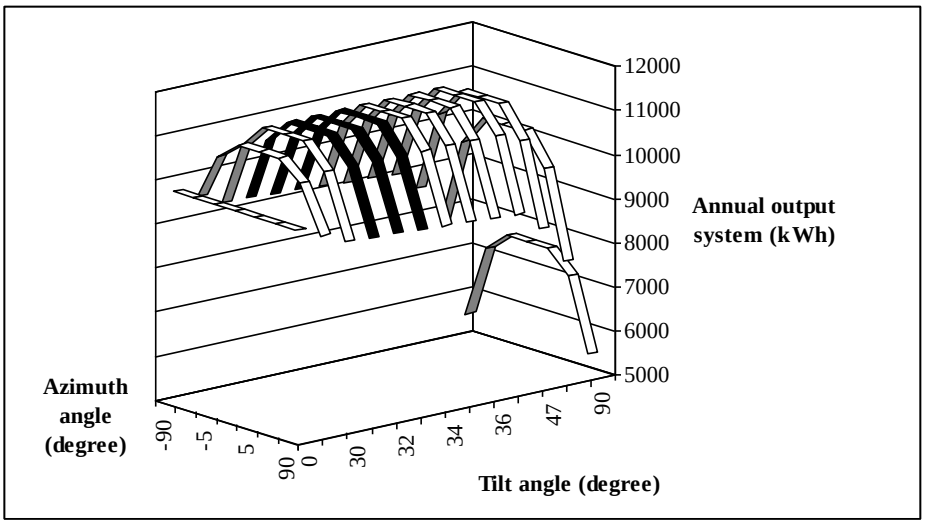

Fig. 4.15. Annual output system for various surface orientations (tilt and azimuth angle)

Based on this characteristic, the system could maximize annual output of the system at azimuth angle 0^o (pure facing to South) and tilt angle between 30-34^o.

Conducted to energy and environment aspect, reduction in CO_2 gas emission as an impact of PV system utilization is further target that must be fulfilled. Theoretically, the surface orientation which could maximize of annual energy production, have meaning also as a surface orientation which could maximizing of CO_2 gas emission reduction. Reduction in CO2 gas emission by implementing a PV is calculated as the difference between corresponding emission and that of a conventional source.

As tools for analysis, two software packages, i.e. RETScreen V3.2 and HOMER Ver. 2.68 beta were used in simulations, and simulation results is shown in Fig. 4.16.

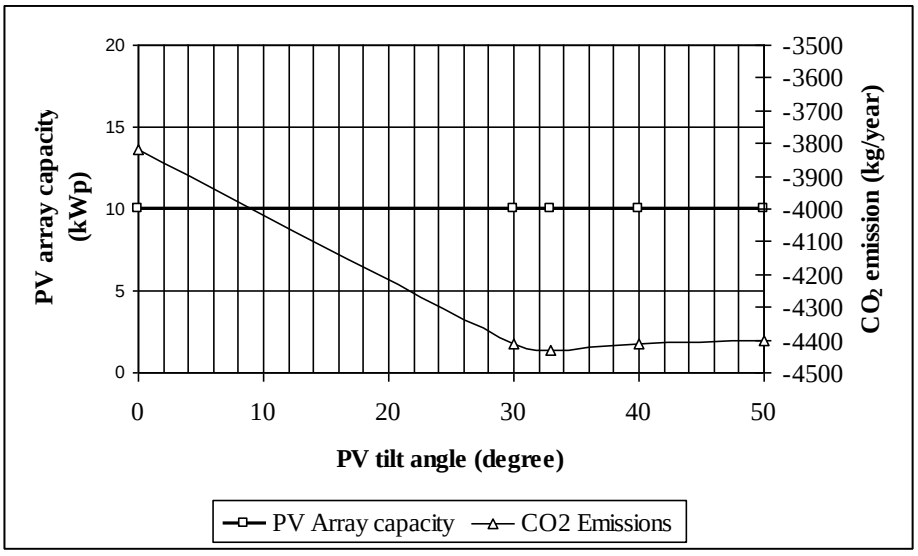

Fig. 4.16. CO_2 emission at various of tilt angle (slope) for South face PV array (0^o of azimuth angle)

Fig. 4.16 shows CO_2 gas emission reduction as a function of tilt angle, at the fixed surface azimuth angle. It can be predicted that reduction of Greenhouse gas (GHG) emission at the optimum tilt angle is equivalent with reduction 4430 kg CO_2/year.

4.3. Electrical characteristics of pc-Si and a-Si modules

4.3.1. I-V and P-V Characteristic of PV modul and PV array

Simulation results of *I-V-P* characteristic of PV array based on *I-V-P* characteristic of PV module are shown in Figs 4.17-18. Figs 4.17 and 4.18 show the comparison of *I-V* and *P-V* characteristics for a single module and PV array system of pc-Si and a-Si, which implement series and parallel circuits of PV modules, in the same time i.e., December and June (at noon), under Hungarian solar radiation at surface orientation position 30^o for tilt angle and -5^o for surface azimuth angle (5 degree to East for South Facing). In Fig. 4.19, characteristic of insolation and kWh output of PV array, either for pc-Si or a-Si are presented, and in Fig. 4.20, comparison of temperature characteristic (either ambient temperature or module temperature) of grid system for December and June for pc-Si and a-Si are presented.

It may be observed, that with a change in season (comparison between December and June), the output current of the PV module/array system and the output power, are increased.

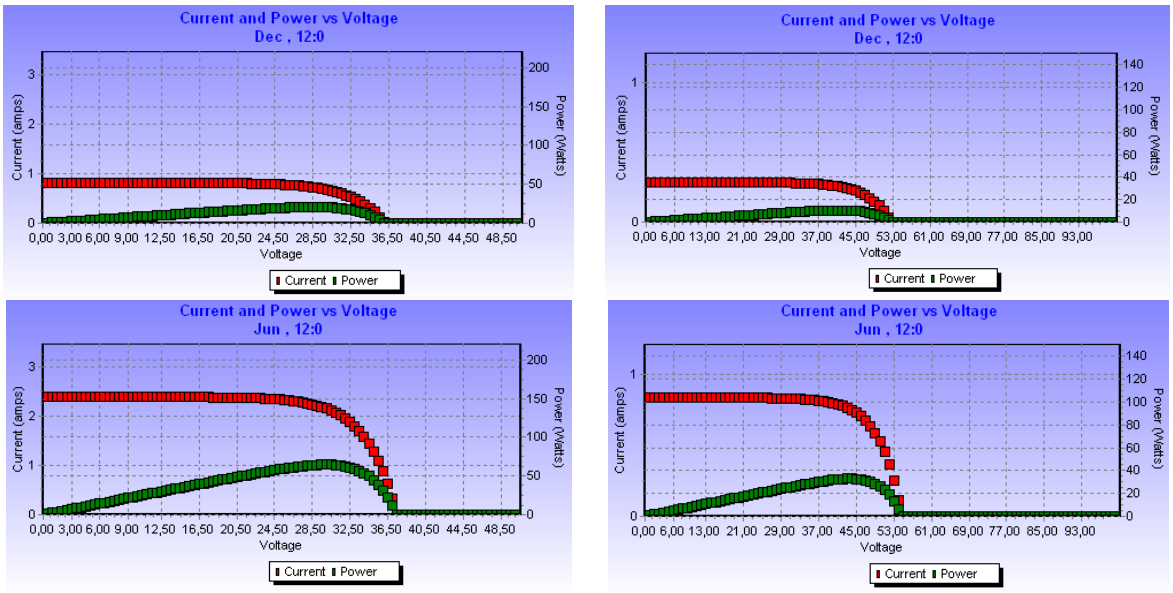

(a) pc-Si (b) a-Si

Fig. 4.17. *I-V* and *P-V* characteristics of single PV module for pc-Si and a-Si

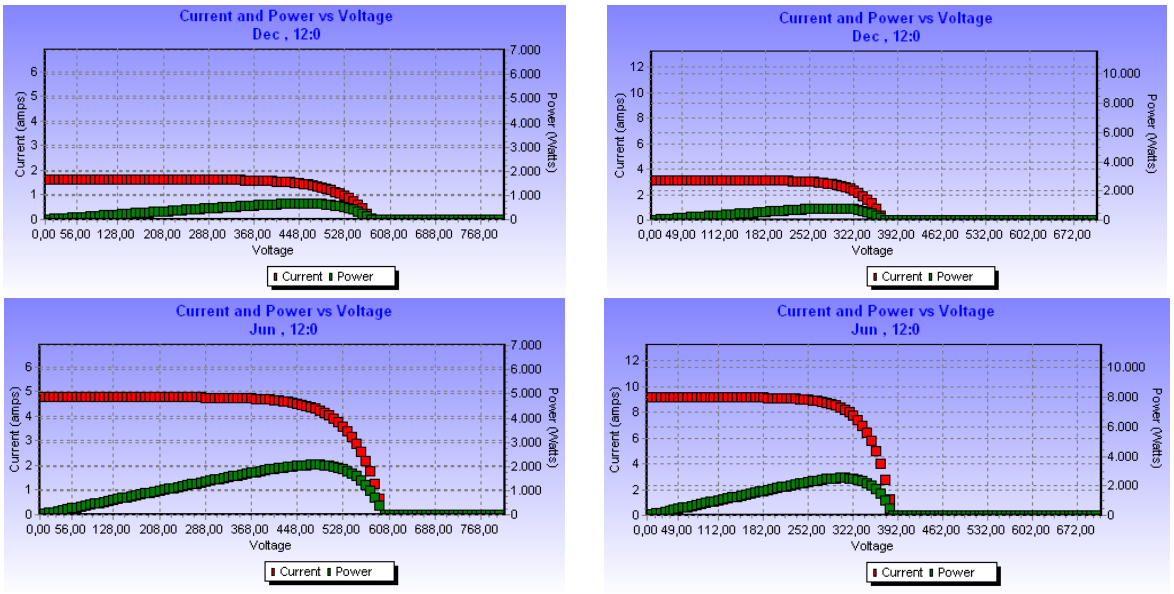

(a) pc-Si (b) a-Si

Fig. 4.18. *I-V* and *P-V* characteristics of pc-Si and a-Si of PV array system

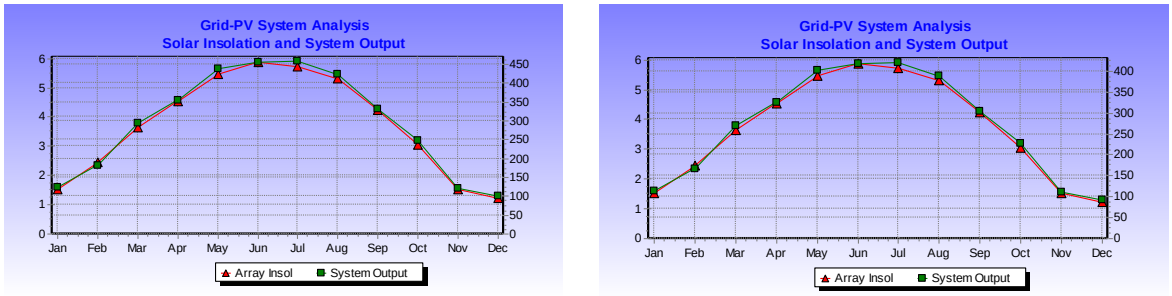

(a) pc-Si (b) a-Si

Fig. 4.19. Comparison of output sytem (kWh) for pc-Si and a-Si

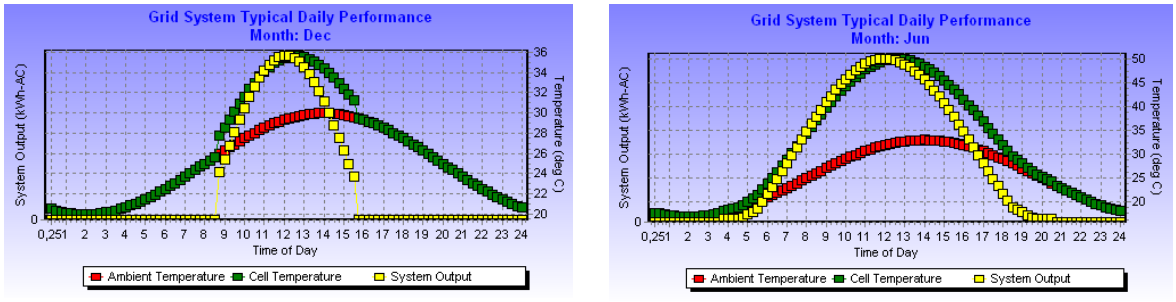

Fig. 4.20. Comparison of typical grid system for December and June for pc-Si and a-Si

4.3.2. I-V-P characteristics as function of climate condition

Figs 4.21-22 show the relationship between output current, voltage and power of the pc-Si and a-Si PV modules, under constant module temperature and at different irradiation, and vice versa, based on PV*SOL 3.0 software packages.

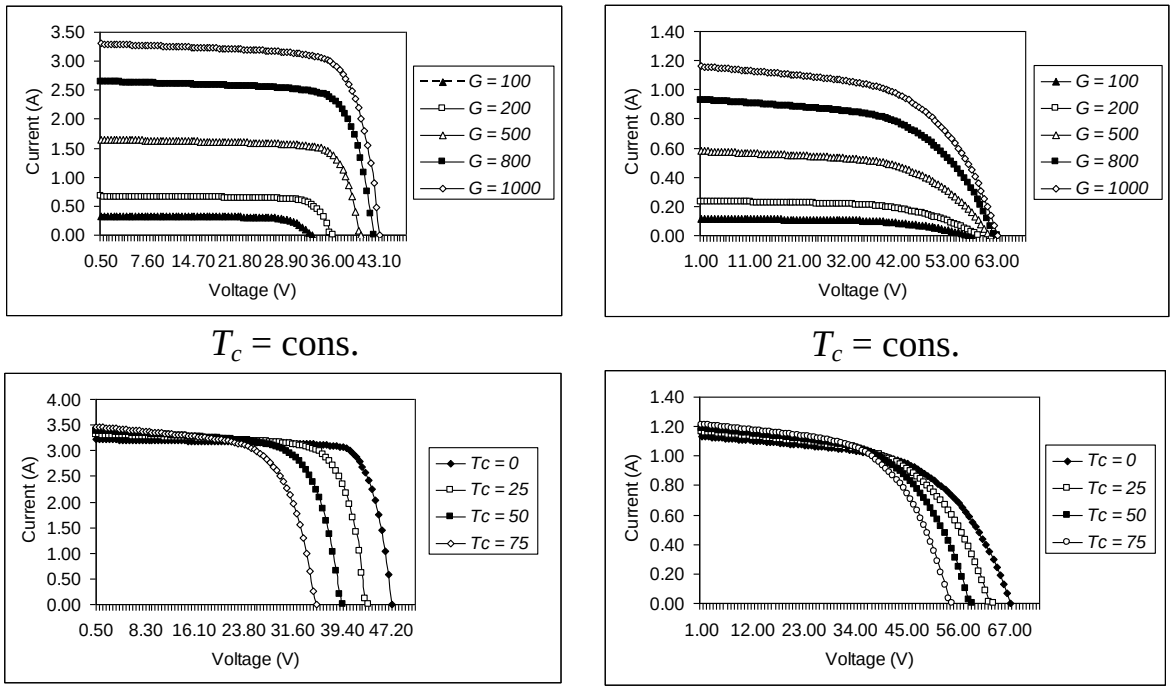

T_c = cons. T_c = cons.

G = cons. G = cons.

(a) pc-Si (b) a-Si

Fig. 4.21. The *I-V* module characteristics, based on PV*SOL 3.0

Based on characteristics in Fig. 4.21, it's clear that at constant module temperature, increasing of irradiation give big affect (proportional) on a short circuit current (I_{sc}) value but small effect on the open circuit voltage (V_{oc}) value. In other side, it can be observed that increasing of module temperature at constant irradiation will increase a short circuit current (I_{sc}) slightly and decrease the open circuit voltage (V_{oc}) proportional.

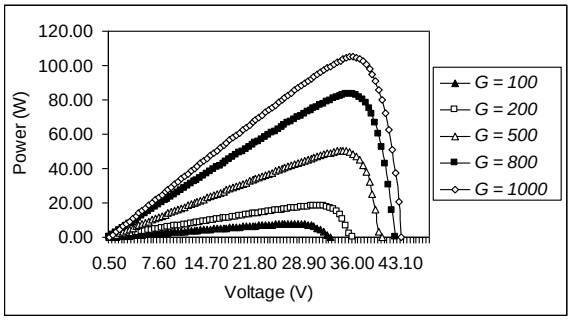

T_c = cons.

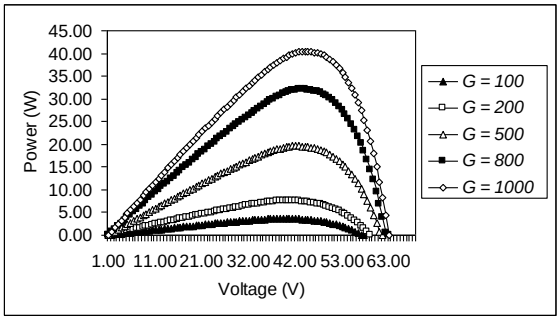

T_c = cons.

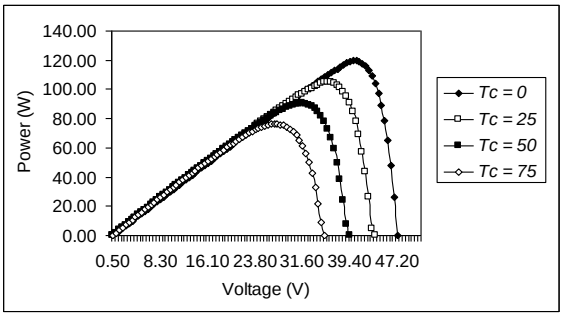

G = cons.

(c) pc-Si

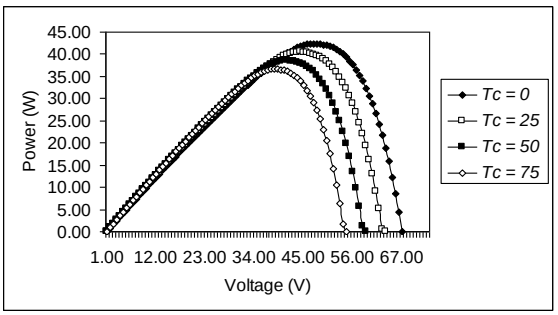

G = cons.

(d) a-Si

Fig. 4.22. The *P-V* module characteristics, based on PV*SOL 3.0

Based on Fig. 4.22, it can be seen also that at constant module temperature, increasing of irradiation give significant affect on the output power of PV module (*P*). Meanwhile, increasing of module temperature at constant irradiation will great affect on decreasing of output power (*P*) PV module. This phenomena illustrated that output power (*P*) PV module is affected indirectly by ambient temperature, T_a.

As a general performances, the change in relative efficiency of two PV module respect to variation of the solar irradiance and the ambient temperature, are given in Figs 4.23-24 (simulation by PV*SOL 3.0 software packages). Principally, at T = 25°C and G = 1,000 W/m^2, the relative efficiency is 1.0, and usually this condition used as reference or standard test conditions (STC).

Both figures shows that the relative efficiency of module is nearly constant over a wide range of intensities, and only dropping sharply below 20% of the standard 1,000 W. Variations in temperature cause the curve to shift upwards (if colder) or downwards (if warmer). It clear also that ASE-100 (wafer based crystalline silicon technology) is more sensitive to temperature changes than DS-40 (thin film technology).

Both figures shows that the relative efficiency of module is nearly constant over a wide range of intensities, and only dropping sharply below 20% of the standard 1,000 W. Variations in temperature cause the curve to shift upwards (if colder) or downwards (if warmer). It clear also that ASE-100 (wafer based

crystalline silicon technology) is more sensitive to temperature changes than DS-40 (thin film technology).

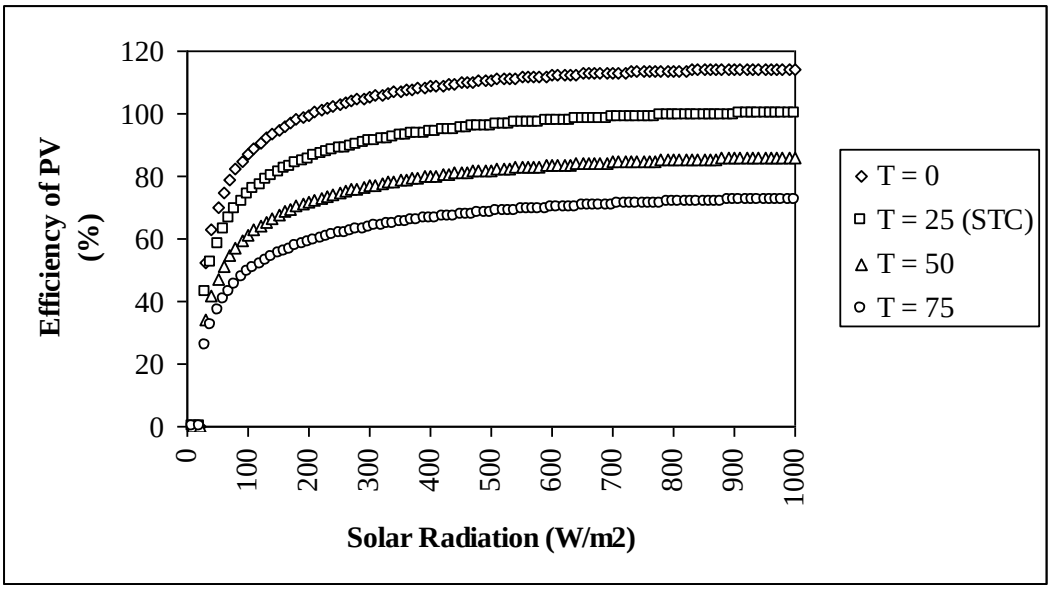

Fig. 4.23. Relative efficiency of PV module at different temperatures for pc-Si

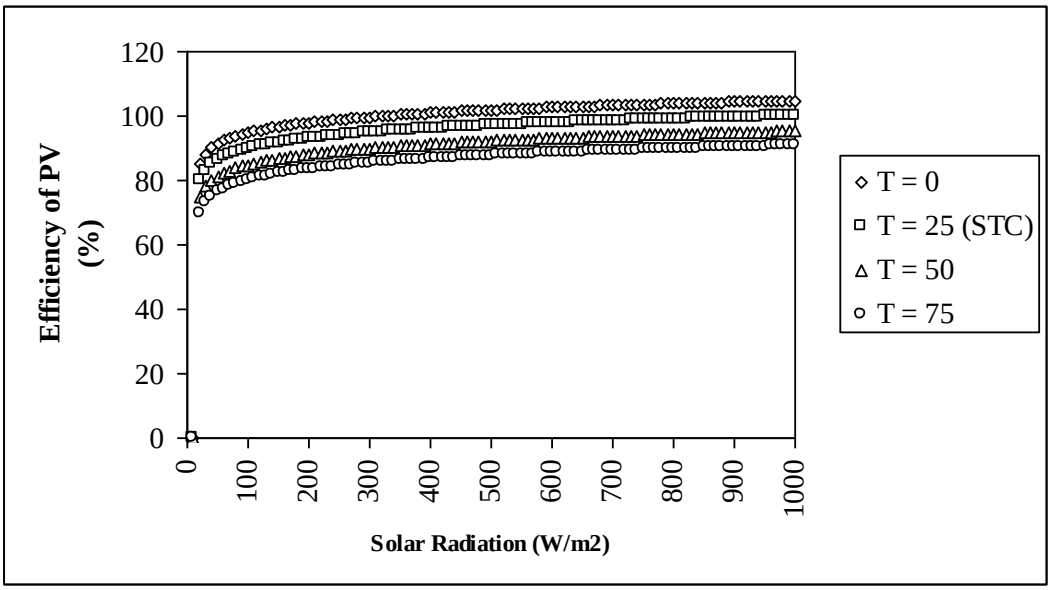

Fig. 4.24. Relative efficiency of PV module at different temperatures for a-Si

4.3.3. Maximum power point tracking of PV modules

The output power of PV modules can be evaluated through *I-V-P* characteristics and strongly affected by many factors, such as irradiance, temperature, material and process control system (usually is implemented in the electronic power system). The PV operating point can be determined at any point on the *I-V-P* curves, and the power has a maximum power point (MPP) at a certain working

point with coordinates V_{mp} voltage and I_{mp} current, at which the PV cell operates with the maximum efficiency and produces the maximum output power.

As a preliminary phase to understand the voltage critical values of each module at different weather conditions, simulation of MPPT line characteristics at various weather conditions have been performed, either for pc-Si or a-Si. In Figs 4.25-26, the MPP ideal conditions of ASE-100 and DS-40 modules are presented.

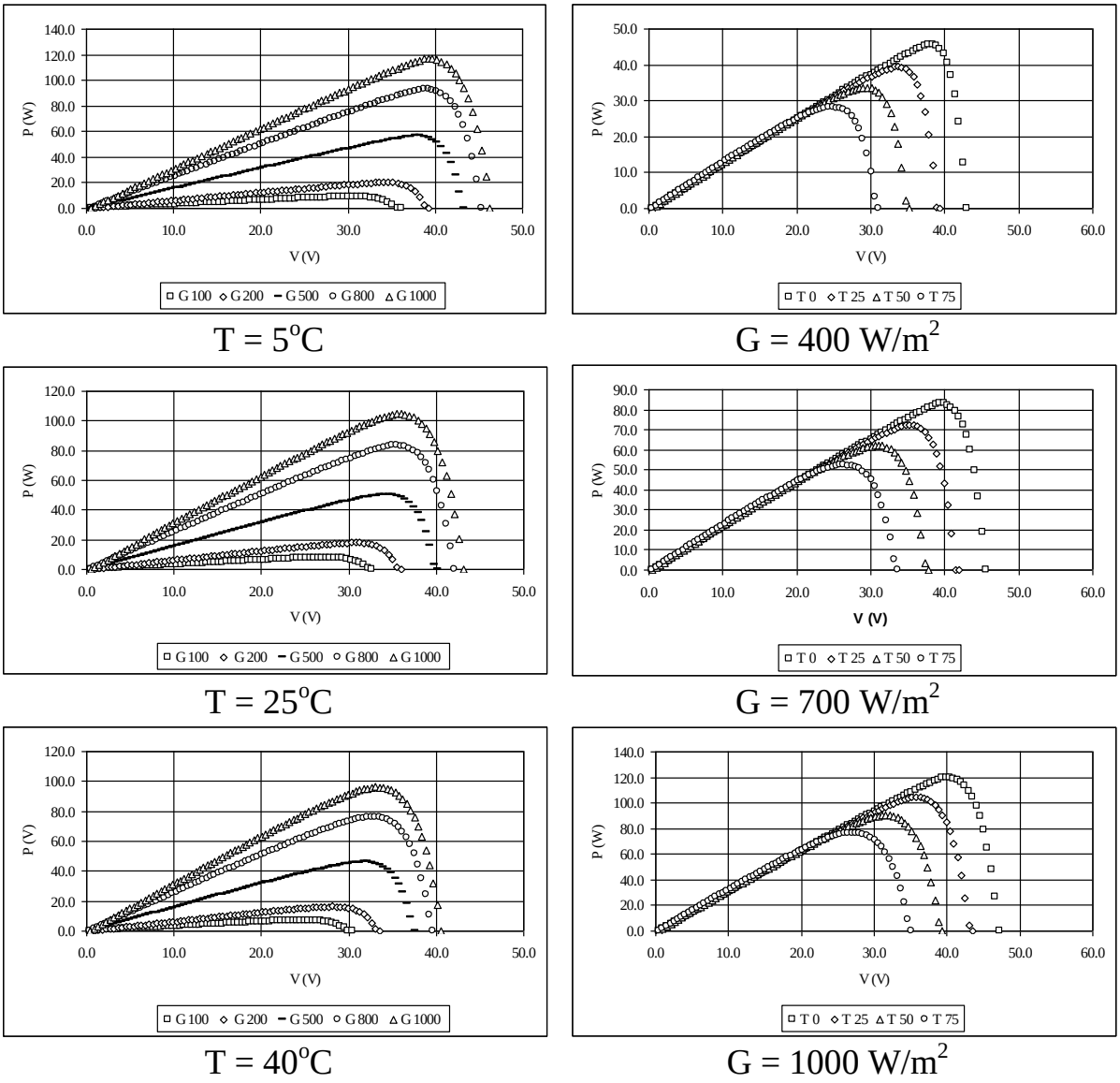

Fig. 4.25. Ideal MPPT characteristic of pc-Si PV module at various G and T_a

Based on Fig. 4.25 and Fig. 4.26, it's clear that the output power of a PV module is influenced by solar radiation incident on the system and cell and ambient temperatures. As solar irradiance increases, the short circuit current, maximum power, and conversion efficiency increases. It is proven that as ambient temperature increases the open circuit voltage decreases, which leads to the reduction of maximum power.

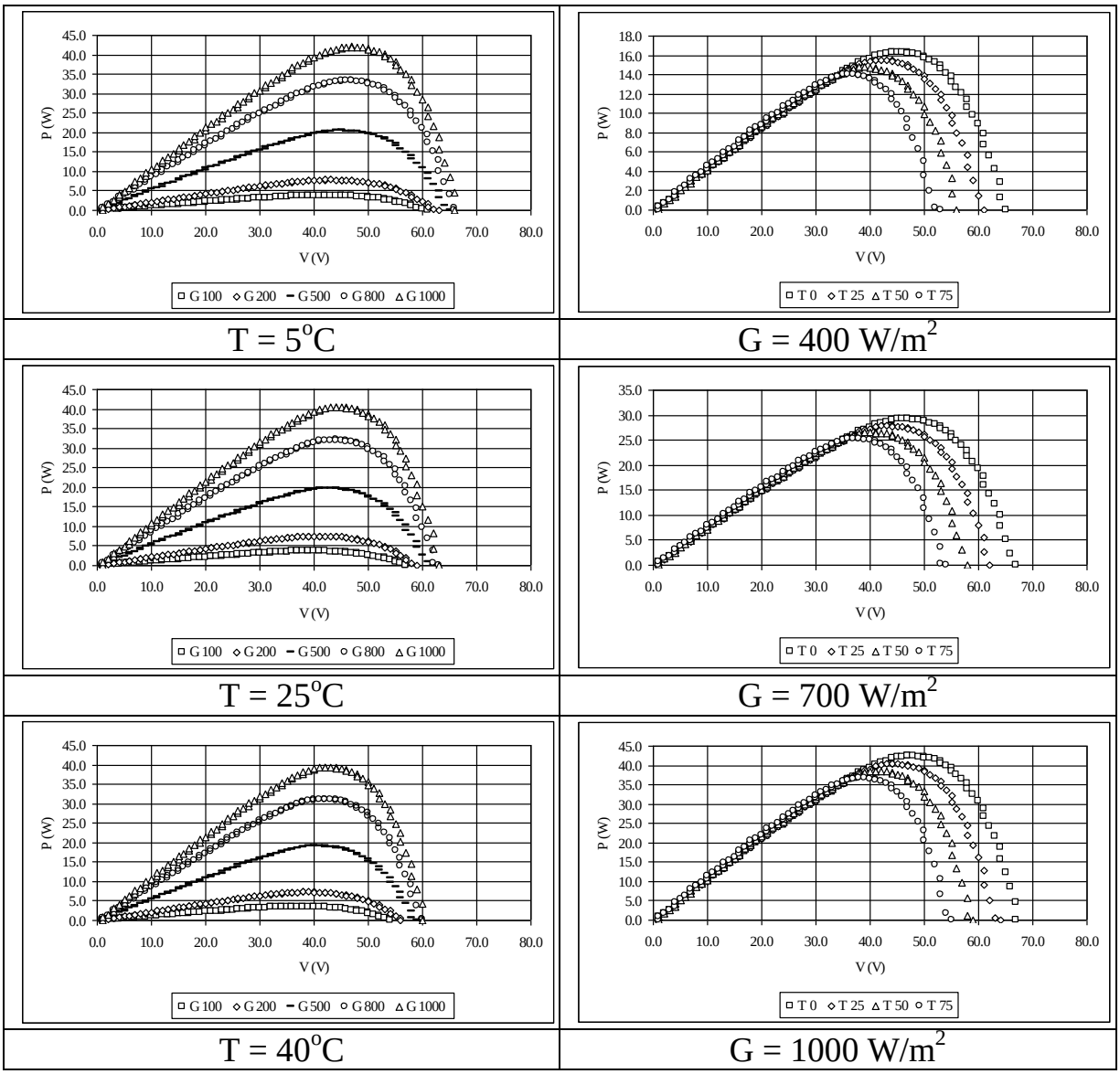

Fig. 4.26. Ideal MPPT characteristic of a-Si module at different *G* and *T*

Based on Figs 4.25 and 4.26 also, it is found that the MPPT line characteristics of PV module are situated around critical value.

4.4. Thermodynamic performance of PV modules

Based on Table 3.1 (available in chapter 3) and general PV modules characteristics as mentioned in chapters 4.3.2 and 4.3.3, other information such as T_c, I_{sc}, V_{oc}, I_{mp}, V_{mp} (at variations of G and T_a) can be determined and furthermore can be used in determining of Fill Factor (*FF*), and the calculation results are shown in Table 4.4 and Table 4.5.

In order to obtain the thermodynamics performance of both PV modules, data in Tables 4.4-5 and equations were mentioned in chapter 3, have been used in analysis.

Table 4.4. Characteristic of pc-Si based on annual climates of Gödöllő

Month	T_c	I_{sc}	V_{oc}	P_{mpp}	V_{mp}	I_{mp}	FF
	(°C)	(A)	(V)	(W)	(V)	(A)	(-)
January	1.88	0.77	26.60	16.10	22.70	0.71	0.79
February	5.60	1.08	27.50	23.16	23.30	0.99	0.78
March	11.92	1.36	27.20	28.79	23.10	1.25	0.78
April	18.73	1.63	27.10	33.64	22.90	1.47	0.76
May	24.82	1.73	26.50	34.38	22.30	1.54	0.75
June	28.10	1.73	26.20	33.55	21.80	1.54	0.74
July	30.38	1.94	26.30	37.58	21.90	1.72	0.74
August	29.80	1.88	26.30	36.29	21.90	1.66	0.73
September	24.42	1.78	26.90	35.70	22.40	1.59	0.75
October	17.30	1.55	27.30	32.10	23.00	1.40	0.76
November	8.64	0.93	26.60	19.19	22.40	0.86	0.77
December	3.25	0.65	26.20	13.12	22.00	0.60	0.77

Table 4.5. Characteristic of a-Si based on annual climates of Gödöllő

Month	T_c	I_{sc}	V_{oc}	P_{mpp}	V_{mp}	I_{mp}	FF
	(°C)	(A)	(V)	(W)	(V)	(A)	(-)
January	2.04	0.18	62.00	6.26	43.00	0.15	0.56
February	5.87	0.26	63.00	8.82	43.00	0.21	0.55
March	12.34	0.32	62.00	11.00	42.00	0.26	0.55
April	19.33	0.39	61.00	13.04	42.00	0.31	0.55
May	25.49	0.41	60.00	13.60	41.00	0.33	0.56
June	28.84	0.40	60.00	13.21	41.00	0.32	0.55
July	31.15	0.46	60.00	15.00	41.00	0.37	0.55
August	30.55	0.44	59.00	14.59	41.00	0.36	0.56
September	25.03	0.42	60.00	14.01	41.00	0.34	0.56
October	17.73	0.37	61.00	12.37	42.00	0.29	0.55
November	8.84	0.22	62.00	7.51	42.00	0.18	0.55
December	3.36	0.15	62.00	5.23	42.00	0.12	0.55

The variation of energy, exergy, power conversion and maximum efficiencies of PV modules, against time (in the month) are shown in Fig. 4.27 and Fig. 4.28 for pc-Si and a-Si, respectively. The energy efficiency for pc-Si varies from a minimum of 39.9% at December to a maximum of 56.4% at June, meanwhile for a-Si varies from a minimum of 34.8% at December to a maximum of 52.9 at June. The exergy efficiency for pc-Si varies from a minimum of 10.9% at June to a maximum of 12.6% at February, meanwhile for a-Si varies from a minimum of 3.5% at June to a maximum of 4.9% at December. In summary, average thermodynamic efficiencies (included energy efficiency, exergy efficiency,

power conversion or electrical efficiency and electrical maximum efficiency) both PV modules during a year are shown in Table 4.6.

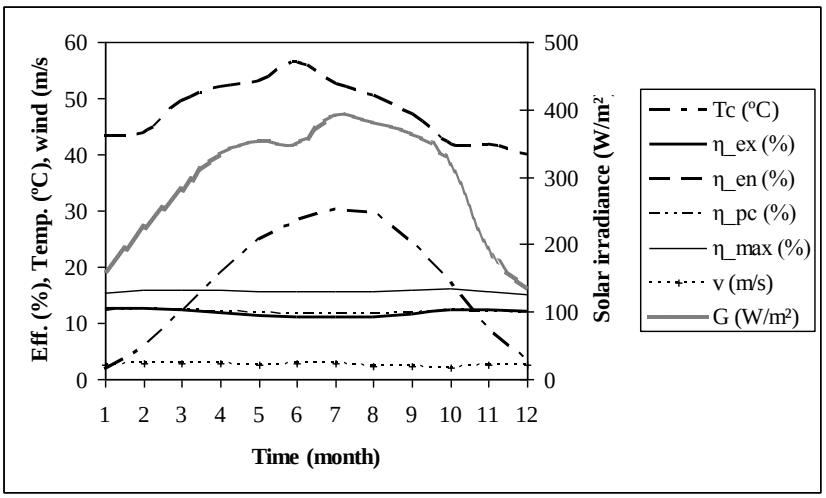

Fig. 4.27. Variation of thermodynamic efficiencies of pc-Si during a year

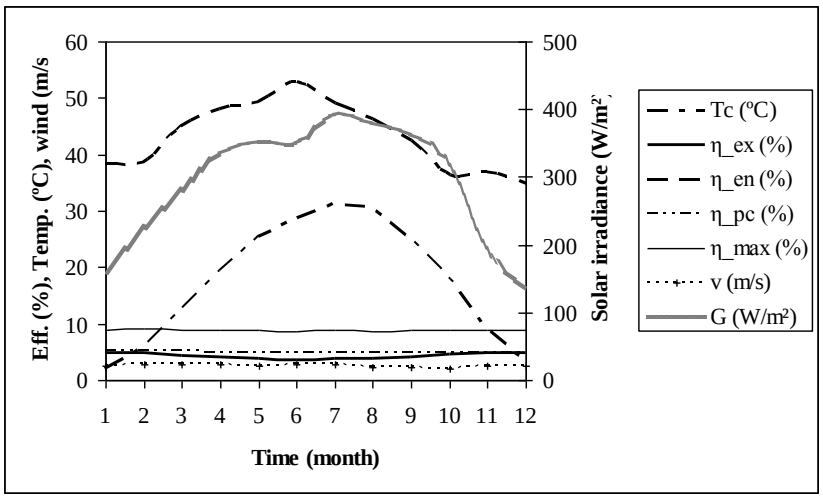

Fig. 4.28. Variation of thermodynamic efficiencies of a-Si during a year

Table 4.6. Average thermodynamic efficiencies of PV modules during a year

Thermodynamic performances		Average in year		
		pc-Si	a-Si	a-Si
η_{en}	= efficiency of energy (%)	47.66	43.20	43.20
η_{ex}	= efficiency of exergy (%)	11.82	4.30	4.30
η_{pc}	= efficiency of power conversion (%)	11.94	4.91	4.91
η_{max}	= efficiency of electrical maximum (%)	15.72	8.88	8.88

The results showed that energy efficiency of PV modules higher than exergy efficiency, due to the energy efficiency is based on the electrical energy and the thermal energy (which available on the PV surface) as an output, meanwhile

exergy efficiency considers only electrical energy as an output (the thermal energy is viewed as losses and is not taken into account as an output). Based on Figs 4.27 and 4.28, it is found that thermodynamic efficiencies of PV modules in power conversion (η_{pc}) and exergy (η_{ex}) are slight different, either for pc-Si or a-Si. The efficiency maximum (η_{max}) is higher than other efficiencies, because this efficiency calculates the maximum electricity generated (as function of I_{sc} and V_{oc}). The results showed also that performance evaluations of PV modules with exergy analysis will lead us getting a realistic values rather than energy analysis, if compared to efficiency power conversion (efficiency of electric). The exergy efficiency of PV module decreases with solar irradiance in higher temperature (in June, July and August). If the temperature decreases, the trend in exergy efficiencies changed (increasing).

4.5. Actual efficiencies of exergy and power conversionof PV modules

To verify the results shown in Figs 4.27-28 and Tabel 4.6, hourly data based on experimental is also used in PV modules analysis. But, due to based on theoretical approach we saw that power conversion and exergy efficiencies are the most important efficiencies for evaluating PV modules, further analysis based on experimental are just given on the two efficiencies.

Figs 4.29 and 4.30 show the variation of solar irradiance, G (W/m^2), exergy of solar energy, Ex_{solar} (in W/m^2), the power supplied by the PV modules, P (in W/m^2), exergy loss, Ex_{loss} (in W/m^2), exergy efficiency, η_{ex} (%) and power conversion efficiency, η_{pc} (%), during the day, based on experimental.

Solar irradiance (G), exergy solar *(Ex_{solar})*, electric power *(P)* and Exergy loss *(Ex_{loss})* are based on active surface area of module, i.e. 0.83 m and 0.79 m, for pc-Si and a-Si, respectively. Ex_{loss} is evaluated as a consequence of the irreversibilities of the process. Data for evaluation is based on Gödöllő climate in May 02, 2007, and due to unavailable information about temperature and wind velocity, evaluation have performed at constant temperature, i.e. average temperature in May, 16.48^{o}C, which available in Table 4.1. Exergy efficiency and power conversion efficiency in an experimental case are calculated based on actual electricity generated, as an output.

Based on Figs 4.29-30, in view of average effective sun hour in that day, it can be seen that the average of η_{ex} and η_{pc} for pc-Si PV module are 12% and 11%, respectively; meanwhile for a-Si PV module are 4% and 3.8%, respectively, for that day. In this case, due to the solar irradiance (G) is always larger than the solar radiation exergy ($\dot{E}x_{solar}$), and actual electricity generated is used for both analysis, the power conversion efficiency of the PV modules is always smaller than the exergy efficiency.

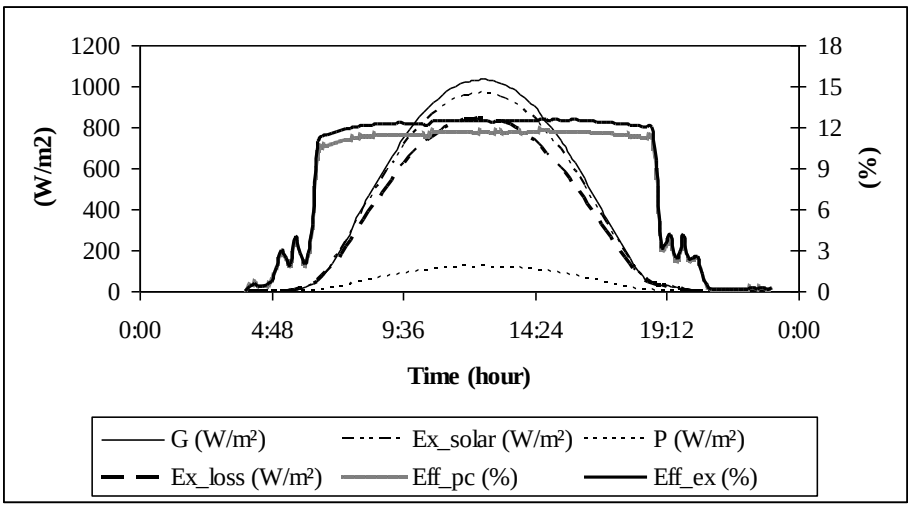

Fig. 4.29. Variation of exergy, power conversion efficiencies and other parameters of pc-Si PV module on a typical day in Gödöllő

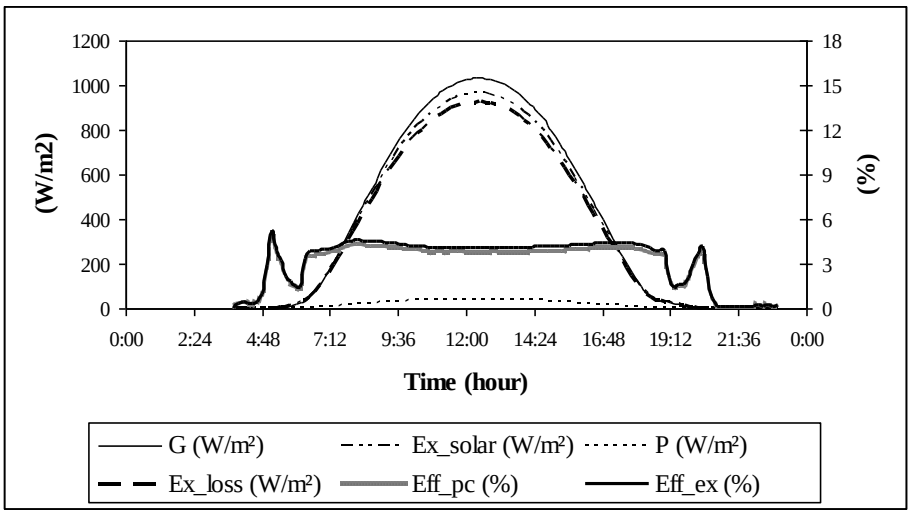

Fig. 4.30. Variation of exergy, power conversion efficiencies and other parameters of a-Si PV module on a typical day in Gödöllő

As expected, the energy and exergy efficiencies of pc-Si PV module higher than a-Si PV module. It is reasonable that in order to get more realistic modelling of PV systems, application of exergy analysis are strongly encouraged. The thermodynamic characteristics showed that both the PV modules, in average, have low exergy efficiencies, i.e. 12% and 4% equal with anergy (energy losses) 88% and 96% for pc-Si and a-Si, respectively.

4.6. Comparison of efficiency exergy based on thermodynamic approach and photonic energy models

In section 4.4, efficiency exergy theoretically has been evaluated by using thermodynamic approach. In this section, efficiency exergy based on

thermodynamic approach will be compared by efficiency exergy which calculated by using others method, i.e. photonic energy method.

In the photonic energy method, calculated are performed by varying wavelength of the visible spectrum, for a given range of 400 to 800 nm. Figs 4.31-32. shows the variation of available of photonic energy (chemical potential), and exergy of PV modules corresponding to the available of photonic energy during a year. If available of photonic energy is known, the exergy of PV can be determined through correlation as described in section 3.4.2. As an approach, the values of η_{pc} in this evaluation are taken from Table 4.6.

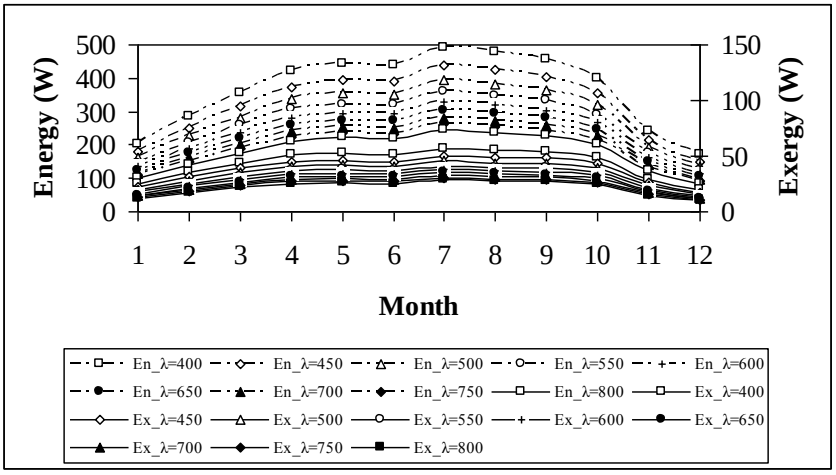

Fig. 4.31. The photonic energy and exergy of pc-Si PV module (yearly base)

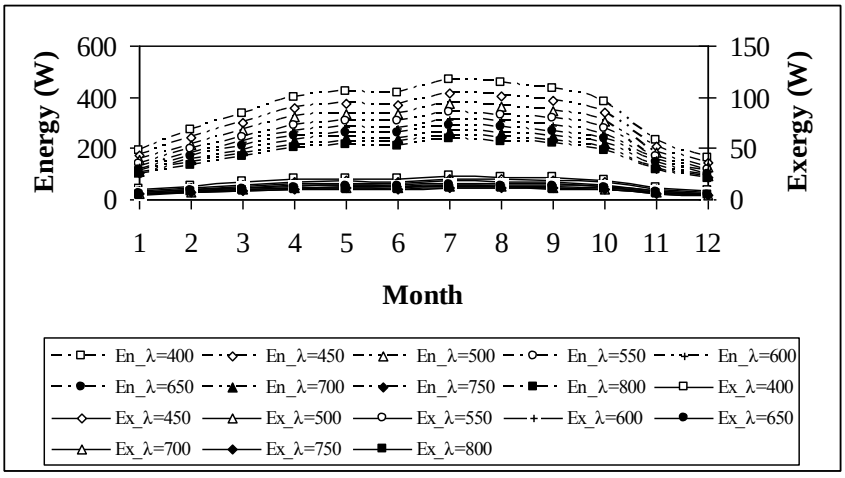

Fig. 4.32. The photonic energy and exergy of a-Si PV module (yearly base)

Comparison between efficiency exergy based on photonic energy, exergy efficiency based on thermodynamic approach and and energy efficiency is shown in Figs 4.33-35.

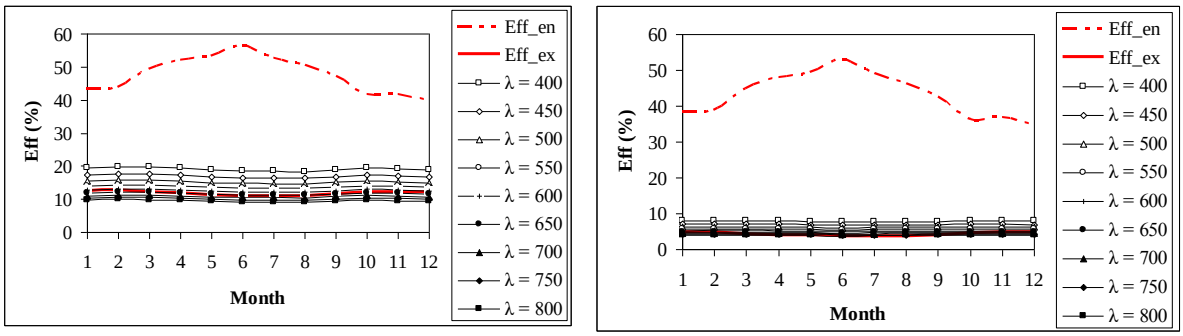

a). pc-Si b). a-Si

Fig. 4.33. PV energy and exergy efficiencies based on two approach

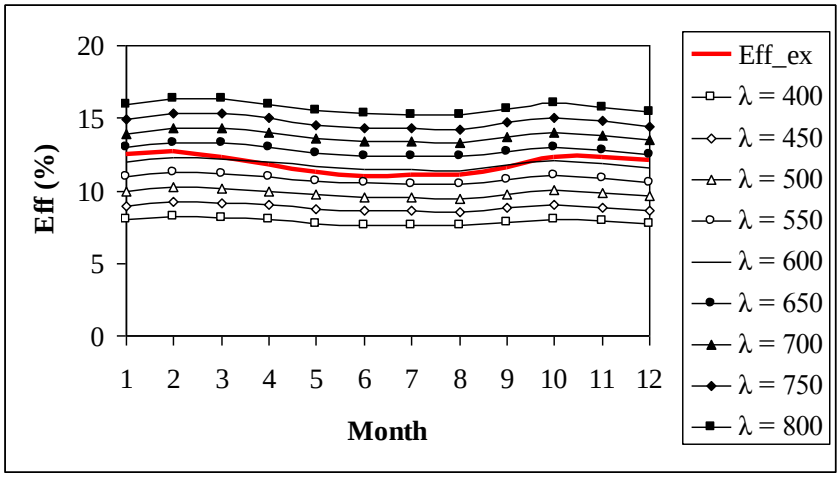

Fig. 4.34. PV exergy effeciencies based on photonic energy and thermodynamic approach (pc-Si)

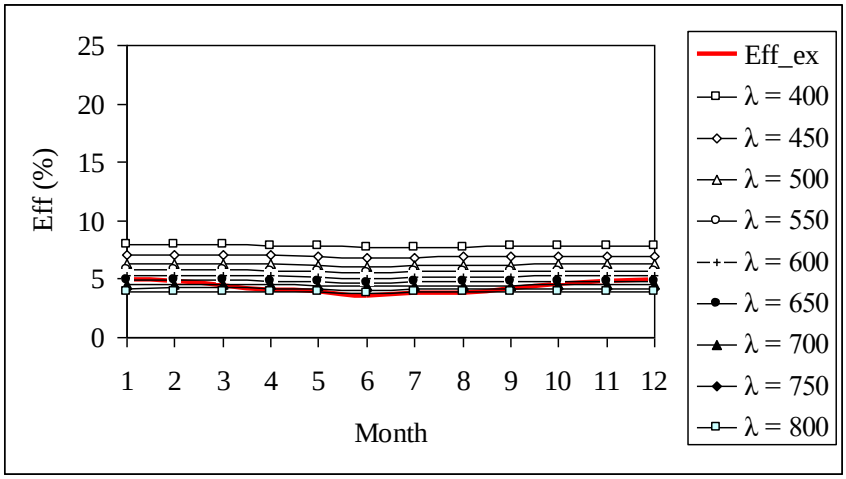

Fig. 4.35. PV exergy effeciencies based on photonic energy and thermodynamic approach (a-Si)

Based on Fig. 4.33, it can be seen that energy efficiency of PV higher than exergy efficiency of PV, because in the energy efficiency terminology, the thermal energy and electrical energy are taken into account as an output of

energy of the PV system. Meanwhile, in the exergy efficiency terminology, the thermal energy is viewed as losses and is not taken into account as an output.

Based in Figs 4.34-35, it can be seen that for the same case, exergy efficiency based on "thermodynamic approach" is spread between exergy efficiency values based on "photonic energy" in the varying wavelength of the visible spectrum.

4.7. Fill factor effects on exergetic performances of PV modules

Variability of fill factor (*FF*) on exergy performance of pc-Si and a-Si PV modules have been evaluated, and the results are shown in Figs 4.36-37.

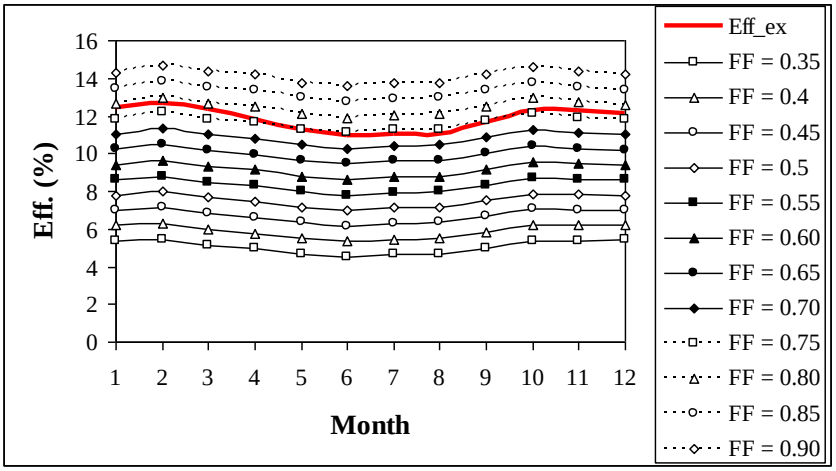

Fig. 4.36. Effect of fill factor (FF) on the exergy performance (pc-Si)

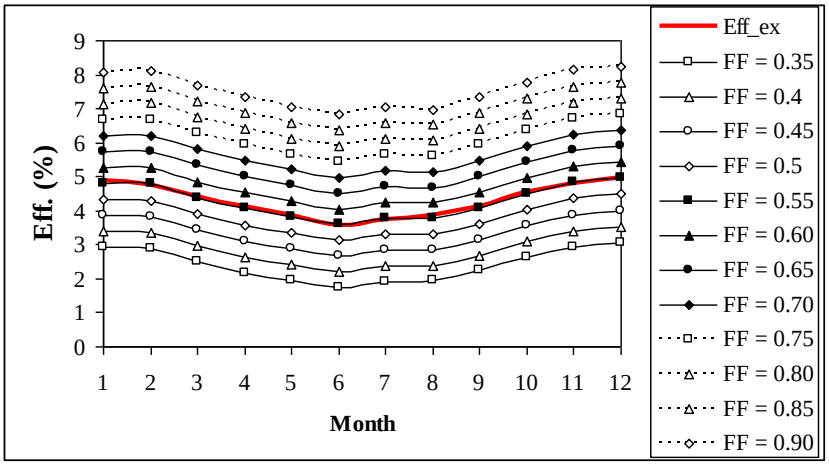

Fig. 4.37. Effect of fill factor (FF) on the exergy performance (a-Si)

The Fill Factor (*FF*) measures of quality of the PV cell. It is evaluated by comparing the maximum power (P_{max}) to the theoretical power that would be output at both the V_{oc} and I_{sc} together. A larger fill factor is desirable, and typical fill factors range from 0.5 to 0.85.

In Lab. scales, generally the FF values of PV cell are 0.80 for pc-Si and 0.74 for a-Si.

Based on simulation it is found that yearly average of *FF* for pc-Si, in range between 0.75 – 0.80, and for a-Si in range 0.50-0.60 (see Figs 4.36-37).

4.8. Spectral irradiance effects on performances of PV module

The performance of photovoltaic (PV) systems is influenced by spectrum of solar irradiance even under the same solar irradiance conditions. In term of wavelength (λ), the spectrum (light) of solar irradiance can be divided into three main regions i.e. ultraviolet region with λ < 0.4 μm (~ 5% of the irradiance), visible region with 0.4 μm < λ < 0.7 μm (~ 43% of the irradiance) and infrared region with λ > 0.7 μm (~ 52% of the irradiance).

In order to get real phenomena and correlation about effects spectral on the PV performance in term of exergetic, as an initial study, the characteristic of spectral solar irradiance in Gödöllő, as presented in Fig. 4.38 will be interpreted.

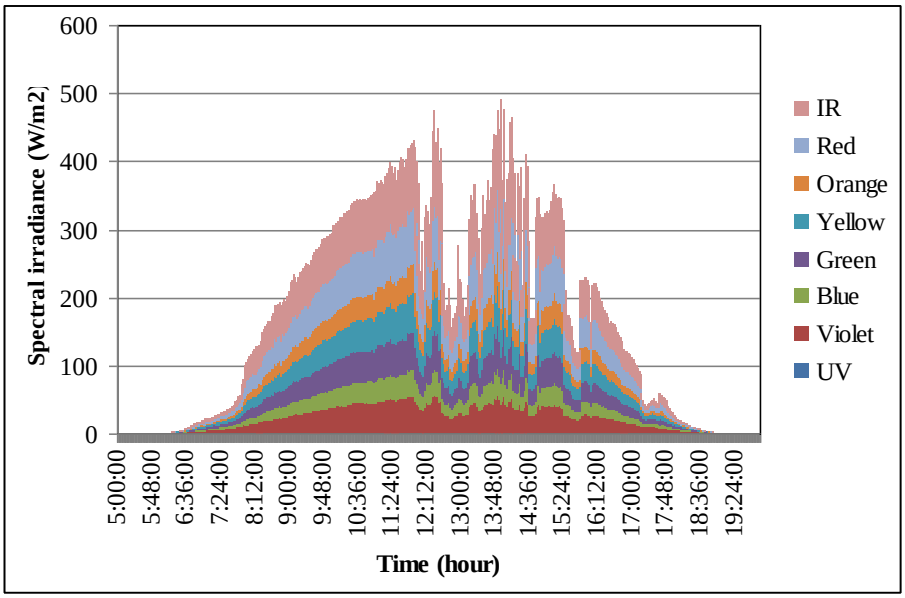

Fig. 4.38. Spectral irradiance characteristic in Gödöllő climates

Based on Fig. 4.38, it clear that although the red spectral irradiation (in visible region) and infra red (in invisible region) have the lower energy (and exergy), as a consequences of high wavelength, nevertheless both are more important than the rest due to their give big distribution on the whole day (not just in solar peak hours).

Physically, light with energy too high or low is not usable by a PV systems to produce electricity (called as optical losses: thermalization and non-absorption).

4.9. New scientific results

The new scientific results of my PhD work can be summarized as follow:

1. I have proven that the maximum annual output of the small scale (up to 10 kWp) capacity of grid-connected PV array system, can be obtained at the tilt angle in the range of 30° to 34°. Various values of tilt angle in this range, will affect on the annual output (an electric energy production) between 1-6%.

   The overall array performance for a different surface azimuth angle less than 5° either to East or to West, in case of facing to South, will affect on the annual output less than 1%.

2. I have evaluated the yearly thermodynamics performances of two most frequently applied photovoltaic modules theoretically, i.e. polycrystalline silicon, pc-Si (which included wafer based crystalline silicon technology), and amorphous silicon, a-Si (which included thin film technology), in view of energy and exergy.

   It is found that energy efficiency (η_{en}) of PV modules 75% and 90% higher than exergy efficiency (η_{ex}), respectively for pc-Si and a-Si, due to the energy efficiency is based on the electrical energy and the thermal energy (which available on the PV surface) as an output, meanwhile exergy efficiency considers only electrical energy as an output.

   It is also found that thermodynamic efficiencies of PV modules in power conversion (η_{pc}) and exergy there are differences, specifically 1% and 12%, respectively for pc-Si and a-Si.

   The efficiency maximum (η_{max}) are 25% and 52% higher than η_{ex}, 24% and 45% higher than η_{pc}, respectively for pc-Si and a-Si, because η_{max} is calculated based on I_{sc} and V_{oc}, as ideal values.

   The results showed that performance evaluations of PV modules with exergy analysis will lead us getting a realistic values rather than energy analysis, if compared to efficiency power conversion (efficiency of electric).

3. I have evaluated exergy efficiency and power conversion efficiency based on operational data.

   Compared to theoretical evaluation, in case of η_{ex} it is found that difference the theoretical and experimental efficiencies are 1.5% and 7%, respectively for pc-Si and a-Si, meanwhile in case of η_{pc} it is found that the difference between theoretical and experimental efficiencies are 8% and 22%, respectively for pc-Si and a-Si.

   In general, it can be stated that the difference of values between theoretically and experimentally in terminology of efficiencies exergy and power conversion are less than 25%.

4. I have compared two exergetic methods for evaluating of PV modules performance based on “thermodynamic approach for solar energy” and “photonic energy”, theoretically. Performance evaluation by photonic energy method was performed in the range of wavelength 400-800 nm.

   It is found that exergy efficiency based on “thermodynamic approach for solar energy” is spread on the exergy efficiency based on ”photonic energy” in the range of wavelength 550-650 nm and 600-800 nm, respectively for pc-Si and a-Si.

   It is also proving that both methods of the PV exergy assessment give more realistic values rather than the PV energy assessment.

5. I have investigated of the fill factor effect (*FF*) on the exergetic efficiency of PV modules, theoretically. Based on evaluation, it was found that yearly average of *FF* for pc-Si PV module is in range between 0.75-0.80, and for a-Si PV module, in range between 0.50-0.60.

   Compared to *FF* values in Laboratory scale, it is found that existing *FFs* are equal for pc-Si and lower 19-32% for a-Si.

6. I have investigated a spectral irradiance characteristic, as initial stage in order to find the effect of spectral irradiance on the exergetic of PV modules performances.

   It has been concluded that the red spectral (in visible region) and infra red spectral (in invisible region) are more important than the rest, due to their distribution on the whole day (not just in solar peak hours). Nevertheless, both have lower energy (and also exergy), as a consequences of a high wavelength.

   As an important irradiance element in visible region, the red spectral have an average irradiance 200 W/m^2, in between time 08:00-16:00. Meanwhile, as an irradiance element with highest energy, the violet spectral have an average irradiance 25 W/m^2, in the same time interval. Difference of solar irradiance between red and violet spectral in that time interval is 87.5%.

5. CONCLUSIONS AND SUGGESTIONS

Based on this work, all the relevant parameters, conducted to the photovoltaic (PV) modules performances have been identified and elaborated. The existing of 10 kWp grid-connected PV array system, which used two PV modules technologies i.e. wafer based crystalline silicon (pc-Si type) and thin film (a-Si) as main components, have been evaluated. It is clear that the installation having the right position, conducted to surface orientation in order to maximize the yield of electric energy.

The thermodynamics performances of PV modules have been evaluated either theoretically or experimentally, in view of energetic (involves only the First Law Thermodynamic) or exergetic (involves both the First and Second Law of Thermodynamics). Based on theoretical evaluation, it is found that average energy and exergy efficiencies during a year were 47.66% and 11.82% for pc-Si, and 43.20% and 4.30 for a-Si. Meanwhile based on experimental in specific day, it is found that an average exergy efficieny during effective sun hours were 12% and 4%, for polycrystalline silicon and amorphous silicon.

As an expected, the energy and exergy efficiencies of pc-Si PV module is higher than a-Si PV module. Finally, in order to get more realistic modelling of PV systems, application of exergy analysis are strongly encouraged.

Beside as a comparison purpose, further outcome of this research is trying to find a possibility to increase the performances both solar PV modules, in PV array system at Szent István University.

As a follow up of this research, sequences activities below needs to be implemented, in order to achieve further research outcome.

- Further parametric studies, in order to obtain a deep correlation between climatic and operating parameter, and finally other possibility to optimize and increase the PV module performance can be found.
- Collects comprehensive operational data of a 10 kWp grid-connected PV array system at Szent István University.
- Conducted an available spectral measurements data to the concept exergetic performances based on photonic energy.
- Develop/Integrate correlation about the energy - exergy mathematical model of PV system into the block oriented solution algorithm on the MATLAB/Simulink block libraries.
- Develop the real time and transient software for exergy analysis based on calculations method that have been elaborated in this research.
- Make a colaboration and synergy with Institute of material, in order to perform comprehensive research, included in view of material aspects.

6. SUMMARY

In this research comprehensive evaluation of two photovoltaic (PV) modules technologies i.e. polycrystalline silicon (pc-Si) included wafer based crystalline silicon technology, and amorphous silicon (a-Si) included thin-film technology, as components of grid-connected PV array at Szent István University (SZIU), have been performed in view energetic and exergetic. It is well known that energy evaluation is more suitable for energy balance when we design a system, while exergy evaluation is more appropriate when we evaluate the performance of a system qualitatively.

First of all, evaluation on the existing grid-connected PV array system in view of macro model has been performed in order to find the best surface orientation of PV module, which maximize the yield of electric energy.

Furthermore, thermodynamic performance of polycrystalline silicon and amorphous silicon PV modules are evaluated in term of efficiencies of energy (η_{en}), exergy (η_{ex}), power conversion (η_{pc}) and maximum/theoretical (η_{max}). Based on this evaluation, we will know which the most important of efficiencies, conducted to PV modules performance.

Exergy efficiency (η_{ex}) and power conversion efficiency (η_{pc}) of PV modules are simulated (yearly base) by two methods i.e. “thermodynamic approach method“ and “photonic energy method“, and after that are evaluated based on operational data for a specific day. Sensitivity of fill factor (FF) on exergetic performance have been evaluated also in this research.

As one of an important aspect in the utilization of solar energy, effect of spectral irradiance on the PV modules performance has been initialized also in this research.

Based on study and discussion of the results, in general it can be concluded that the energy efficiency is higher than theoretical, power conversion and exergy efficiencies throughout the year. Based on exergy analysis, it clear that there is an opportunities to increase the real of PV modules performances (in this case pc-Si and a-Si), until close to the theoretical efficiency (as an ideal value), which can be performed through various field of research and methods. Currently, one of a method i.e. tandem cells method (multi junction method) has been offered and used widely in the world, in order to increase the power conversion efficiency of PV systems (solar cells/module).

10.14751/SZIE.2013.026

7. ÖSSZEFOGLALÁS (SUMMARY IN HUNGARIAN)

FOTOVILLAMOS MODULOK ENERGETIKAI MODELLEZÉSE HÁLÓZATRA KAPCSOLT RENDSZEREKBEN

A disszertációban bemutatott kutatás átfogó értékelést ad kétfajta fotovillamos (PV) modul technológiáról, a polikristályos szilícium (pc-Si), amely a szelet alapú kristályos szilícium technológiához, és az amorf szilícium napelemekről (a-Si), amely vékonyrétegű technológiához tartozik. A kétfajta modultípus a Szent István Egyetemen (SZIE) található hálózatra visszatápláló PV erőmű alkotóelemei, amelyekre a kutatás folyamán energetikai és exergetikai vizsgálatok és elemzések készültek. Az energetikai értékelések a tervezés során kialakuló energia-egyensúly meghatározására alkalmasak, amíg az exergetikai értékelések leginkább akkor használatosak, amikor a rendszer teljesítményét minőségileg vizsgáljuk.

Első lépésben a hálózatra visszatápláló PV rendszer vizsgálata történt makro modellel, amely során meghatározásra került az optimális felületorientáció, amellyel maximalizálható a mező által termelhető villamos energia mennyisége.

Ezt követően meghatározásra került a polikristályos, illetve az amorf szilícium PV modulok termodinamikai teljesítménye a teljes (villamos és termikus) energiaátalakítási hatásfok (η_{en}), az exergetikai hatásfok (η_{ex}), a villamos energiaátalakítási hatásfok (η_{pc}) és a maximális (elméleti) villamos energiaátalakítási hatásfok (η_{max}) segítségével. A számításokból megállapítható, hogy melyik hatásfok van a legnagyobb hatással a PV modulok teljesítményváltozására.

Egész évre vonatkozó szimulációval kétféle módon is elemzésre került a fotovillamos modulok exergetikai és az energiaátalakítási hatásfoka, nevezetesen „termodinamikai megközelítéssel“ illetve „foton energia módszerrel“, amelyek segítségével a vizsgálatok egy adott napra vonatkozóan is elkészültek. A számítások során az exergetikai teljesítmény segítségével a kitöltési tényező (fill factor, *FF*) érzékenységvizsgálata is elkészült.

Jelen dolgozatban úgyszintén meghatározásra került a napsugárzás spektrális hatása a fotovillamos modulok teljesítményére vonatkozóan, amely a napenergia hasznosításnál rendkívül fontos szempont.

Az eredmények kiértékeléséből általánosságban megállapítható, hogy a teljes energiaátalakítási hatásfok az egész év folyamán meghaladja az exergetikai és a villamos hatásfokat. Exergetikai elemzésekből az is megállapítható, hogy lehetőség van a PV modulok (pc-Si és a-Si) villamos hatásfokának a maximális hatásfok értékek közeli növelésére. A PV rendszerek (PV cellák/modulok) energiaátalakítási hatásfokának növelése érdekében jelenleg elsősorban a több határréteges cellák alkalmazása javasolt.

APPENDICES

A1. Bibliography

1. ABRAMS, Z. R., GHARGHI, M., NIV, A., GLADDEN, C., ZHANG, X. (2012): Theoretical efficiency of 3rd generation solar cells: Comparison between carrier multiplication and down-conversion, *Solar Energy Materials & Solar Cells*, 99, pp. 308–315.
2. AKHMAD, K., KITAMURA, A., YAMAMOTO, F., OKAMOTO, H., TAKAKURA, H., HAMAKAWA, Y. (1997): Outdoor performance of amorphous silicon and polycrystalline silicon PV modules, *Solar Energy Materials and Solar Cells*, 46, pp. 209-218.
3. AIR JIANG, J., LIANG HUANG, T., TUNG HSIAO, YING, HONG CHEN, C., (2005): Maximum power tracking for photovoltaic power systems, *Tamkang Journal of Science and Engineering*, 8 (2), pp. 147-153.
4. AZMI, M., MALIK, A.Q. (2001): Optimum tilt angle and orientation for solar collector in Brunai Darussalam, *Renewable Energy*, 24, pp. 223-234.
5. BENARD, A. (2006): Design of alternative energy systems course notes – solar power, *Michigan State University College*, spring 2006.
6. Best research-cell efficiencies, on line at: www.nrel.gov/ncpv/images/efficiency_chart.jpg, accessed on December 19, 2012.
7. Can thin film solar modules be the right choice for a sustainable future, on line at: www.greensolar.hu/sites/default/files/EuropeanEnergyInnovation-GreenSolar.pdf, accessed on December 19, 2012.
8. CHANG, T. P. (2008): Study on the optimal tilt angle of solar collector according to different radiation types, *International Journal of Applied Science and Engineering*, 6 (2), pp. 151-161.
9. CHRISTENSEN, C.B., BARKER, G.M., (2001): Effects of tilt and azimuth on annual incident solar radiation for United States location, *Proceedings of Solar Forum*, 2001, Washington DC-USA, April 21-25.
10. CLEMENTE, I. C., 2005. Quantitative subsurface defect evaluation by pulsed phase thermography: depth retrieval with the phase: Fundamentals of Infrared Radiation. On line at: http://archimede.bibl.ulaval.ca/archimede/fichiers/23016/apb.html, accessed on December 19, 2012.
11. DINCER, I., CENGEL, A. Y., (2001), Energy, entropy and exergy concepts and their roles in thermal engineering, *Entropi*, 3, pp. 116-149.
12. DURISCH, W., TILLE, D., WÖRZ, A., PLAPP, W., (2000): Characterisation of photovoltaic generators. *Applied Energy*, 65, 273-284.

13. FARKAS, I., SERES I., (2008): Operational experiences with small-scale grid-connected PV system, *Mechanical Engineering Letter - Szent István University*, 1, pp. 64-72.
14. Hahn-Meitner, Production of Amorphous silicon: Institut Berlin, on line at: www.sunenergysite.eu/en/technologies.php, accessed on December 19, 2012.
15. HUSSEIN, H.M.S., AHMAD, G.E. AND EL-GHETANY, H.H., (2004): Performance evaluation of photovoltaic modules at different tilt angles and orientations. *Energy Conversion & Management*, 45, pp. 2441-2452.
16. Insolation, on line at: www.geog.ucsb.edu/ideas/Insolation.html, accessed on December 19, 2012.
17. JOSHI, A.S., DINCER, I., REDDY B.V., (2009), Performance analysis of photovoltaic systems: a review, *Renewable and Sustainable Energy Reviews*, 13, pp. 1884-1897.
18. KABELAC, S., (2008): Thermodynamic basic of solar radiation, *The 5th European Thermal-Sciences Conference 2008, The Netherlands*, online at: http://www.eurotherm2008.tue.nl/, accessed on December 19, 2012.
19. KACIRA, M., SIMSEK, M., YUNUS, B., SEDAT, D., (2004): Determining optimum tilt angles and orientations of photovoltaic panels in Saliurfa, Turkey. *Renewable Energy*, 29, pp. 1265-1275.
20. KING, D. L., BOYSON, W. E., KRATOCHVIL, J. A., (2004): Photovoltaic array performance model, Sandia National Laboratories, Albuquerque, New Mexico.
21. KLISE, G.T., STEIN, J. S. (2009), Models used to assess the performance of photovoltaic systems, *Sandia report: SAND2009-8258*, on line at: http://photovoltaics.sandia.gov/Pubs_2010/PV%20Website%20Publications%20Folder_09/Klise%20and%20Stein_SAND09-8258.pdf
22. LABUHN, D., KABELAC, S., (2001): The spectral directional emissivity of photovoltaic surfaces, *International Journal of Thermophysics*, 22 (5), pp. 1577-1592.
23. MARCEL, S., HULD T.A., DUNLOP, E.D., OSSENBRINK H.A., (2007): Potential of solar electricity generation in the European Union member states and candidate countries, *Solar Energy*, 81, pp. 1295-1305.
24. MARKVART, T., (1996): Solar electricity, Chichester, UK, John Wiley & Sons.
25. MASTERS, G.M., (2004): Renewable and efficient electric power system, *Wiley-Interscience, New Jersey*.

26. Orion Energy Corporation, NSol Version 4 - PV System Sizing Program, Frederick, Maryland USA, www.orionenergy.com.
27. PEARSALL, N.M., Hill, R., (2001): Photovoltaic modules, systems and application, *Northumbria photovoltaics applications centre* – University of Northumbria at Newcastle.
28. PETELA, R., (2003): Exergy of undiluted thermal radiation, *Solar Energy*, 74, pp. 469-488.
29. PETELA, R., (2010): Engineering thermodynamics of thermal radiation for solar power utilization, *McGrawhill, New York*.
30. Geographical Assessment of Solar Resource and Performance of Photovoltaic Technology, Photovoltaic Geographical Information System (PVGIS), on line at: http://re.jrc.ec.europa.eu/pvgis/, accessed on December 19, 2012.
31. RAZYKOV, T.M., FEREKIDES, C.S., MOREL, D., STEFANAKOS, E., ULLAL, H.S., UPADHYAYA, H.M., (2011): Solar photovoltaic electricity: current status and future prospects, *Solar Energy*, 85, pp. 1580–1608.
32. ROSEN, M. A., BULUCEA, C. A., (2009): Using exergy to understand and improve the efficiency of electrical power technologies, *Entropy*, 11, pp. 820-835.
33. SAHIN, A.D., DINCER, I., ROSEN, M.A., (2007): Thermodynamic analysis of solar photovoltaic cell systems, *Solar energy materials & solar cells*, 91, pp. 153-159.
34. SANDNESS, B., (2003), *Exergy efficient production, storage and distribution of solar energy*, PhD thesis, Department of Physics, Faculty of Mathematics and Natural Sciences, University of Oslo, Norway.
35. SANTARELLI, M., MACAGNO, S., (2004): A thermoeconomic analysis of a PV-hydrogen system feeding the energy requests of a residential building in an isolated valley of the Alps, *Energy Conversion and Management*, 45, pp. 427–451.
36. SERES, I., FARKAS, I. (2007): Development of a 10 kWp Photovoltaic System — Efficiency Analysis, *Proceedings of ISES World Congress 2007 (Vol. IV)*, September 18-21, Beijing, China, pp. 1652-1656.
37. SHUKUYA M., HAMMACHE A., (2002): Introduction to the concept of exergy, *VTT Research notes 2158, Julkaisija–Utgivare-Publisher*, on line at: http://www.vtt.fi/inf/pdf/tiedotteet/2002/T2158.pdf.
38. SKOPLAKI, E., BOUDOUVIS, A.G., PALYVOS, J.A., (2008): A simple correlation for the operating temperature of photovoltaic modules of arbitrary mounting, Solar Energy Materials & Solar cells, 92, pp. 1393-1402.

39. Solar Power – Technologies, PV cells and modules, on line at: www.greenrhinoenergy.com/solar/technologies/pv_modules.php, accessed on December 19, 2012.
40. TSAI, H.L., TU, C.S., SU, Y.J., (2008): Development of generalized photovoltaic model using Matlab/simulink, *Proceeding of the World Congress on Engineering and Computer Science (WCECS) October 22 – 24, 2008, San Fransisco, USA*, online at: http://www.iaeng.org/publication/WCECS2008/WCECS2008_pp846-851.pdf
41. WALL, G., (2007): On education towards sustainable development, *Department of Education, Göteborg University, Sweden*, online at: http://www.exergy.se/ftp/oetsd.pdf
42. WALDAU, A.J., (2004), Status of thin film solar cells in research, production and the market, *Solar energy*, 77, 667-678.
43. WALUKIEWICZ, W. New concepts and materials for solar power conversion, *Material science division, Lawrence Berkeley National Laboratory*, on line at: arlevents.com/energy/presentations/7th/Walukiewicz.ppt, accessed on December 19, 2012.
44. WENHAM, S.R., GREEN, M.A., WATT, M.E., CORKISH, R., (2007): Applied photovoltaics. *Earthscan, London*.
45. What is ultraviolet radiation - Sunlight and radiation, on line at: http://www.healthycanadians.gc.ca/environment-environnement/sun-soleil/radiation-rayonnement-eng.php, accessed on December 19, 2012.
46. WOYTE, A., (2003): Grid-connection of photovoltaic systems, on line at: http://www.esat.kuleuven.be/electa/publications/fulltexts/pub_1146.pdf, accessed on December 19, 2012.
47. ZEMAN: Solar cell operating principle, Delf University of Technology, on line at: www.ocw.tudelf.nl/courses/microelectronics/solar-cells/lectures/, accessed on December 19, 2012.

A2. Publications related to the thesis

Refereed papers in foreign languages:

1. **Rusirawan, D.** and Farkas, I. (2012): Spectral irradiance effects on exergetic performances of photovoltaic module: initial study, Mechanical Engineering Letter, Szent István University, Vol. 8 (submitted).
2. **Rusirawan, D.** and Farkas, I. (2012): Thermodynamic efficiencies of solar photovoltaic modules, Environmental Engineering Management Journal (accepted for publication). (IF: 1.004*).
3. **Rusirawan, D.** and Farkas, I. (2012): Availability of the photovoltaic modules in view of photonic energy, Scientific Monograph: Applications of Physical Research in Engineering, Part 1, pp. 42-61.
4. **Rusirawan, D.** and Farkas, I. (2011): Characterizations based an experimental of two photovoltaic module technologies, Mechanical Engineering Letter, Szent István University, Vol. 6, pp. 112-122.
5. **Rusirawan, D.** and Farkas, I. (2011): The photovoltaic modules performance based on exergy assessment, Hungarian Agricultural Engineering No. 23, pp. 53-56.
6. **Rusirawan, D.** and Farkas, I. (2011): Simulation of electrical characteristics of polycrystalline and amorphous PV modules, Electrotechnics Electronics Automatics, Vol. 59, No. 2, pp. 9-15.

Refereed papers in Hungarian:

7. **Rusirawan D.**, Farkas I. (2012): Napelem modulok teljesítmény növelése érdekében kidolgozott technológiák, Mezőgazdasági Technika, LIII. Evfolyam, július 2012, 5-7. o.
8. Farkas I., **Rusirawan D.**,Galambos E. (2012): Hálózatra kapcsolt napelem mező cella/modul alapú modellezése, Magyar Energetika, XIX évfolyam, 2. sz., 6-9. o.

International conference proceedings:

9. **Rusirawan, D.** and Farkas, I. (2012): Electrical and exergetic efficiencies of polycrystalline and amorphous silicon, Eurosun 2012 conference, September 18-20, 2012, Rijeka, Croatia, p. 8.
10. **Rusirawan, D.** and Farkas, I. (2012): Exergetic based of photovoltaic modules characteristics, Conference X, Engineering and Application of Mechanical Engineering in Industry, ITENAS Bandung, Indonesia, January 17-18, 2012, pp. 119-127.

11. **Rusirawan, D.** and Farkas, I. (2011): Exergetic analysis of photovoltaic modules based on photonic energy, Proceeding of Scientific Works in Physics – Research – Applications – Education (PRAE) 2011, October 13-14, 2011, Nitra, Slovakia, pp. 119-124.
12. **Rusirawan, D.** and Farkas, I. (2011): Exergetic assessment of polycrystalline and amorphous photovoltaic modules in different methods, Proceeding of the 2nd International Conference in Agricultural Engineering, Synergy 2011, October 9-15, 2011, Gödöllő, Hungary, p. 6.
13. **Rusirawan, D.** and Farkas, I. (2011): MPPT algorithm effect on the performance of a small scale grid-connected PV array system, Solar World Congress 2011, August 28-September 2, 2011, Kassel, Germany, p. 12.
14. **Rusirawan, D.** and Farkas, I. (2011): Thermodynamic analysis of a 10 kWp grid-connected photovoltaic array system, CIOSTA 2011, June 29-July 1, 2011, Vienna, Austria, p. 10.
15. **Rusirawan, D.**, Seres, I. and Farkas, I. (2010): Exergy analysis of grid-connected photovoltaic array system, Conference IX, Engineering and Application of Mechanical Engineering in Industry, ITENAS Bandung, Indonesia, November 9-10, 2010, pp. 36-44.
16. **Rusirawan, D.** and Farkas, I. (2010): Cell/module based modelling of grid-connected photovoltaic array system, International Congress Energy and the Environment 2010, Vol. I, Opatija, Croatia, October 18-22, 2010. pp. 59-68.
17. **Rusirawan, D.**, Seres, I. and Farkas, I. (2009): Energy Production of a 10 kWp grid-connected PV array system after 4 years operation at Szent István University, Conference VIII, Engineering and Application of Mechanical Engineering in Industry, ITENAS Bandung, Indonesia, November 24-25, 2009, pp. 159-164.

Hungarian conference proceeding:

18. **Rusirawan D.,** Farkas I. (2012): Variability of fill factor on exergetic of crystalline and thin film PV modules technologies, Értékteremtő Épületgépészet Konferencia és kiállítás, Gödöllő, 2012. május 24-25, Konferencia Kiadvány, 27-39. o.

International conference abstracts:

19. **Rusirawan, D.** and Farkas, I. (2012): Characteristics of photovoltaic modules in hot climates, 18th Workshop on Energy and Environment, Gödöllő, Hungary, November 22-23, 2012 (submitted).

20. **Rusirawan, D.** and Farkas, I. (2012): Fill factor (FF) effects on exergetic efficiency of photovoltaic modules, 11th International Workshop for Young Scientists (BioPhys Spring 2012), Prague, Czech Republic, May 24-25, 2012, p. 19.
21. **Rusirawan, D.** and Farkas, I. (2011): Characteristics of the photovoltaic modules availability at a predetermined temperature, Book of Abstracts, 17th Workshop on Energy and Environment, Gödöllő, Hungary, December 1-2, 2011, p. 9.
22. **Rusirawan, D.** and Farkas, I. (2011): MPPT analysis of module component of a grid-connected PV array system, Book of Abstracts, 10th International Workshop for Young Scientists (BioPhys Spring 2011), Gödöllő, Hungary, May 26-27, 2011, pp. 44-45.
23. **Rusirawan, D.** and Farkas, I. (2010): A photovoltaic array system performance based on energy and exergy analysis, Book of Abstracts, 16th Workshop on Energy and Environment, Gödöllő, Hungary, November 11-12, 2010, p. 20.
24. **Rusirawan, D.** and Farkas, I. (2010): Energy and environmental aspects of a 10 kW_p grid-connected photovoltaic array, Book of Abstracts, 9th International Workshop for Young Scientists (BioPhys Spring 2010), Nitra, Slovakia, May 20-21, 2010, pp. 33-35.
25. **Rusirawan, D.** and Farkas, I. (2009): Introduction to modelling a generalized photovoltaic array, Book of Abstracts, 15th Workshop on Energy and Environment, Gödöllő, Hungary, November 5-6, 2009, p. 16.

ACKNOWLEDGEMENTS

This PhD work has been carried out at Department Physics and Process Control, Institute for Environmental Engineering System, Faculty of Mechanical Engineering, Szent István University – Gödöllő, during period of September 2009 to October 2012.

I would like to acknowledge my deepest gratitude to my supervisors Prof. Dr. István Farkas, for his valuable advice, excellent guidance and continuous encouragement throughout my research. This dissertation would not have been possible without the generous academic support of him and has been a great pleasure to learn the scientific way of thinking under his supervision. I wish also to extend my sincere gratitude to Dr. István Seres, for his valuable help, in provide data, throughout my research.

I would like to acknowledge and extend my heartfelt gratitude to the General Directorate of Higher Education (GDHE) of Republic Indonesia, the Hungarian Scholarship Board, Kocsis Károly Research Grant Szent István University – Gödöllő and Institut Teknologi Nasional (ITENAS) - Bandung, for their supports which have made the completion of this project possible.

It has been a great pleasure to work in the Department Physics and Process Control in Szent István University. I wish to express my special thanks to all members of Department Physics and Process Control, for their helpful attitude, and creating a friendly environment conducive for my progress. Thanks to Ivett Kocsány and Erik Galambos, who taught me a Hungarian language, and also help me to translate my dissertation to Hungarian.

To my wife Noorita Tetriana, my sons Farizi Nadhir Mahandika and Istvan Azka Fakhrusy, my gratitude goes to them all for providing me a warm and happy family and for their patience living in completely different in weather and culture. Last but not least, I would like to thanks to my big family in Indonesia for their moral support that made it possible for me and my family to be here.